High Impact Polypropylene –Structure Evolution and Impact on Reaction

Dissertation

zur Erlangung des

Doktorgrades der Ingenieurwissenschaften (Dr. Ing.) der

Naturwissenschaftliche Fakultät II - Chemie, Physik und Mathematik der Martin-Luther-Universität Halle-Wittenberg

vorgelegt von Herrn

Miguel Angel Plata Acevedo

geb. am 18.03.1985 in Bogota

Abstract

This work focuses on the effect of reaction conditions, in particular prepolymerization conditions, on resulting particle morphology and how in turn particle morphology influences process kinetics in the multistage polymerization of heterophasic polypropylene.

Experimental studies were carried out using two industrial Ziegler-Natta catalysts in gas-phase and bulk phase polymerizations using a number of different lab-scale setups.

After establishing reproducibility and reference activity levels, initially a broad screening of the effect of homopolymerization and prepolymerization conditions on particle morphology was performed. The results clearly showed for both catalysts studied, that prepolymerization is essentially required in order to obtain good catalyst activity and that addition of small amount of ethylene during prepolymerization is an effective handle to adjust particle morphology. By addition of ethylene, bulk density of the resulting polymer is reduced and correspondingly porosity (measured by Hg-porosity measurements) is increased. Sorption measurements in a high-pressure sorption balance reveal for the samples with lower bulk density faster mass-transfer rates.

Polymerization activity in the matrix stage (either performed as gas-phase or bulk-phase polymerization) is for both catalysts studied basically not affected by ethylene in the prepolymerization step. Also crystallinity of the matrix polymers is not affected by ethylene in the prepolymerization step.

During the rubber-phase polymerization, the samples with ethylene in the prepolymerization step showed surprisingly lower activities compared to the samples without ethylene in the prepolymerization step. There are indications that ethylene incorporation in the rubber step is slightly higher for samples with ethylene during the prepolymerization step.

Simulation studies show that the samples with ethylene in the prepolymerization step reduce the mass-transfer limitations for ethylene in the heco-stage, which helps to better exploit the catalyst capabilities for ethylene incorporation.

Abstract

Diese Arbeit untersucht die Auswirkungen von Reaktionsbedingungen, insbesondere der Prepolymerisation auf die Partikelmorphologie und darauf, wie diese die Prozesskinetik in der mehrstufigen Polymerisation von heterophasischem Polypropylen beeinflussen.

Die experimentellen Untersuchungen zur Gasphasen und Masse-Polymerisation wurden unter Verwendung von zwei industriellen Ziegler-Natta-Katalysatoren in verschiedenen Laborreaktorsystemen durchgeführt.

Nach Erreichen von Reproduzierbarkeit und Referenzaktivitäten wurde zunächst ein breites Screening über den Einfluss von Homo- und Prepolymerisationsbedingungen auf die Partikelmorphologie durchgeführt. Die Ergebnisse zeigen für beide untersuchten Katalysatoren, dass eine Prepolymerisation zwingend erforderlich ist um gute Aktivitäten zu erhalten. Die Zugabe einer kleinen Menge an Ethylen während der Prepolymerisation ist eine wirksame Methode zur Einstellung der Partikelmorphologie. Durch die Zugabe von Ethylen wird die Schüttdichte des Polymers verringert und entsprechend die Porosität (gemessen durch Quecksilber Porosimetrie) erhöht. Sorptions-messungen in einer Hochdruck-Sorptionswaage zeigen für Proben mit geringerer Schüttdichte schnellere Stoffaustauschraten.

Die Aktivität während der Matrix-Homopolymerisation (entweder als Gasphasen- oder Massepolymerisation durchgeführt) wird durch die Zugabe von Ethylen bei der Prepolymerisation für keines der beiden untersuchten Katalysatorsysteme wesentlich beeinflusst. Auch die Kristallinität der Homopolymere wird durch Ethylen in dem Prepolymerisationsschritt nicht beeinflusst.

Während der nachfolgenden Copolymerisation zeigten die Proben mit Ethylen in der Prepolymerisation überraschend geringere Polymerisationsaktivitäten auf. Es gibt Hinweise darauf, dass der Ethyleneinbau in der Copolymerisation bei Proben mit Ethylen während der Prepolymerisation etwas höher ist.

Simulationsrechnungen zeigen, dass die Proben mit Ethylen in der Prepolymerisation die Stofftransportbeschränkungen für Ethylen in der Copolymerisation reduzieren. Dadurch kann das Potential des Katalysators für den Ethyleneinbau besser genutzt werden.

Diese Arbeit ist Teil des Forschungsprogramms des Dutch Polymers Institut (DPI), Projekt # 785

Acknowledgments:

<u>For all those who did NOT believe in me</u>

Table of contents:

1 Introduction

1.1 Polypropylene market and applications

Polymers are with an annual worldwide production of more than 300 Mio tons an important class of materials used in many applications. About 50 million tons were demanded for Europe. Polyolefines, mostly polyethylene (PE) and polypropylene (PP) do account for almost half of the polymers produced. Polypropylene is one of the most important plastics in the market. With a production of approximately 10 million tons in Europe in 2016, polypropylene shares around 19 percent of the market. Just in Germany about 25% were consumed. In Europe, PP is the second most used and produced polymer following polyethylene. The demand for this material has been growing at a rate of 4.4% per year between 2013 and 2016 [1].
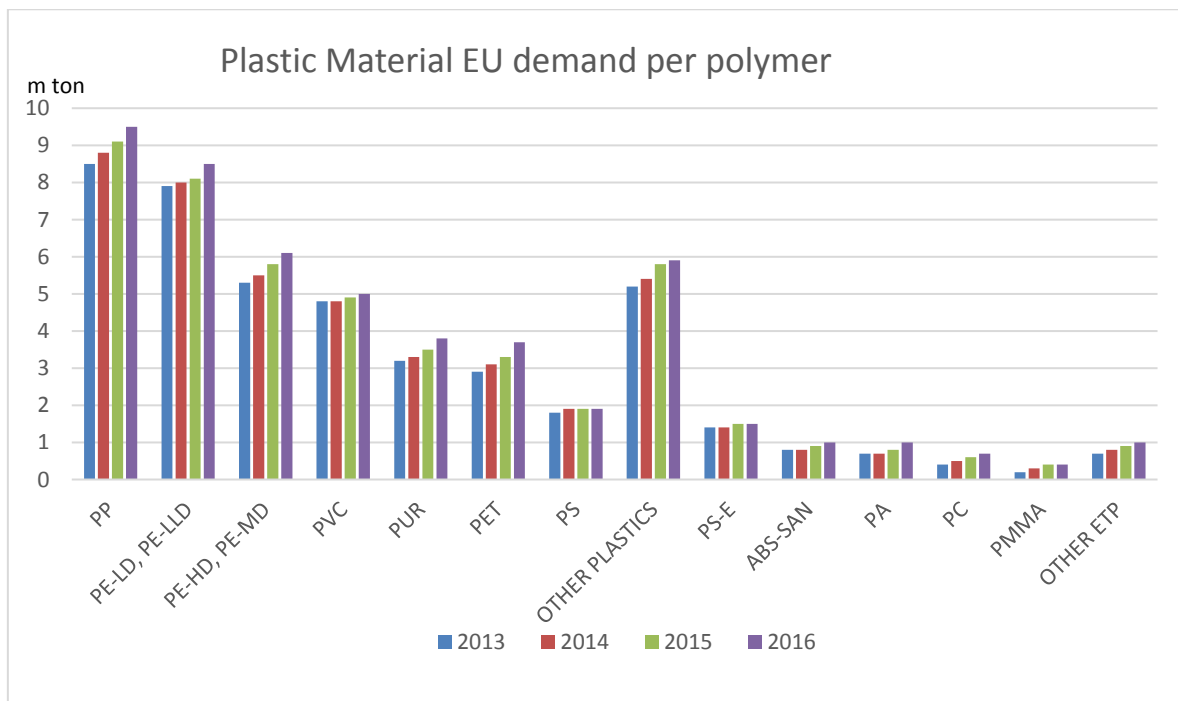
Figure 1 : Plastic demand in EU from 2013 to 2016 [1]
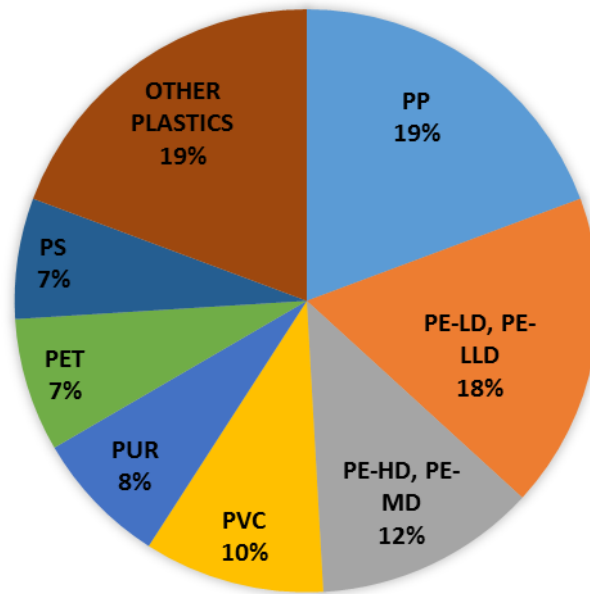
Figure 2: European plastics converter demand by polymer types in 2016 [1]

Polypropylene (PP) is widely used in many high-volume applications due to its versatility and attractive price/performance ratio [2]. High volume applications for PP are in consumer products, packaging, film, textile and in the automotive industry.

One of the advantages of iPP is that it can be applied easily using different processes such as injection moulding, blow moulding and extrusion. High molecular weight grades are suitable for extrusion blow molding, meanwhile low molecular weight grades are more suitable for are used for injection- and compression-molding. Research in the development of this polyolefin have been dedicated to both increase mechanical properties such as the melt strength for film and foam production and high heat distortion temperatures which are now competing with other polymers [1].

1.2 PP microstructure and properties

Polypropylene as a macromolecule has its own stereochemistry. Its chains can be spatially arranged in three different ways: as atactic, syndiotactic and isotactic polymer [3], as shown respectively in Figure 3, Figure 4, and Figure 5.
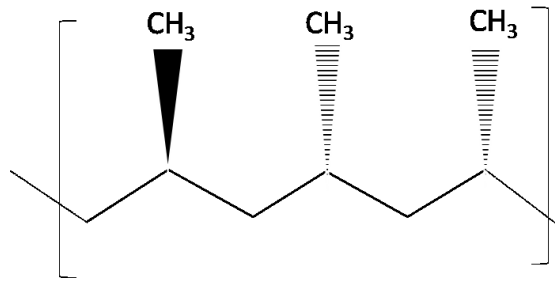
Figure 3: Atactic form of PP
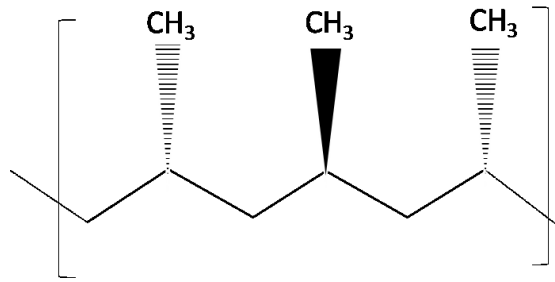
Figure 4: Syntactic attachment form of PP
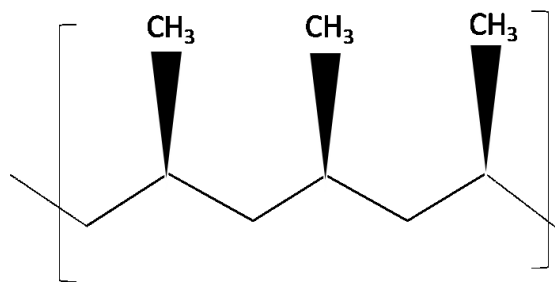
Figure 5: Isotactic PP

The tacticity or stereoregularity of the polymer molecule is of profound importance for the properties of the polymer. The mechanical and physical properties of polypropylene will be affected if the tactility is changed since it is the force that acts between adjacent polymer chains. Tacticity and stereoregularity of the polymer is mainly controlled by the catalyst used for production of the polymer [4].

Atactic polypropylene is completely amorphous (soft and sticky). In this type of tacticity the chains do not have any consistent placement of the methyl groups. The random positioning of the methyl groups prevents crystallization [4].

Syndiotactic polypropylene can be produced by e.g. certain metallocene catalysts [5]. In this case chains are a result from the head-to-tail addition of

propylene monomer units. The methyl groups are alternatively placed with respect to the polymer backbone. Syndiotactic polypropylene has the ability of crystallization and is used for film and fiber manufacturing [5].

The breakthrough for PP was the introduction of stereospecific catalysts (e.g. Ziegler-Natta) which enabled the production of predominantly isotactic polypropylene, which is semi-crystalline. Isotactic PP results from the head-to-tail addition of propylene monomer units, where all the methyl groups are placed on one side of the chain respect to the polymer backbone [6].

Through this head-to-tail addition, isotactic PP is able to line up and form a crystalline structure. Some of the most known features of isotactic PP are: low density, high thermal stability, and good solvent resistance. However, the poor impact property of isotactic polypropylene limits some of its applications [7]. High crystallinity is therefore important for the production of polypropylene. To improve this stereoregularity some donors are given in the polymerization reaction [8].

Furthermore, commercial PP type are distinguished in three different type groups:

- Homopolymer
- Random copolymers
- Heterophasic copolymers

Homo-PP grades are characterized by high crystallinity values, a relatively high melting temperature and a fair modulus value [9].

Random polypropylene contains low levels (1.5-7%) of ethylene or other olefin comonomers. They have a lower degree of crystallinity and melting point than Homo-PP. Random polypropylene is suitable to be process as thermoplastics. [10].

Heterophasic propylene copolymers consist of a polymer matrix of isotactic polypropylene homopolymer and a dispersed rubbery ethylene-propylene copolymer not miscible with the matrix phase [11]. For heterophasic copolymers (Hecos) the content of ethylene is typically between 20 and 60 wt%. While the matrix gives good stiffness, the elastomeric phase improves impact strength and low temperature behavior [9].

Polypropylene can be mixed with other polymers, which leads to important mechanical and chemical changes on its final properties. Furthermore, it can be blended to contain high amount of foams, talc and other agents to produce polymer blends that are bi-phasic [12].

1.3 Production of Polypropylene

Polypropylene is entirely produced by coordinative polymerization, with the help of organometallic catalysts.

Commercially predominately supported Ziegler-Natta catalysts are used, also supported metallocene catalysts can be used, however the fraction produced by Ziegler-Natta catalysts is by far higher, mainly for cost reasons [13].

Polypropylene Homo- and copolymers are produced commercially in three different process types: liquid slurry, bulk and gas phase processes and combinations thereof using different types of catalyst systems [14].

In liquid slurry processes, the polymerization is carried out in an organic diluent such as hexane. Operation of slurry plants is expensive due to the separation of the diluent. Hence slurry plants are more and more replaced by more cost-efficient bulk or gas-phase processes [15].

In bulk polymerization, the condensed monomer is used as dispersion media. Hence separation of the polymer is less costly compared to slurry processes. In addition, the monomer concentration is higher, hence higher reaction rates are possible [16].

Example for bulk processes are e.g. the spheripol process licensed by Basell and the Mitsui Hipol II process licensed by Mitsui.

The gas phase polymerization process is widely used for propylene polymerization. In this process, gaseous monomer (and co-monomers) are polymerized mostly over a solid Ziegler-Natta or a metallocene catalyst system. Catalyst components may be premixed and injected to the reactor in activated form or they may be injected separately [16] [17]. Homogenous mixing of the components is quite important to avoid any non-uniform distribution of catalyst.

Heat removal is harder than in slurry processes due to the absence of a liquid medium in the reaction zone. Avoiding particle sintering or changes in polymer properties is imperative during the design of the reactor [18].

Continuous stirred bed reactor (e.g. Novolen process), horizontal compartment reactors (Amoco process) and fluidized bed reactors (Unipol PP process) are used for propylene polymerization in the gas phase [19] [17].

Among the current technological and commercial processes are:

(a)   Novolen process for gas-phase polymerization licensed by Lummus Novolen Technology.

(b)   Unipol PP process for gas-phase polymerization licensed by Grace technology.

(c)   Spheripol bulk/gas-phase processes licensed by LyondellBasell

(d)   Borstar PP (Figure 6) bulk/gas-phase process licensed by Borealis.

(e)   Amoco gas-phase process licensed by Ineos [20].

High impact polypropylene (hiPP) is a propylene homopolymer reinforced by an elastomeric phase, and is made in at least two reaction steps. In the first step, the homopolymerization of propylene leads to the formation of an initial isotactic polypropylene (PP) matrix. Once the initial PP particles have reached a sufficient degree of polymerization, a copolymerization step is used to form a separate elastomeric phase in the still-active homopolymer particles [7].

The typical polymerization process for HiPP begins in a first reactor where a suitable catalyst will be used to achieve a defined Homo-PP morphology. In the second part this powder will continue to react in a second reactor with also a defined concentration of ethylene and propene. It should be noted that the temperature, pressure and concentration of the monomers can vary from one reactor to another thus producing a completely different polymer in each stage of the process. The final product from this process is strictly bi-phasic copolymeric material, but it is commonly referred to as an impact block copolymer [21].

In addition, the rubber one the second reactor can also find its way to the surface of the particles, which can cause stickiness, lump formation, reactor fouling and a number of other unfortunate incidents. It is also well known that changing the internal morphology of this type of particle can lead to changes in the mass transfer regime, and therefore reaction rates and macromolecular properties inside the particles [21].
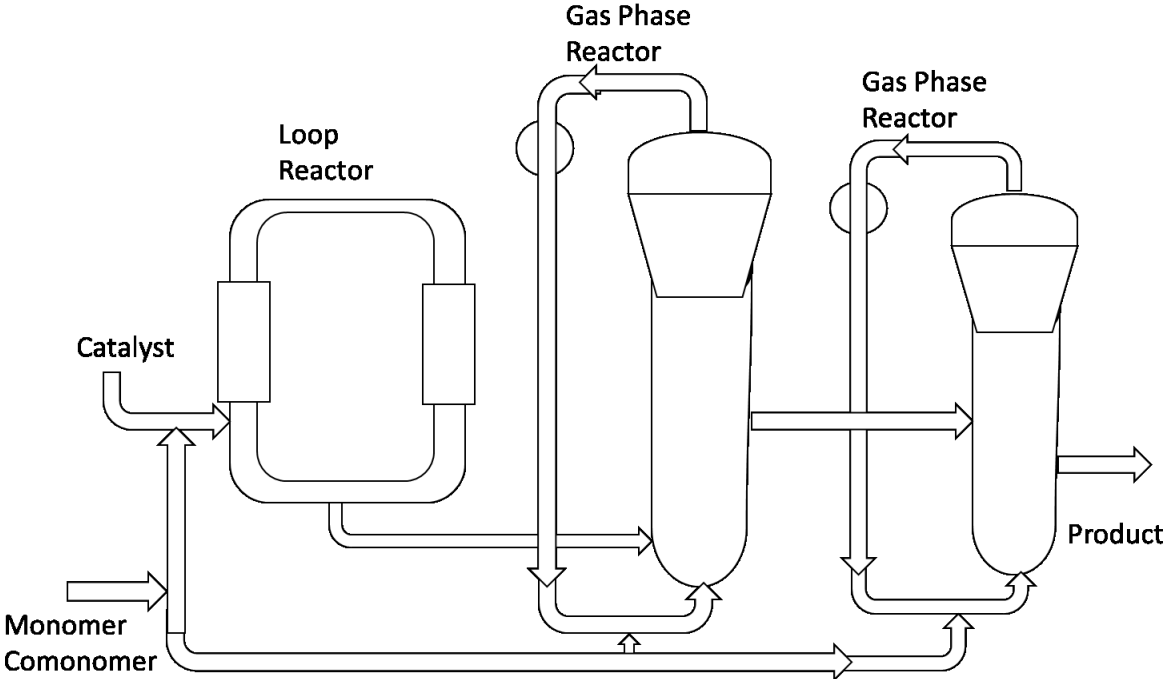
Figure 6: Borstar process for hiPP production

2 Theory and literature review

2.1 The role the particle in olefin polymerization

Supported catalysts are used for the polymerization of ethylene, propylene and/or α-olefin co-monomers, in gas or liquid phase processes. Tree types of supported catalyst are known (Ziegler–Natta, metallocene, and chromium-based systems). In all of them, the active sites are deposited on and inside porous solid supports. High specific surface area has a great importance since they maximize the number of accessible active sites per unit volume. Typical values for specific surface areas varying from 10 to 250 m²/g [22].

Ziegler-Natta (ZN) catalysts are made of a silica and magnesium dichloride ($MgCl_2$) support, while metallocenes are being supported on a variety of inorganic and organic carriers. Phillips catalysts are mostly supported on silica or silica/alumina [23].

The nature of catalyst types and supporting techniques has been already deeply studied [24] [25] [26] [27]. The different supports with individual physical properties will influence the development of polymerization and therefore the powder morphology, heat and mass transfer profiles during the polymerization. Nevertheless, the different types of support have a number of aspects in common from the point of view of modelling single particle growth [28].

The polymerization begins when a catalyst particle is injected into the reactor. One or more monomers, either in the form of a gas or liquid, are inserted in the continuous phase of the reactor. To reach the active sites, regardless nature of the phase, monomer must diffuse through the boundary layer around the catalyst and through its pores. After reaching the active sites, the polymerization will take place [29] [30].

In several processes, pre-polymerized catalysts are used, in which case the active sites will be pre-covered with a layer of polymer [25] [31]. It has been shown that pre-polymerization, done at milder polymerization conditions in a separate reactor, is a very useful technique to enhance catalyst stability as well as activity, and to eliminate the formation of hot spots in the catalyst particles [32] [33].

As the reaction takes places the polymer layer around the catalyst will grow and fill up the pores. Two possible scenarios can happen at this state:

➢ The support ruptures into many fragments (micrograins). Nevertheless, the particle retains its component parts because the polymer holds them together. In this case, pre-polymerization is a technique to improve and control the fragmentation step. From the engineering point of view, fragmentation is an advantageous phenomenon. Fragmentation leads to porosity and therefore facilitates monomer to access faster the actives sites [34].

➢ On the other hand, catalyst support could be also too strong and the particle does not break. The polymer layer will grow and therefore not only the pores will be filled up but also the length scale for diffusion of monomer will increase. At thick polymer layers the polymerization can be monomer-starved [35] [36]. Olefin polymerization is also a highly exothermic reaction [31] [36] [37], thus the heat generation rate can be very high inside the particles. Hot spots and agglomerations will appear if the heat of polymerization cannot be efficiently removed through the porous polymer matrix and fragmentation.

Catalyst fragmentation for Ziegler- Natta, metallocenes and Phillips catalyst has been studied over the last decades [37] [38] [39] [40] [34] [41]. The mechanism of growth by coordinative polymerization is explained in Figure 7.
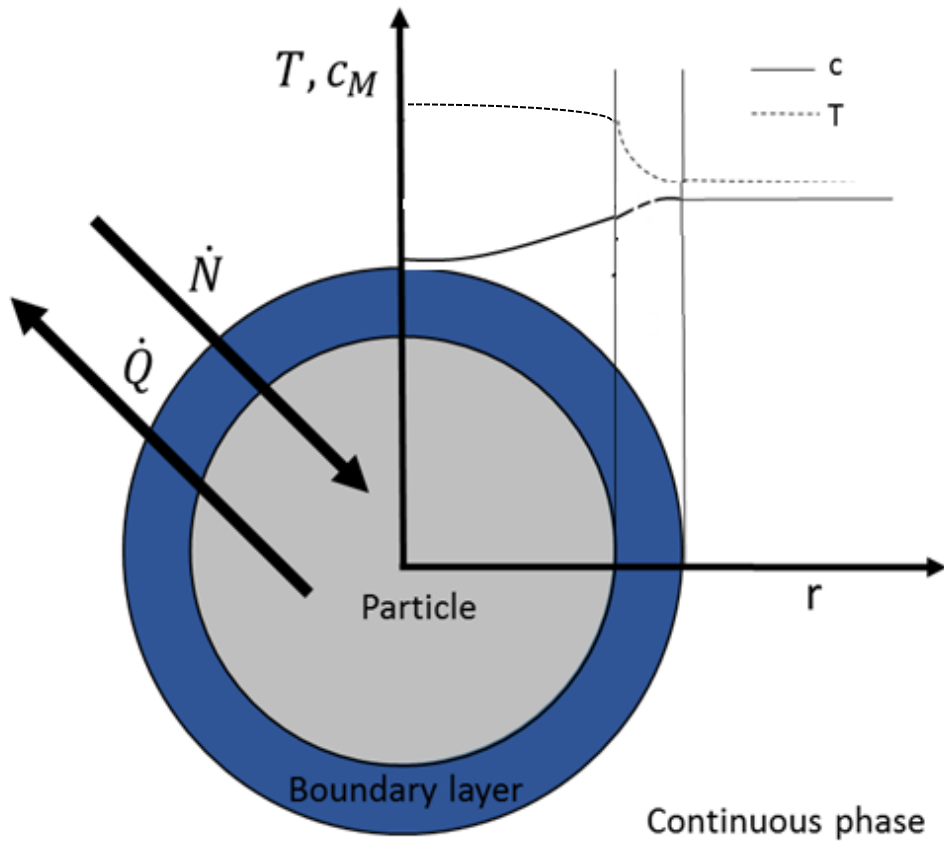
Figure 7: Mass and energy transport during particle growth

2.2 Morphology models

To describe the particle growth process in a polyolefin production several models have been proposed. Following are the most important models:

2.2.1 Core-Shell model

The Core-Shell model is the most simplistic of all models from the transport point of view. In this model, the catalyst is assumed as a compact particle which does not break up. All monomer surrounds the catalyst and reacts at the surface of the catalyst. Thus the growing polymer layer –and therefore the mass-transfer resistance- increases its radius, as the polymerization goes on [19].
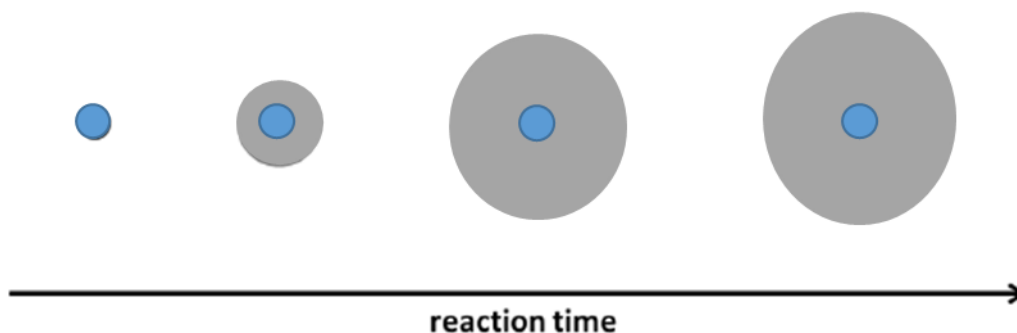
Figure 8: Core-Shell Model

Figure 8 shows the main concept of the core-shell model. Monomers must be transported through the polymer phase (growing grey color) and polymerize at the outer surface of the catalyst particle (fixed blue particle).

Beagley et. al. described a polypropylene polymerization using the core shell model [42]. Schmeal et al. also made some mathematically approaches to describe this model and use it for Ziegler-Natta polymerization [43]. Crabtree et. al. used this model to describe the activity and molecular weight in a slurry reaction of polyethylene [44].

The core-shell model predicts severe mass-transfer resistances for modern high-active catalyst systems.

The simplicity of this model makes it useful as a basis for further development of more elaborated models. Modern investigation reveal that highly active catalysts used nowadays fragment in early stages of the reaction [45].

2.2.2 Quasi-homogeneous particle models

Quasi-homogeneous particle models were proposed by Schmeal et. al. [46] [47] and Singh and Merill [48]. In quasi-homogenous model approaches, polymer and catalyst are treated as one single phase. There are two main versions of quasi-homogeneous particle models, the uniform site model and the polymeric flow model [49] [43].

In the uniform site model the sites are distributed evenly distributed in the polymer phase. In the polymeric flow model, catalyst is distributed within the polymer formed during polymerization, radial concentration gradients for the catalyst are the consequence. In both models, the polymer particle is treated as a compact particle without pores. With these assumptions the diffusion length would equal the particle radius.

reaction time
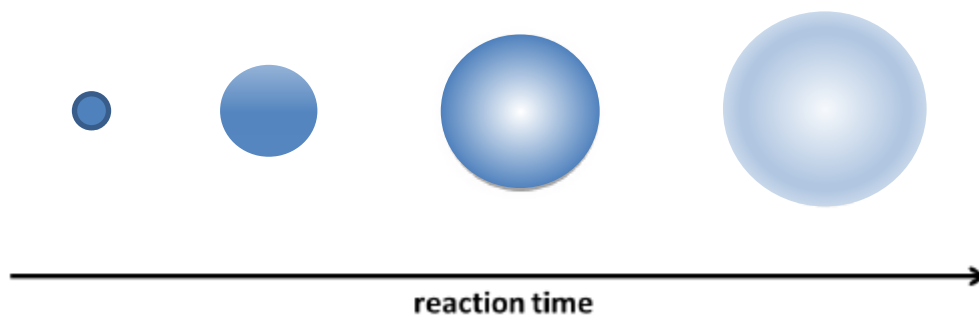
Figure 9: Quasi-homogeneous model

2.2.3 Multi Grain model

The multigrain model is a heterogeneous model treating catalyst and polymer as separate phases and considering particle porosity. It is assumed that in very early stage of polymerization the catalyst disintegrates into fragments, which polymerize according to a core-shell morphology and build together a porous macro particle. Yermakov et al. were the first to describe this model and use it to estimate concentration profiles in the polymer particle. This model is nowadays the most used to describe an olefin polymerization [50].

The multigrain model is based on the fact that polymer grows around catalyst grains. Each grain grows polymer independently of its neighbors and has a diameter of around 1 micron. Together they form part of larger agglomerate which defines the porous network of the catalyst [51] [52].

Nagel et al defined that every agglomerate or macroparticle consist of a large number of microparticles or micrograins, each having active sites in the center. The micrograins themselves consist of a catalyst fragment surrounded by a

polymer layer (core-shell morphology). Number and radius of the micrograins are adjustable parameters [53]. An assumption of this model is that catalyst fragmentation occurs immediately when the reaction begins.

Mass-transfer limitations are for the multigrain model much less severe compared to other particle models and mass-transport of monomer can also be explained for modern, high active catalysts. [54].

Mass transport is divided into two different mechanisms, pore diffusion and in some cases even convection in the macroparticle and film diffusion through the polymer layer of the micrograins. Film diffusion of the micrograins can be explained by Fick's diffusion [55]. The relevant length for film-diffusion is therefore the micrograin radius.

Hutchinson et al. studied heat and mass transfer with this model in detail [56]. Figure 10 shows a schematic representation of the multigrain model:
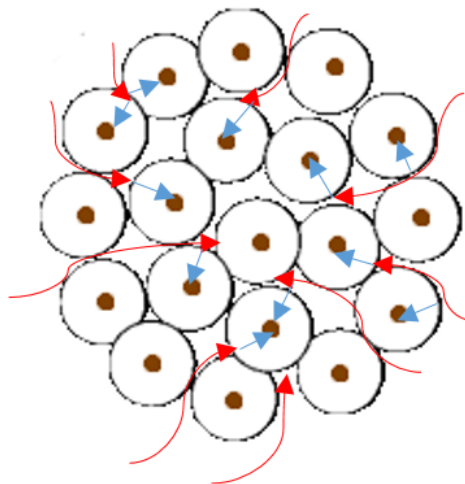
Figure 10: Multigrain Model (red line pore diffusion in the macroparticles - blue line film diffusion in the microparticles)

2.2.4 Catalyst fragmentation

The multigrain model assumes that the catalyst particle breaks up into fragments in the initial phases of the polymerization, which is in line with experimental observations [57] [58].

The common understanding for this catalyst fragmentation is, that polymer is first formed in the pores of the catalyst. The expanding polymer volume is then building up hydraulic pressure, which is relaxed by fragmentation of the catalyst support [59] [60].

While the multigrain model assumes that this fragmentation takes place in the initial stages of the polymerization, the model does not describe the fragmentation process itself.

A number of models has been developed to study the fragmentation process, e.g. by Fink [61], by Chiovetta [62] [63], later by Kitelssen [64] [7]and Mc Kenna [65] [66] [67] [68], and by the group of Kosek [69].

2.3   Rubber distribution in the heco-stage

During matrix polymerization, it is generally accepted, that particle morphology basically follows catalyst morphology [70], the so called "replication phenomena", a porous catalyst particle will lead to a porous matrix polymer particle.

During heco-stage, now an amorphous, elastomeric material is produced. Distribution of this EPR material can be described via different routes:
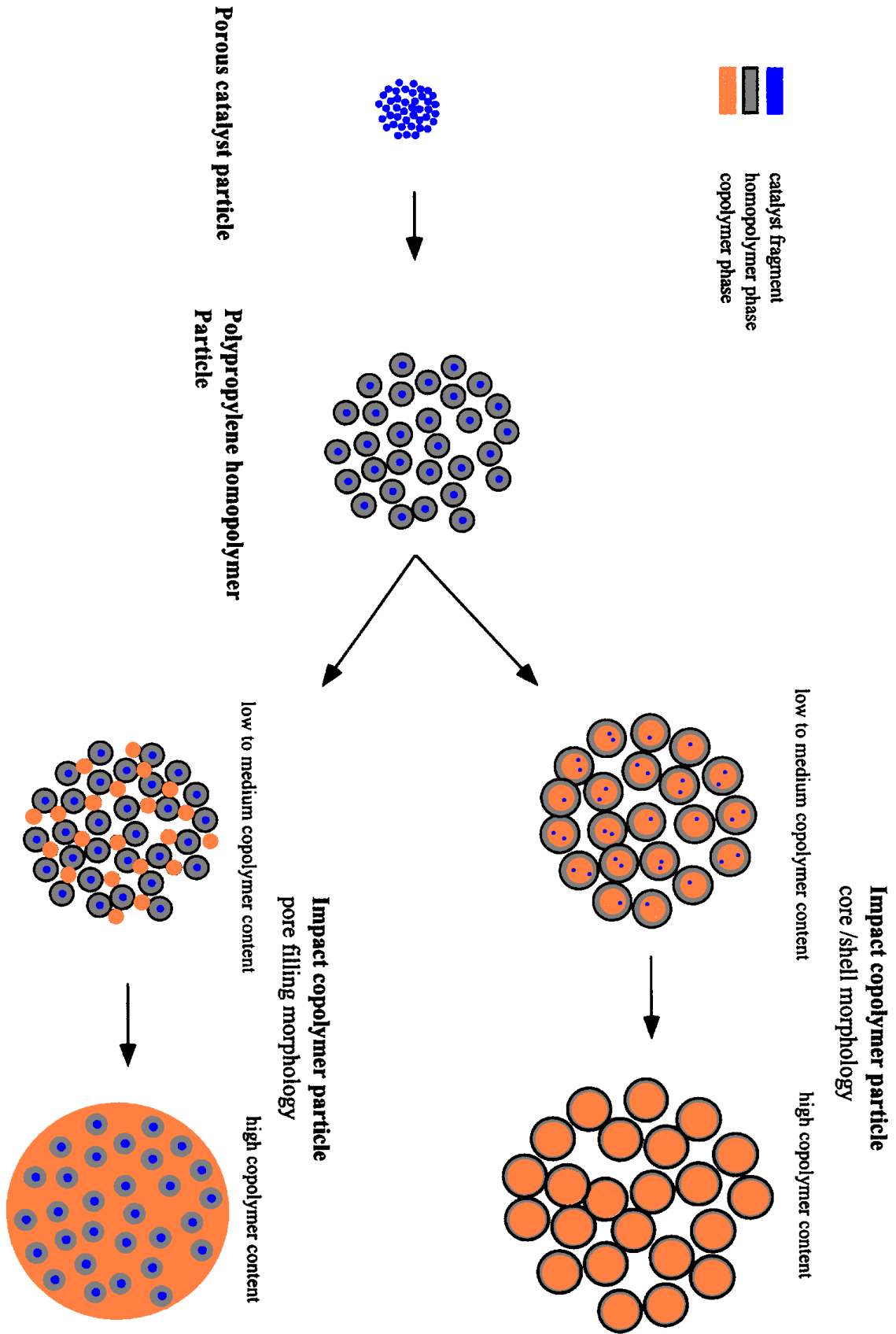
Figure 11: Morphology model of the impact propylene copolymers [71]

One way of dispersion of EPR is the so called ''core-shell'' micro-morphology. In this case the EPR is generated and retained within the micro-particles. However, transmission electron microscopy (TEM) of the sectioned and stained impact copolymer shows that the majority of the amorphous EPR actually migrates into the interstices of the homopolymer particle. Very little EPR remains inside of the micro-particles [71]. In case of a low to medium concentration EPR this will probably be found as a rubbery particle intimately dispersed within the pre-existing voids of the homopolymer matrix [72].

As the concentration of EPR increases, the copolymer phase becomes the continuous phase and the particle is acknowledged to be a free flowing elastomeric polymer. This type of dispersion builds a heterophasic structure and it is known as the 'pore filling' model [73]. The pore filling model of impact copolymer indicates that the porosity of the polymer granule will have a major change. By this model, high concentrations of EPR will be added. Therefore, the obtained copolymer particles possess little or no porosity. As the copolymer phase is added, the porosity of the granule will steadily decrease [74] [75].

The formation of rubber predominately on the surface of the particle will not only cause stickiness, lump formation, reactor fouling but also it will reduce the total copolymer content and its distribution [76]. Morphology of the original PP matrix is very important since the EPR tends to disperse in well-defined areas [18] [77].

2.4   Prepolymerization

One critical aspect of polymerization with modern, highly active polymerization catalyst is particle overheating, especially in the beginning of polymerization. Temperature increases of 30 K or more up to melting of the polymer are reported in literature [31]. These strong temperature increases can destroy the catalyst by thermal deactivation [78] and also influence particle morphology [22].

One well-known and industrially applied technique for preventing catalyst overheating and improving of particle morphology is prepolymerization [79] [80] [32] [81].

Prepolymerization means the start of the reaction in mild conditions. While starting the polymerization in mild conditions, i.e. at low temperature and/or lower monomer concentration, polymerization rate and therefore also heat production is reduced.

Prepolymerization is usually run only up to very low yields, thus its contribution to the final polymer product is in terms of product properties usually negligible. However, the influence on the polymerization process can be significant. By prepolymerizing in mild conditions up to polymerization degree of e.g. $5^3 = 125$, for high active catalysts this is less than 1% of the final productivity, the particle diameter is roughly increasing by a factor of 5 and the (external) particle surface is increasing by a factor of 25. Thus, prepolymer entering the main polymerization reactor has much more at transfer area available for heat removal compared to 'virgin' catalyst. Although heat transfer coefficients decrease with increasing particle size, the temperature difference between particle and surrounding bulk phase needed in order to remove the heat of reaction is significantly lower for prepolymer in comparison to virgin catalyst polymerizing at the same rate.

Due to the lower rate at the beginning of the polymerization, catalyst fragmentation occurs in a more controlled manner [33] and particle morphology can be improved [82] [83] [68].

In industrial scale production processes, prepolymerization is carried out as a separate continuous process step, e.g. in stirred tank reactors or loop reactors ("baby loop") [80].

In lab-scale batch or semi-batch polymerization experiments, prepolymerization is often carried in a non-isothermal procedure: catalyst is injected at low temperature and then the reactor is heated up to main polymerization temperature [84] [78] [85] [81], which typically takes in between 10 to 15 minutes.

One motivation for such a procedure are often safety aspects (reduction of injection pressure). Due to the non-isothermal procedure, the prepolymerization is somehow a bit undefined, e.g. the end of prepolymerization, the start of the main polymerization and degree of prepolymerization at the start of the main

polymerization are not really precisely known, kinetics during prepolymerization is continuously changing due to heating-up of the reactor.

In open literature, there is only little systematic work on the prepolymerization process as such available.

Pater and Weickert [85] studied prepolymerization of a supported Ziegler-Natta catalyst in propene bulk polymerization. Kinetics and the role of prepolymerization and hydrogen were investigated. In this studies, a calorimetric method was used. It was shown that prepolymerization step can increase the polymerization rate in the main polymerization stage. The prepolymerization prevents the particles from a thermal runaway during the main polymerization due to the enlargement of outer surface area at a relatively low polymerization rate.

2.5   Literature review on morphology development during production of high impact polypropylene.

Comparing studies from other polyolefins to HiPP, only limited number of studies on this impact copolymer morphology have been published. One of the first studies on the morphology of high impact polypropylene was done by Kaguko et al. [34] [86]. These authors studied morphology by examining the distribution of rubber sites using TEM and a staining technique. Three levels of morphology were proposed in these studies. Primary crystallites conformed a basis morphology, which will expand into mesostructures and these again by growing will compose macrostructures. 3

Debling and Ray [87] [88] also investigated morphology development of heterophasic copolymers. They found that the larger pores do not seem to fill up completely, and can be found on the surface even when the particles contain 70% rubber with respect to total particle weight. Surprisingly, they found decreasing bulk densities with increasing rubber content. This seems counter intuitive since the rubber is filling the pores in the particle, and unless there is some dramatic change in the external particle morphology, the loss of porosity should correspond to an increase in the bulk density.

Debling and Ray [18] [87] [88] agreed with Kaguko's representation of particle morphology. Their investigation introduced melded mesostructures (called lumps) which are built inside the particle as the rubber content increases. It was also noticed, that EPR tends to prefer or grow in defined areas of the original amorphous iPP. This selected–growing-effect is discussed in terms of decreasing of the viscosity of the EPR.

Cecchin et al. [89] analyzed also this theory and proposed that the representation where the EPR ruptures the PP layer is not correct. Rubber forms a continuous network even at low EPR contents. Therefore, the idea that the rubber forms below the surface of the PP, then ruptures it before flowing out, was questionable. They also claimed to see lamellae of PE surrounding the PP "sub-globules" in the particle (here sub-globule refers to an assembly of micro grains, much smaller than the macroparticle, but probably bigger than the individual crystals) in one set of experiments, and of polybutene in a second experiment where first PP, then PB was produced.

With these studies it was concluded that the reaction occurs around the proposed subglobules and that the active sites (in particular sites that are specific to ethylene and do not polymerise propylene) are "convected" to the upper layer of the subglobules. The authors base their arguments on the observation of the formation of crystalline lamellae at different moments during the polymerization.

A study from the Lyon group [24] using atomic force microscopy (AFM) to examine the repartitioning of the EPR inside particles showed that very little rubber actually seemed to flow out of the growing particles, but rather that when it was seen on the surface it actually formed there [90]. In the case of low to moderate rubber contents of (10-35% w/w), most of the reactions takes place on the actives sites located at the surface of the particle building an EPR layer and covering HiPP particles.

One of the biggest challenges during the production of HiPP is agglomeration of particles und subsequent overheating due to accumulation of sticky rubber on the surface. In order to prevent this, procedures are known [90] to deactivate existing active sites on the particles surfaces by addition of anti-static agents.

D. Yang et. al. focused their studies on the relationship between the morphology of the initial iPP powder, and the final properties of the impact copolymer [91] [92]. In their studies morphology of polypropylene is investigated as a result of macromolecular architecture. Except for a compositional analysis of the final powders, the impact of process conditions is not discussed [93] [94].

From the point of view of mass transfer many studies explain the importance of diffusion through polymer and also the diffusion through the pores. Both diffusion can have an impact on the reaction rate thus on the final properties of the gained powder. The polymerization reaction implies a growth of the particle and therefore a simultaneous changing of the particle morphology during the different phases. It is to be expected that this will also impact how mass transfer occurs. For instance, Kittilsen et al. showed that at high rubber loadings, the rate of polymerisation was lower than for similar particles at lower rubber contents [7].

Tong et al. [95] investigated mass transfer resistance and resistance during the polymerization. The major resistances were in the micropores of the isotactic PP matrix. They reported low rubber concentration at the surface of a HiPP particle for low rubber loadings. Also at higher rubber loading very small amount of EPR was found inside of the pores. These founding was a step to analyse closer the impact of the morphology of iPP and how mass transfer can impact the structure of the particles.

Mc Kenna et. al [24] studied rubber distribution in HIPP particles. They found difference in the composition of rubber throughout the particles and attributed these to difference in the chemistry of the active sites across the particle and to mass transfer resistances.

Kosek et. al. have published some works on modelling of the degassing in the final PP powders. These investigations were based on experimental tomography investigations and model-based reconstruction of the particles by statistical morphology-descriptors [96] [97].

Kröner et. al. analysed in [98] the balance of mass-transfer and reaction in HiPP. Mass-transfer in HiPP particles was experimentally studied by sorption measurements and both diffusion coefficients and relevant sorption lengths were determined. It was clearly shown that the effective length-scale for

diffusion is between the particle radius and the classical "micrograin" radius of the multigrain-model. For the selected catalyst and a fixed homopolymerization step, a correlation for effective length-scale of diffusion in relation to yield was derived. Reaction-diffusion simulations with the derived mass-transfer model revealed significant mass-transfer limitations for ethylene during the heco stage.

2.6 Sorption of gases in polymers

A sorption process is the solubilization of penetrants into the polymer phase [99]. Studies in this process are done to determine equilibrium concentrations and to estimate of mass transport parameters.

The sorption of gases has been studied in great detail for a large number of natural and synthetic rubbers, semi-crystalline polymers, and polymeric composites with a wide variety of organic and inorganic penetrants [100] [101].

A key concept underlying the quantification of the sorption of gases is the free volume of the polymer phase. Typically, sorption characteristics are strongly dependent on the nature of the polymer and penetrant, and on the physical state of the polymer. Significant amount of gas can be absorbed in amorphous materials because of their relatively large free volume [100] [101] [102].

The solubility and diffusion coefficients have been proven not so trivial to determine, since both transport parameters vary widely depending on the nature of polymer and penetrant, and more profoundly with a great number of physical properties and constants. These parameters and properties are: The Lennard-Jones force constant, molecular size, molecular weight, sorption temperature, monomer concentration, crystalline fraction, glass and melting temperature, fraction free volume, tacticity, stereoregularity, average molecular weight and functional groups of the polymer [100] [101].

To describe sorption into polymers, a large number of models of varying degrees of sophistication have been put forward [102] [103] [10]. Gas sorption into polymers is often commonly expressed in terms of the solubility of a gas in a polymer matrix, following an either Henry's law or Flory-Huggins theory and

Langmuir adsorption of gas in microscopic voids. More fundamental approaches, in which gas sorption has been related to physical properties of a polymer matrix, have also been developed. However, those approaches remain semi-quantitative and lack, in particular and unequivocal explanation of the nature of the distribution of a penetrant in a matrix [102]. On the following chapter some sorption models will be explained.

2.6.1 Henry's Law

The sorption of gases into a polymer can be treated as a classical thermodynamic sorption of a gas into a liquid for a single component [104].

$$\varphi_i \cdot p_i = x_i \cdot \gamma_i \cdot H_i \tag{1}$$

Assuming a case if ideal gas behavior and liquid phase (φ, γ=1):

$$p_i = x_i \cdot H_i \tag{2}$$

The mole fraction of the penetrant can be substituted by the molar concentration [55] [105]:

$$c_i = p_i \cdot H_i^* \left[\frac{mol}{l_{amorphous}}\right] \tag{3}$$

This equation describes the simplest behavior that can be observed in a sorption isotherm. Such sorption isotherms are observed for light gases such as hydrogen and inert gases in rubbery polymers [106] [107].

In the case of semi-crystalline polymers the solubility coefficients have been determined for a great amount of penetrants ranging from inert gases up to higher hydrocarbons [106]. One of these researches was done by Stern. In his research for semi-crystalline polymer it was found that both critical temperature

of the penetrant and sorption temperature influence the Henry's solubility parameter H* [106]. His empirical equation for calculation of Henry coefficient for different penetrants is shown at equation (4):

$$log(H^*) = -2,38 + 1,08 \left(\frac{T_c}{T}\right)^2 \qquad (4)$$

Ever since the success of Henry's Law to determine experimental solubilities, this thermodynamic model has been used indiscriminately, and deviations started to arise. Stern et al. studied these deviations and proposed the following equation [106]:

$$log\left(\frac{p_{dev}}{p_c}\right) = A_1 + B_1 \left(\frac{T_c}{T}\right) \qquad (5)$$

Where, p_{dev}, is the pressure at a 5% deviation from the Henry's Law solubility. This deviation occurs due to the plasticizing effect of the penetrant. The adjustable parameters A_1 and B_1 were found to be 3.025 and 3.50 respectively.

According to Hutchinson et al. equation (5) is useful to determine where more complex thermodynamic models must be used to predict sorption [107].

2.6.2 Flory-Huggins Theory

The Flory Huggins theory has been specially developed to describe the solubility of low molecular weight monomers into a polymer. As the complexity of the gases (CO_2 and higher hydrocarbons and vapors) as well as the temperature rises, strong deviation from Henry's law and consequently non-linear sorption isotherms are observed. The polymer phase is considered as a lattice. Each of these lattices is statistically occupied by whether segments of the polymer chain or by the dissolved low molecular component [100] [107]. Historically the Flory-Huggins equation is defined as [108] [109]:

$$ln(a) = \ln\left(\frac{p}{p_{sat}}\right) = \ln(\phi) + (1-\phi) - \frac{1-\phi}{r_s} + \chi(1-\phi)^2$$

(6)

Where:

$a =$ The penetrant activity in the gas phase contiguous to the polymer

$p/p_{sat} =$ The pressure and saturation vapor pressures of the gas

$\phi =$ The volume fraction of penetrant solved in the polymer

$r_s =$ Total number of segments per chain

$\chi =$ The *Flory Huggins* interaction parameter.

The segment number for the case of polymers is around 10000 thus the expression $\frac{1-\phi}{r_s}$ is almost negligible. The left side of equation (6) ($a=p/psat$) describes an assumption that only is valid for ideal gases. Small polymer gas interactions are given for the case $\chi>2$. In the other hand $\chi \leq 0.5$ indicates strong interactions between non-cross-linked polymer and monomer [100].

At the beginning the Flory Huggins model was supposed to be independent from the temperature. Over the year it was found that the interaction parameter χ was

an empirical parameter that depends on temperature and penetrant concentration. Frequently, the Sanchez-Lacombe equation is used to explain the interaction parameter in an empirical form [100].

$$\chi = \frac{A_2}{T} - B_2 [-]$$

(7)

From experiments, it has been found that this interaction parameter is not constant. Meier et al. considered that the Interaction parameter is the same for liquid and gas [45]. Later it was found that the Flory's Interaction parameter is not only dependent with temperature but also pressure can influence the value of χ. This parameter increases exponentially with pressure, and can be expressed as [110]:

$$\chi = \frac{A_3}{p_{sat}} e^{B_3 * p} [-]$$

(8)

2.6.3 Other gas solubilities models

2.6.3.1 Semi empirical model for polyolefins.

As the concentration of the adsorbed monomer rises, neither Henry's law nor Flory Huggins model are valid. Concentration dependence was studied by Hutchinson, et. al. Experimental sorption in polyolefins revealed that the solubility parameters can be expressed as [107].

$$C = S_c \cdot P \cdot e^{\sigma \cdot C} [mol / l_{amorphous}]$$

(9)

Where C is the concentration of the penetrant dissolved in the polymer at the pressure P, S_c is a limiting value of penetrant solubility into the polymer. σ is constant characterizing the concentration dependence of solubility. This model implies that when c → 0 , Henry's Law is obeyed.

2.6.3.2 Dual sorption model

Another model, which combines the temperature and pressure dependence of the sorption isotherms for glassy polymers, is the dual sorption model. In this model parameters such as pressure, temperature, sorption capacity, and concentration are considered [100] [111]:

$$C = H^* \cdot p + C'_H \frac{b \cdot p}{1 + b \cdot p} \ [mol/l_{amorphous}] \tag{10}$$

With:

H* = Henry's law parameter characterizing concentration and temperature of the sorbed monomer.

C_H' = Langmuir sorption capacity, which characterize sorption into the non-equilibrium excess volume associated with the glassy state.

b = adjustable pressure affinity parameter.

2.7 Mass Transport during the sorption

Mass transfer in olefin polymerization is complex and occurs via various mechanisms such as:

- Convection – transport by pressure gradient in the reactor
- Pore diffusion in the pores of the polymer particle
- Diffusion though the polymer matrix to the active sites of the catalyst.

In this work we focus on the mass transfer on the particle level, where diffusion through the polymer matrix and pore diffusion in the pores of the particle are dominant. Since diffusion coefficient in pore diffusion are typically a magnitude larger compared to diffusion in the polymer phase, diffusion through the polymer is the limiting case discussed here.

2.7.1 Fick's diffusion

In the mid of 19th century Fick proposed his laws of mass diffusion which are analogous to with Fourier's law of heat conduction [112] :

$$J = -D\nabla C \tag{11}$$

For a spherical particle the material balance results in the well-known transient diffusion equation for a sphere:

$$\frac{\partial c_m}{\partial t} = \frac{D}{r^2}\frac{\partial}{\partial r}\left(r^2\frac{\partial c_m}{\partial r}\right) \tag{12}$$

with the boundary conditions $\left.\frac{\partial c_m}{\partial r}\right|_{r=0}$ and $c_m\left(r = r_{particle}\right) = c_{gas\ phase}$.

Eq. (12) describes only mass-transfer, for a particle with reaction, a reaction term has to be added. Crank derived in [55] analytical solutions for various diffusion problems. The solution of equation (12) results for the amount of sorbed mass in a spherical morphology to:

$$\frac{m(t)}{m_{eq}} = 1 - \frac{6}{\pi^2} \sum_{n=1}^{\infty} \frac{1}{n^2} e^{\frac{-D \cdot n^2 \cdot \pi^2 \cdot t}{r^2}} \ [g\ /g] \tag{13}$$

R is the particle diameter and D is the diffusion coefficient.

For a flat morphology in a film an analogy the following analytical solution is obtained:

$$\frac{m(t)}{m_{eq}} = 1 - \sum_{n=0}^{\infty} \frac{8 \cdot e^{\frac{-D \cdot (2n+1)^2 \cdot \pi^2 \cdot t}{4 \cdot l^2}}}{(2n + 1)^2 \cdot \pi^2} \ [g\ /g] \tag{14}$$

2.7.2 Diffusion coefficient

In general terms, diffusion coefficients describe the dynamics or mobility of a penetrant into a polymer [55]. As previously mentioned for solubility, diffusion coefficients are highly related to the very nature of the penetrant and polymer physical and thermodynamic properties and parameters. This means that correlations between properties and diffusion can be made [100].

2.7.2.1　Effect of polymer properties

In order to explain the effect of the polymer on the diffusion coefficients, the concept of "free volume" coming from polymer physics theory must be introduced. Free volume theory is widely used and accepted to explain the diffusion of a sorbed gas into a polymer. The fundamental principle is that diffusion is viewed as a series of activated jumps from one theoretical cavity within the polymer matrix to another. In principle, any modification to the process or condition that might increases the number or size of cavities on a polymer or changes the mobility of polymer chains increases the rate of diffusion. Nevertheless, properties such as crystallinity decrease the size or number of vacancies or immobilize chain segments, thus crystallinity decreases the diffusion rate [100] [113].

Polymer with a small T_g for instance those that have a higher molecular chain possess properties to filter or separate elements since these have more free-volume. Through this volume, the elements have more space to accommodate diffusion steps of both large and small molecular penetrants [100] [113].

Glassy polymers have normally less free volume, are rigid and have restricted chain motions. These properties allow small free-volumes elements to diffuse easier than larger elements since the free volume is not large enough to allow diffusion of larger gas molecules. Depending on the element size and the availability of free volume inside of the polymer, the sieving properties will be suited [100] [113].

2.7.2.2　Effect of pressure and concentration

Pressure can have a significant effect on the diffusion coefficient, since the concentration of penetrants raises,

Increasing the pressure or the concentration of the penetrant will induce a raise of the free volume. Due to the higher amount of penetrants, the chain mobility of the polymer will expand and therefore the diffusion coefficient typically

increases with increasing pressure. However, also opposite behavior has been reported. Due to agglomeration of penetrants, which might inhibit the sorption of penetrants with smaller diameter [100] [113].

2.7.2.3 Effect of temperature

Movement of gas molecules is through a polymer is a thermally activated process, thus diffusion can also be expressed as an Arrhenius-type property [114]:

$$D = D_{o,T} \cdot e^{\left(-\frac{E_D}{R \cdot T}\right)} [m^2/s] \tag{15}$$

E_D, equals the activation energy of diffusion, which can be mathematically expressed as the energy of permeation E_p minus the enthalpy of sorption ΔH_s (Equation (16)). The pre-exponential factor $D_{o,T}$ is only believed to be a compensation factor [114].

$$E_D = E_p - \Delta H_s \ [J/mol \cdot K] \tag{16}$$

2.8 Effectiveness factor

One way to quantify the balance between mass transfer and reaction is the calculation of an effectiveness factor. This factor is defined as the average monomer concentration present during reaction, related to the equilibrium concentration.

For a spherical micrograin cluster, the effectiveness factor can be calculated according to:

$$\eta_{eff} = \frac{\int_0^1 c_M(r_n) \cdot 4\pi r_{cluster}^3 r_n^2 dr_n}{c_{M,eq} \cdot V_{cluster}} = \frac{3 \int_0^1 c_M(r_n) \cdot r_n^2 dr_n}{c_{M,eq}} \qquad (17)$$

If the mass-transfer rates are high compared to the reaction rates, the concentration gradients will be flat, the concentrations within the cluster will approach equilibrium concentration and the effectiveness factor will approach towards one.

If the mass-transfer rates are low compared to the reaction rates, the concentration gradients will be steep, there will be little monomer inside the cluster and the effectiveness factor will approach zero.

In previous studies [98] Kröner has reported for the effectiveness factor for propylene in homopolymerization values in between 0,8 and 1,0, so only minor mass-transfer restrictions for propylene. In the same study, effectiveness factors for ethylene during the rubber polymerization step were calculated to be in between 0,3 and 0,4 which means significant mass-transfer restrictions for ethylene.

3 Aim of investigation and scientific approach

This work has been part of a larger project called "High Impact Polypropylene – Structure Evolution and Impact on Reaction" funded by the Dutch Polymer Institute (DPI).

High impact Polypropylene is a high volume product, but there are still some open questions like the control of rubber distribution and particle morphology or the impact of rubber distribution on reaction. Only little systematic experimental data on factors influencing rubber distribution are available in literature.

Focus of this work is an extensive experimental study on how to control and modify particle morphology during the multistage-stage production process of heterophasic polypropylene materials. Furthermore, the impact of adopted particle morphology on the behaviour in the polymerization process in terms of process kinetics and mass-transfer shall be studied. The obtained data shall be used to improve rubber incorporation while reducing operational difficulties such like agglomeration and fouling. Existing particle models shall be tested and improved.

The experimental study has been carried out with two supported, industrial Ziegler-Natta catalysts supplied by cooperation partners of the DPI.

With these two catalyst, initially a broad screening on of the effect of homopolymerization and prepolymerization conditions on particle morphology and process kinetics shall be carried out. The screening study shall be carried out for both bulk-phase and gas-phase polymerization, which are used both for commercial production if HiPP. The parameters influencing particle morphology while keeping a reasonable activity level shall be identified.

For these main parameters on particle morphology, in a second step a more detailed study shall follow. In particular, the effect of particle morphology on the subsequent process steps shall be studied:

➢ The effect of adopted particle morphology on activity in matrix stage (both gas-phase and bulk polymerization) and particle morphology after matrix stage.

➢ The effect of adopted particle morphology on rubber production (both activity and comonomer incorporation) during heco-stage, carried out as gas-phase polymerizations. Development of particle morphology during heco-stage.

The obtained powders shall be characterized in terms of morphology by methods such like measurement of bulk-density, measurement of porosity and electron microscopy. Furthermore, mass-transfer in the obtained powders shall be studied via sorption measurements and the relevant length scale for diffusion shall be identified.

Finally, the obtained data shall be used and analysed in existing particle models.

4 Experimental polymerization setups and procedures

In this study, a number of different lab-scale polymerization reactors has been used:

- A 5-liter horizontal stirred bed reactor has been used for gas phase polymerizations.
- A 1.9 l vertical stirred tank reactor has been used for bulk phase polymerization of propene
- A 250 ml reaction calorimeter has been used for external prepolymerization reactions in bulk phase

The experimental setups are introduced in the following:

4.1 5-liter gas phase reactor setup

For gas-phase polymerization, an existing 5-liter horizontal stirred tank reactor already known from earlier investigations [115] has been used, (see Figure 12). The reactor is pressure rated up to 40 bars and temperature rated up to 100°C. The horizontal anchor-type stirrer inside the reactor is bound to a gear motor with a magnetic coupling (Büchi) with maximal 800 rotations per minute.

The reactor is equipped with a jacket for adjusting temperatures. Thermostating oil (type Therminol ADX) is circulating through the jacket to a powerful thermostat (type Lauda Proline RP855C with a heating capacity of 3.5KW and a cooling capacity of 1.6 KW). For temperature control, the cascaded loop controller of the thermostat is used.

The reactor is equipped with a number of pipe connections for addition of catalyst and reaction partners. Monomers are fed from the separate purification section (see chapter 4.4) via thermal flow controllers to the reactor. Propene is fed in liquid state; hence the heat of evaporation can be used to increase the cooling capacity of the reactor. Ethylene and hydrogen are fed as gases via flow controllers. The reactor can be inertized with nitrogen and vacuum.

The pressure is measured and the value will be transferred via voltage signal to a proportional-integral-derivative controller (PID). The PID controller compares the set point with the actual reactor value and sends a voltage signal to a control box (Brooks instruments), which regulates the single mass flow of the monomers.

A pressure control-loop regulates the propylene feed. Other monomer can be fed in a fixed ratio to propylene feed. In the case of copolymerization, the feed ratios of ethylene/propylene can be varied depending on the aimed reactor concentration or ethylene incorporation.

The reactor pressure is measured by a pressure gauge (type WIKA IUT-10, pressure range = 0-40 bar, error = 0.15%), temperature in the reactor and the jacked are measured by PT100 thermometers. The reactor is connected to a µ-GC, which enables to monitor and control gas-phase composition. Both gas concentrations of propylene and ethylene are especially important to control the copolymerization stage.

A schematic draft of the setup can be seen in Figure 13.
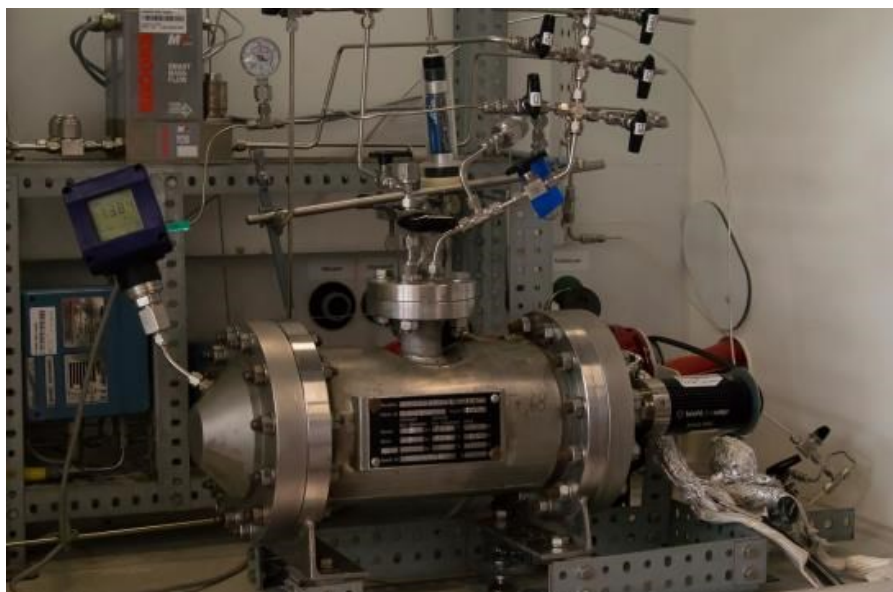
Figure 12: 5 liter gas phase reactor

The reactor is run in semi-batch mode; the monomer flow is controlled by a control loop keeping the reactor pressure constant. In isobaric and isothermal conditions, this flow of monomer resembles the consumption by reaction and is hence an easy experimental access to the gross reaction rate.
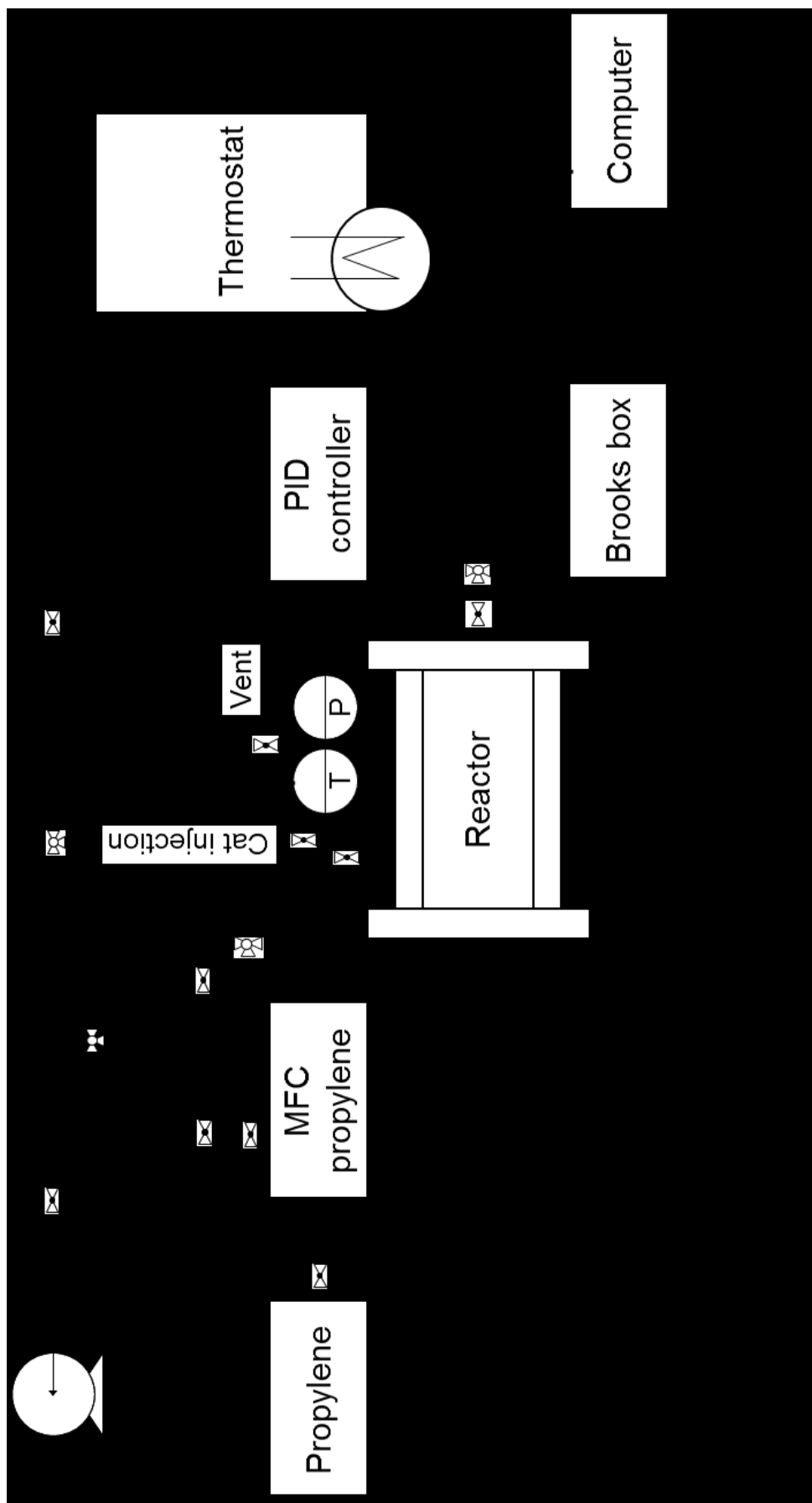
Figure 13: System flow of the 5-liter gas phase reactor

Up to 700 g of polymer can be produced in the reactor per run.

The reactor is connected to a µ-GC for analysis of the gas composition. This enables to monitor and control the propylene / ethylene ratio during copolymerization.

The µ-GC (Varian CP 4900) is equipped with three separation columns. The first column is flushed with argon and it is used for separation and measuring of small molecules such as hydrogen, oxygen and nitrogen. The second and third columns are run with hydrogen as inert media. With these columns monomers, up to six carbon atoms can be detected. Figure 14 shows the calibration of the µ-GC in form of a parity diagram.
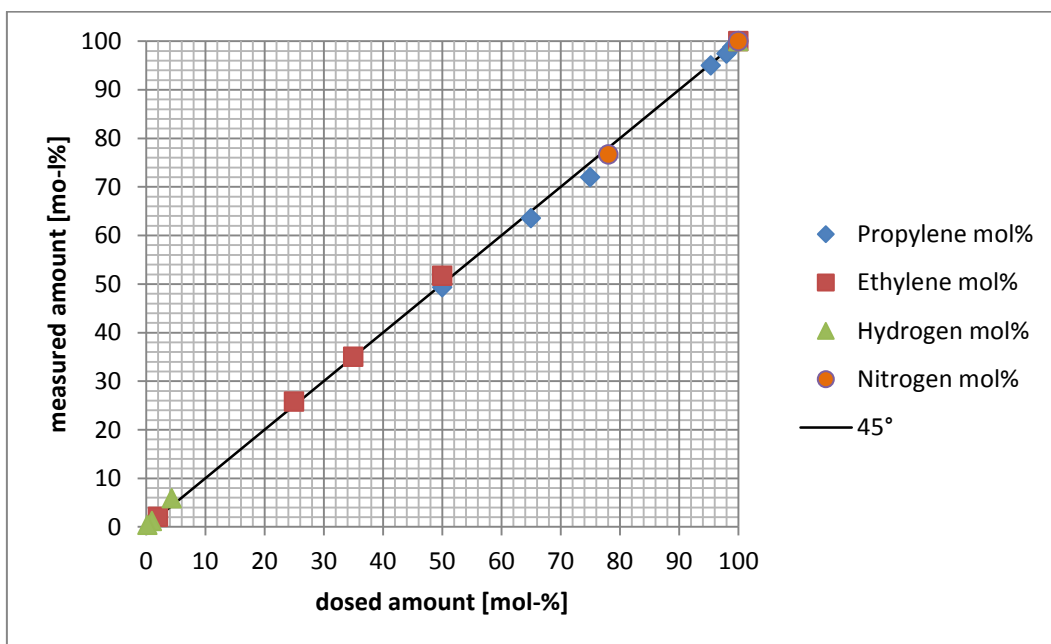
Figure 14: µ-GC Calibration

4.2 The 1,9-liter bulk reactor

For bulk-phase matrix polymerizations an existing 1.9 l vertical stirred tank reactor has been used. This 1,9-liter reactor is pressure rated up to 100 bars and is operated batch-wise. Reaction temperature is controlled by a specific, custom-made, highly dynamic temperature control system. A photo of the reactor is shown at Figure 15 and Figure 16 displays the temperature control system.
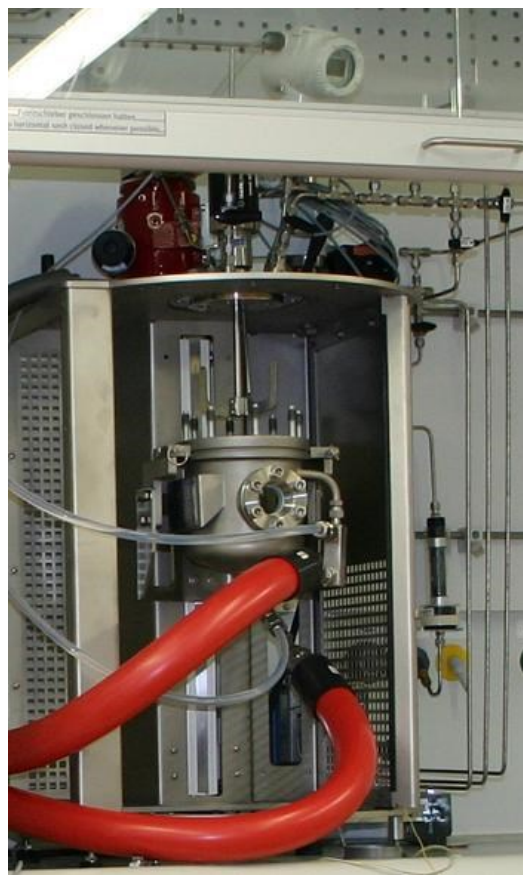
Figure 15: 1,9 liter bulk reactor
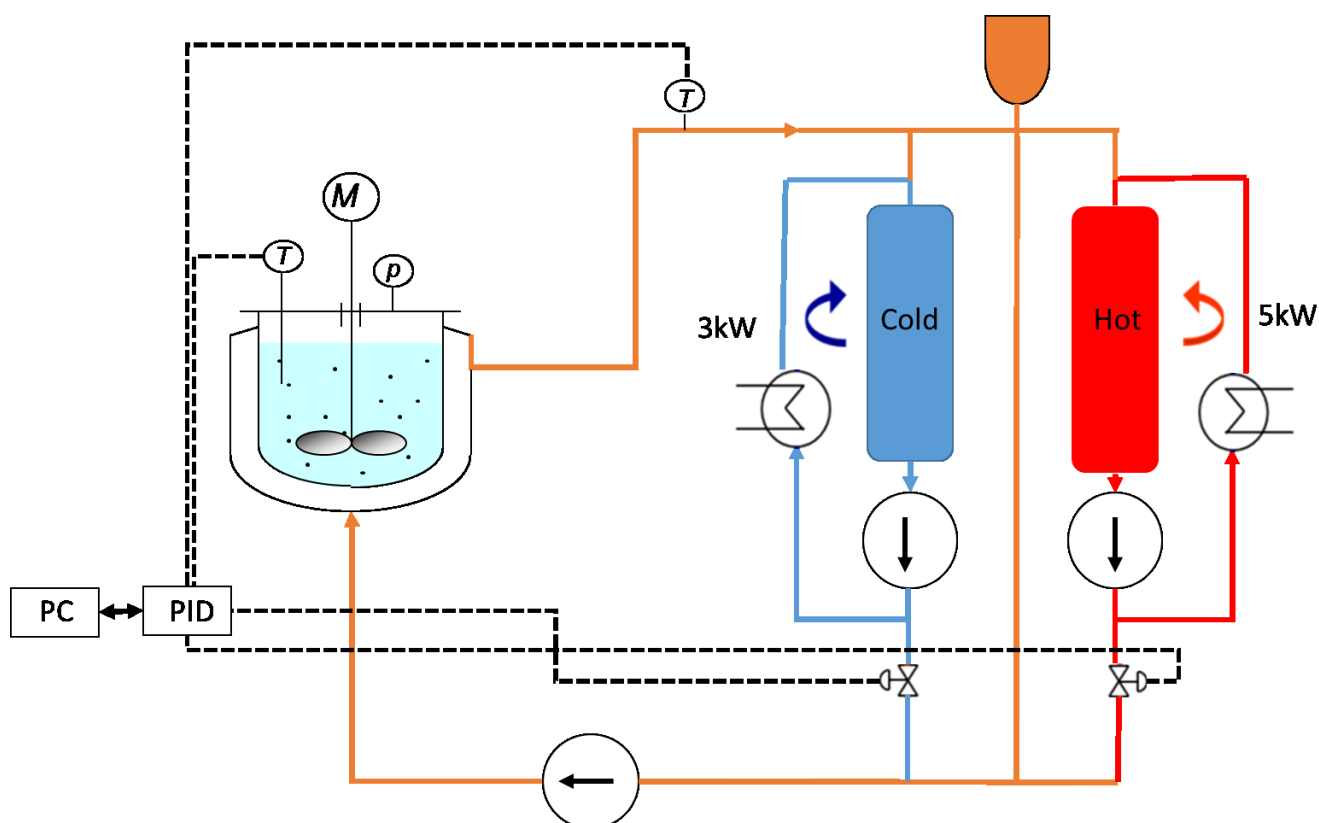
Figure 16: Temperature control system 19-liter reactor (blue line = cold oil, red line = hot oil)

In this reactor bulk polymerizations are carried out in batch-mode, there is no online measurement for rate, the only kinetic information is the obtained yield of the reaction.

4.3 The 0,25-liter heat flow reaction calorimeter

The external prepolymerizations in this work were carried out in experimental setup based on in a commercial 0,25-liter reaction calorimeter (Chemisens, type CPA 202). The existing setup has already been used for external prepolymerization with supported metallocene catalysts, details can be found in former works from AG Bartke.

The reactor is pressure rated up to 100 bars. The complete reactor is submerged in a thermostate bath operating with water, hence the temperature is currently limited to 100°C. The temperature of the bath is set to reaction temperature and thus limits heat losses of the reactor (active insulation).

For this reactor heat is only exchanged via the reactor bottom induced by a Peltier-element, which acts as a "heat pump". The heat flow through reactor bottom is measured via a heat conductivity transducer and is independent of heat transfer conditions, which is a great advantage for polyreactions compared to other calorimeters.

The dynamic energy balance for the calorimeter equals:

$$\dot{Q}_{chem} = \dot{Q}_{heatflow} - P + m * c_p \frac{dT_R}{dt} \qquad (18)$$

The stirring power P can be measured separately via a torque transducer. The chemical heat flow is proportional to the polymerization rate:

$$\dot{Q}_{chem} = rate * (-\Delta H_R) \qquad (19)$$

By rearranging equation (19), (20) and knowing the stirring power P, in isothermal conditions the rate can be calculated according to:

$$rate_{polymerization} \approx \frac{\dot{Q}_{heatflow} - P}{-\Delta H_R} \qquad (20)$$

Integration rate, the yield resp. the degree of prepolymerisation can also be calculated.

Another advantage of the 0,25-liter reactor is that this reactor can be introduced into glove-box for recovery of prepolymerized catalyst under inert conditions.

Figure 17, Figure 18 and Figure 19 show the set-up, the reactor and a schematic representation of the reactor the heat-flow principle:

Figure 17: 0,25-liter reactor set-up
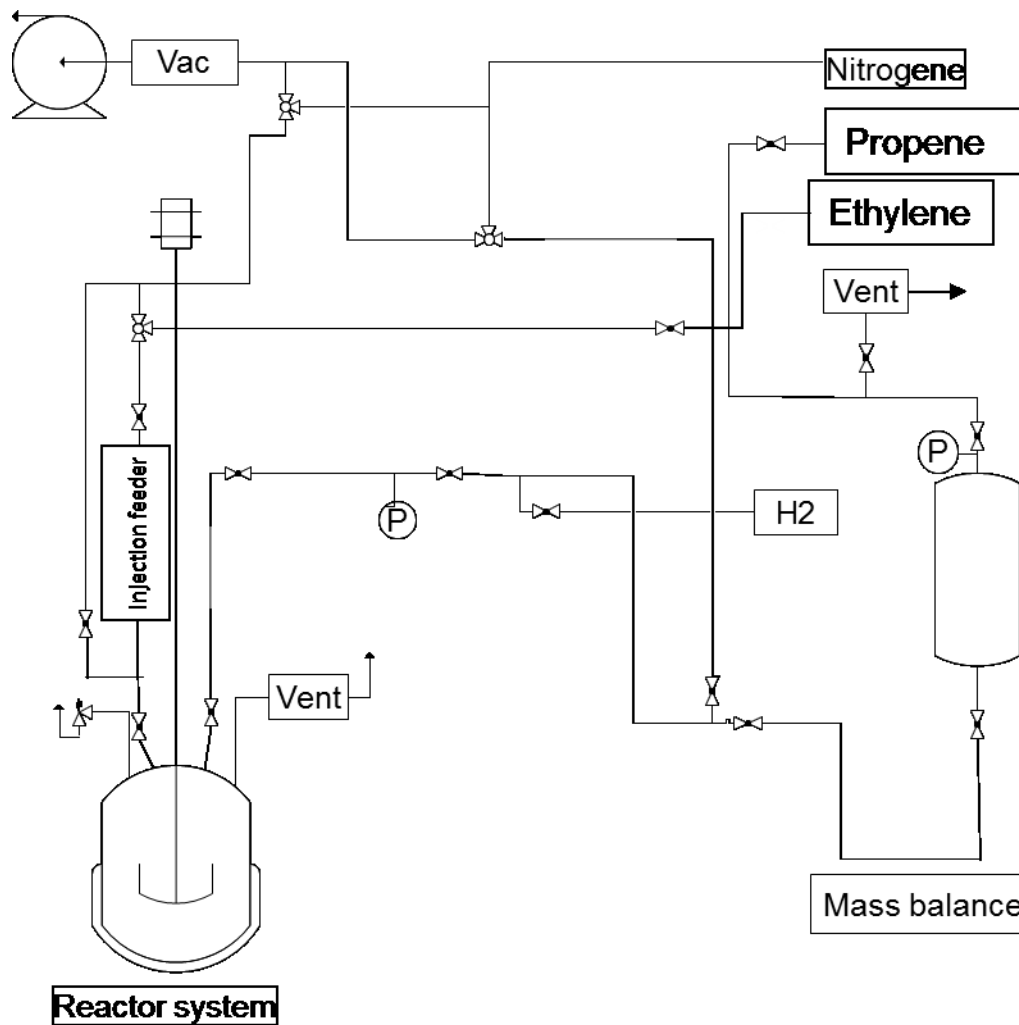
Figure 18: System flow 0,25-liter reactor
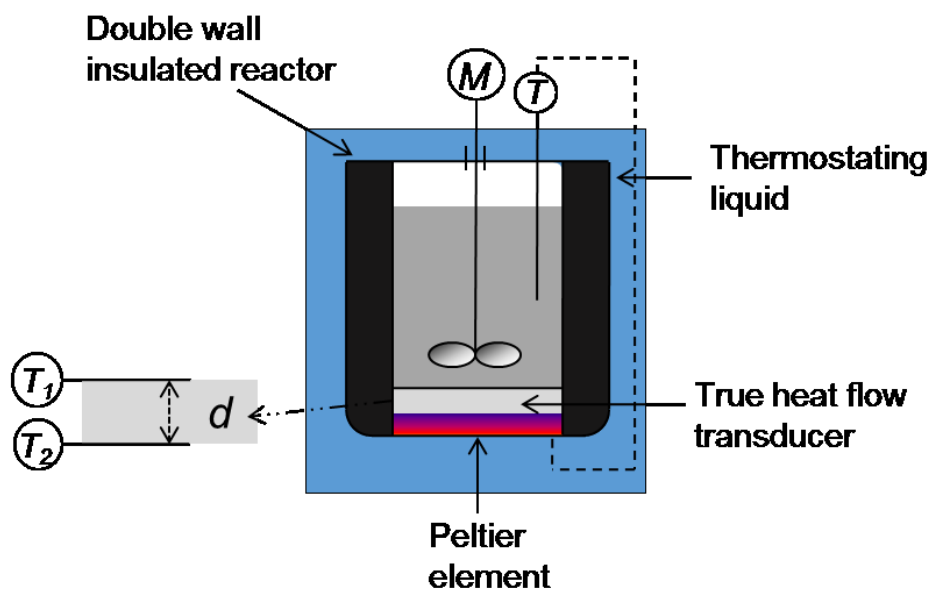
Figure 19: Principle heat-flow calorimeter

4.4 Chemicals and purification and of raw materials

4.4.1 Propylene, ethylene, hydrogen and nitrogen

Liquid propylene and ethylene with a minimum purity of 99.5 % were purchased in gas bottles from Airliquide.

Polyolefin catalysts are very sensitive to impurities such as oxygen, water, CO, CO_2 and sulfur compounds. In order to remove even traces of such impurities, a six stage purification system is installed for both ethylene and propylene. A schematic representation of the purification system and the set-up can be found in Figure 20 and Figure 21:

Figure 20 : Purification set-up
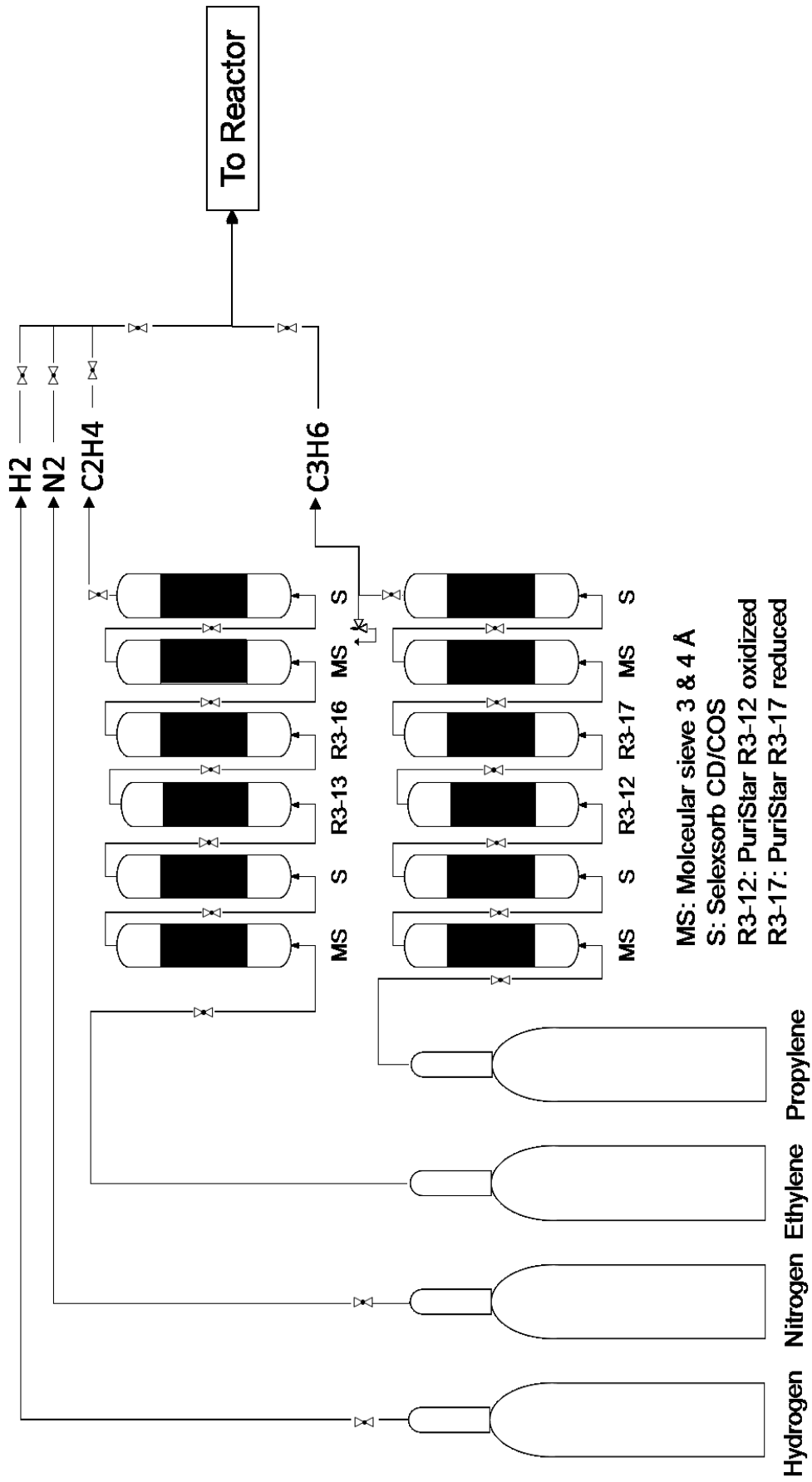
Figure 21: Purification system

The first and fifth column are filled with molecular sieves, which remove molecules below 3 and 4 Å. Main task of the sieve is to remove water traces. Selexsorb COS/CDX is filled in the second and sixth column. Selexsorb removes wide range of polar organic compounds. Afterwards BASF Puristar R3-12 on the third column removes substances such as arsine, phosphine and reactive sulfur. The fourth column contains BASF Puristar R3-17 for propylene and R3-16 for ethylene, which is used to remove traces of CO.

Propylene is recirculated through the purification system to increase the residence time and the contact times between monomer and catalyst. For ethylene no recycle line was needed.

All columns were regenerated if a decline in activity was detected, typically latest after two years.

Hydrogen was used as chain transfer agent in order to control molecular weight and was purchased quality 6.0 (Linde) and used without any further purification.

Nitrogen (house supply) was used as inert gas for reactor inertization and reactor cleaning. An Oxisorb cartridge from Airliquide was installed in the nitrogen pipelines for purification and removal of oxygen.

All gases were stored in gas bottles.

4.4.1 Catalysts, cocatalyst and donor

In this work, polymerization reactions were performed using two 4th generation industrial supported Ziegler-Natta catalysts. Catalyst A and catalyst B were provided from two different polyolefin industries.

External donors were used in this work to ensure high stereo regularity without reducing activity of the catalyst [116]. Diisopropyl-dimethoxy silane (DIPDMS, >90%, Merck) was used together with catalyst A and Dicyclopentyl (dimethoxy) silane (DCP, >98 %, TCI) was used for catalyst B.

Triethylaluminium from Sigma Aldrich with a purity of 93% was used with both catalysts as a cocatalyst.

In order to check the condition of the supplied catalysts and also to ensure our polymerization reactor and procedures, the catalyst suppliers were asked for reference activities of the supplied catalysts.

Reference activity for catalyst A in gas-phase polymerization conditions at 70°C, 20 bar and 1 mol-% hydrogen was indicated to be around 20 $Kg_{pp}/(g_{cat}*h)$.

For catalyst B in bulk-phase polymerization at 80°C, 39 bar pressure and 3 mol-% hydrogen, a reference activity of approx. 45 $Kg_{pp}/(g_{cat}*h)$ was indicated.

4.5 Experimental procedures

4.5.1 Preparation

Due to sensitivity of the used catalysts to oxygen, moisture and other polar components, all reactor setups used have to be cleaned thoroughly prior to used.

All reactor steps were cleaned for at least four hours before starting the reaction. For efficient removal of moisture residues, the reactor setups were heated up to 105 °C (5-liter gas-phase reactor and 1.9-liter bulk reactor) resp. 75°C (250 ml calorimeter) and inertized via multiple flushing with nitrogen followed by discharge and applying vacuum. Minimum five cycles of nitrogen flushing and applying vacuum have been carried out.

Handling of the sensitive catalysts has been done in a Glove Box (Jacomex, France) under inert conditions. For catalyst injection, stainless-steel catalyst feeders (Figure 22) made of Swagelok® piping parts have been used.

Figure 22: Injection feeder

Each stainless steel feeder consists of two chambers. After inertization these feeders have been introduced inside the glove box for loading. In one chamber, around 6 to 14 mg of supported catalyst have been loaded. In the other chamber, co-catalyst and donor have been loaded in a fixed ratio to the catalyst amount. For better distribution, in each chamber, 1ml Primol 352 have been added. The amount of oil is kept constant for all reactions.

4.5.2 Gas-phase polymerization with in-situ prepolymerization

Liquid propylene is used as an injection medium. The reactors will cool down through evaporation heat. Depending on the catalyst activity, the amount of catalyst and setting during the prepolymerization a pressure drop can be measured. The prepolymerization is run for 10 minutes. Typical prepolymerization degrees were between 200 to 400 $g_{polymer}/g_{catalyst.}$

The reactor is afterwards heated up to main polymerization temperature, which typically takes in between 10 to 15 minutes. Due to the non-isothermal procedure, the prepolymerization is somehow a bit undefined, e.g. the end of prepolymerization, the start of the main polymerization and degree of prepolymerization at the start of the main polymerization are not really precisely known, kinetics during prepolymerization is continuously changing due to heating-up of the reactor. Figure 23 shows the in-situ prepolymerization procedure.
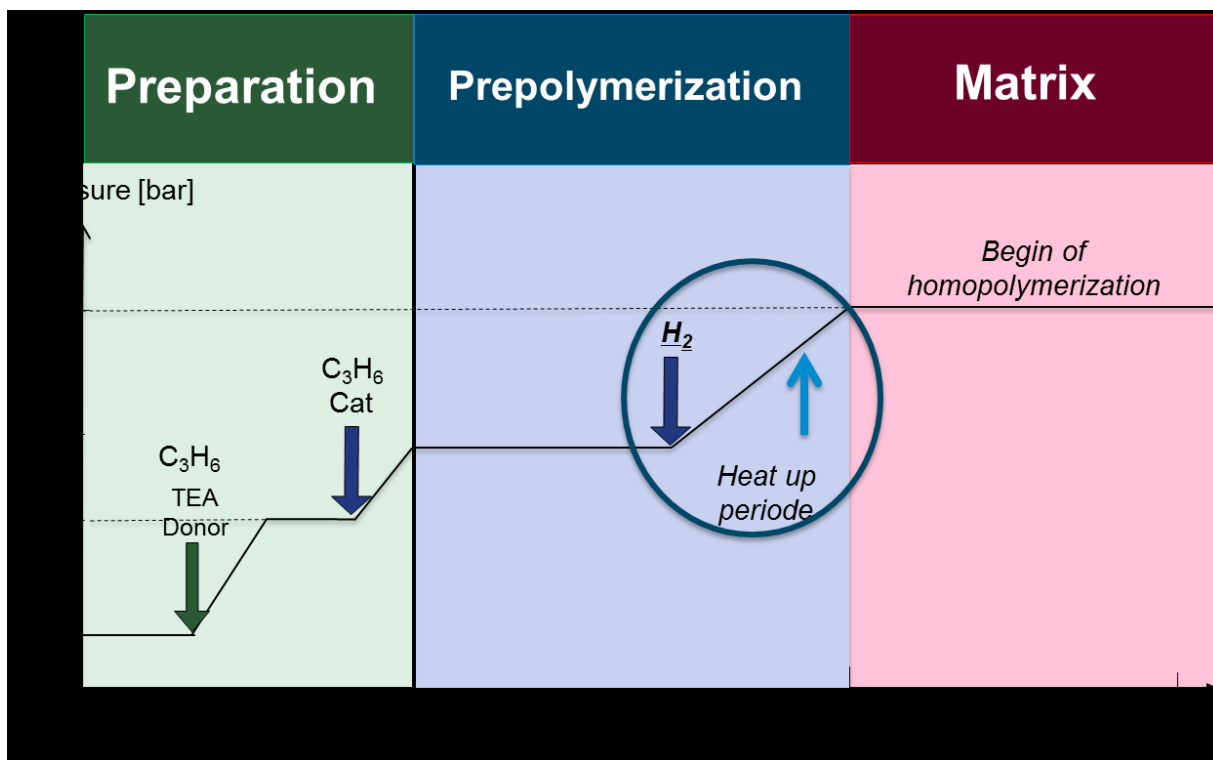
Figure 23: In-situ prepolymerization procedure

4.5.3 Bulk-phase polymerization with in-situ prepolymerization

After the prepolymer is produced by either in-situ or external prepolymerization, the prepolymer is used for further polymerization. Reactor temperature is heated up and hydrogen was given. During the heating phase more monomer is given to the reactor until pressure and temperature are near the setting point. Shortly before reaching the desired pressure and temperature the cascaded closed loops are activated thus isobaric and isotherm conditions are ensured. For the catalyst A, an Al/Ti ratio of 160 and DIPDMS as a donor with a Si/Ti ratio of 10 was recommended. In case of catalyst B, Al/Ti ratio was the same but DCP was used as a donor (Si/Ti = 10).

4.5.4 External prepolymerization in reaction calorimeter

In this work the external prepolymerization reaction is carried out in the 0.25-liter reactor. The benefit of doing external prepolymerization is that prepolymerized powder is synthesized and subsequently recovered from the reactor in inert condition (Glove Box). Heating or transition phases are solved since the recovered prepo-powder can be injected into the polymerization reaction environment.

External prepolymerization has also the advantage of constant and manageable temperatures over the course of the prepolymerization. Settings such as the temperature, the reaction time and monomer concentration can fix the degree of prepolymerization and morphology of the gained powder.
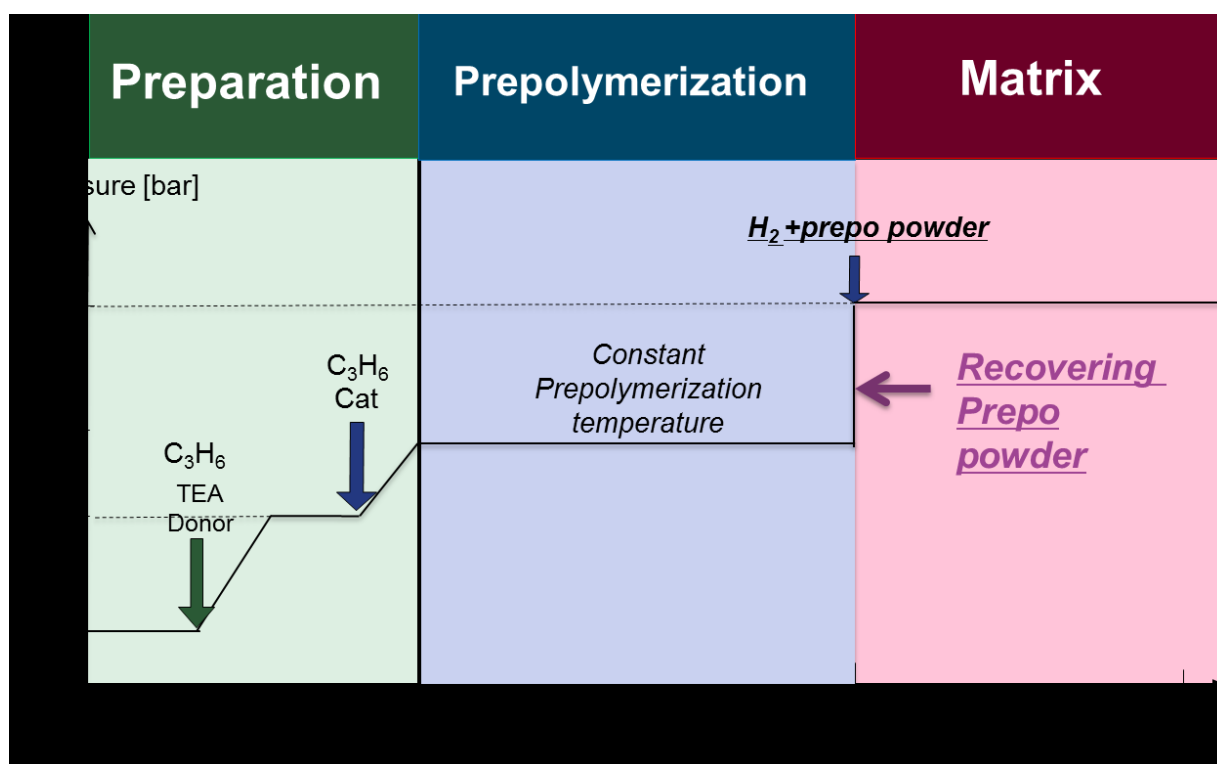
Figure 24: External prepolymerization procedure

As seen in Figure 24 the reactor is cleaned and hold in vacuum. Afterwards the feeder with the donor/TEA/oil mixture is connected to the reactor and flushed

into the reactor by liquid propylene. Shortly after, the feeder with the catalyst/oil is also flushed in the reactor. The prepolymerization reaction is run for 10 minutes and afterwards stopped by removal of the monomer via venting. The reactor is flushed with nitrogen to remove the remaining monomer. The 0.25-liter reactor is dried as fast as possible and into the glove-box. Finally, the prepolymerized powder is recovered in an inert condition and prepared for inject into the polymerization reaction later on.

4.5.5 Gas-phase polymerization with prepolymerized catalysts

Figure 24 shows schematically the reaction procedure for the main polymerization of propylene with prepolymerized catalyst at reaction conditions. Donor and TEA were added with propylene in the inertized reactor at room temperatures. The reactor was then heated up to the desired reaction temperature giving the scavenger time to clean last impurities in the monomer/reactor. The desired amount of hydrogen was given during the heating of the reactor. When a constant reaction temperature was reached, the dried prepolymerized catalyst was injected with liquid propylene. The polymerization as well as the activity measurements directly started with the injection of the catalyst. The reaction was after one hour stopped through pressure release and cooling down the reactor.

4.5.6 Bulk-phase polymerization with prepolymerized catalysts

In a bulk-phase polymerization with prepolymerized catalysts, a prepolymerized catalyst is produced at mild reaction conditions (T=25°C), isolated and stored in the glove-box under inert conditions. First, hydrogen will be given to the reactor. After this, a small amount of TEA as a scavenger for the monomer will be given. The reactor will be filled with liquid propylene until almost obtaining the desired level of filling. The cascaded closed loops are activated to obtain isobaric and isotherm conditions. The prepolymerized catalyst was directly injected at reaction conditions and the main polymerization took place immediately after

the injection. The polymerization was carried out for one hour and stopped by pressure release and cooling of the reactor.

4.5.7 Heterophasic copolymerizations

One of the most important steps during the copolymerization is the transfer into the second stage of the reaction. This transfer should be as fast as possible since copolymer is already being formed at early stages. For all copolymerization, the 5-liter gas phase reactor was used. The experimental steps of the copolymerization reaction in the 5-liter reactor are as the following:

1) µ-GC must be active and columns must be heated up. Connection and bypass between 5-liter reactor and µ-GC must be open.
2) Setting thermostat temperature for the copolymerization. Due to overheating and high reaction rates, thermostat temperature should be approximately 5 to 10°C lower than reactor temperature.
3) Flushing propylene until the desired partial pressure is reached
4) Ethylene feed with maximum flow rate (>750 g/h) until desired absolute pressure for copolymerization is reached

Steady state is reached depending on the ethylene/propylene ratio, but this should take less than 5 minutes. The thermostat temperature and the required partial pressure of propylene were stablished through various rows of experiments.

At the copolymerization stage, constant monomer composition is achieved after 5 minutes. The monomer feed ratios are at steady state related to activity and EPR incorporation rate. An optimized ethylene/propylene ratio was achieved through a row of experiment for concentration between 10 mol-% and 90 mol-%. Monomer composition is within the experimental error constant during rubber phase. Copolymerization times were not varied (1 hour) since matrix morphology was adjusted. EPR incorporation rate is therefore dependent on the morphology of the iPP and not on reaction time. Rubber contents in this study varied from low (15 mol-%) to very high (90 mol-%). Around 1 Kg HiPP is

possible to produce in each reaction. Monomer composition at steady state and reproducibility during copolymerization are shown in Figure 25 and Figure 26.
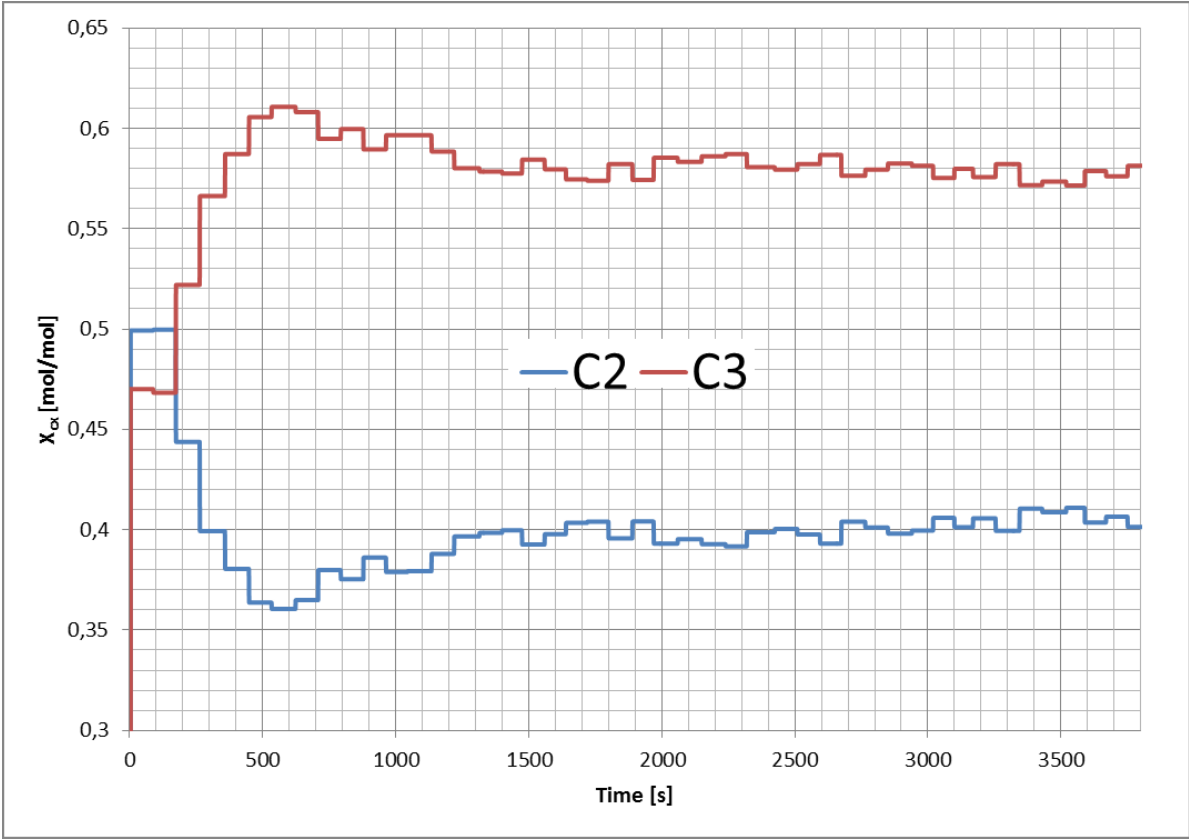
Figure 25: Constant gas composition during rubber step
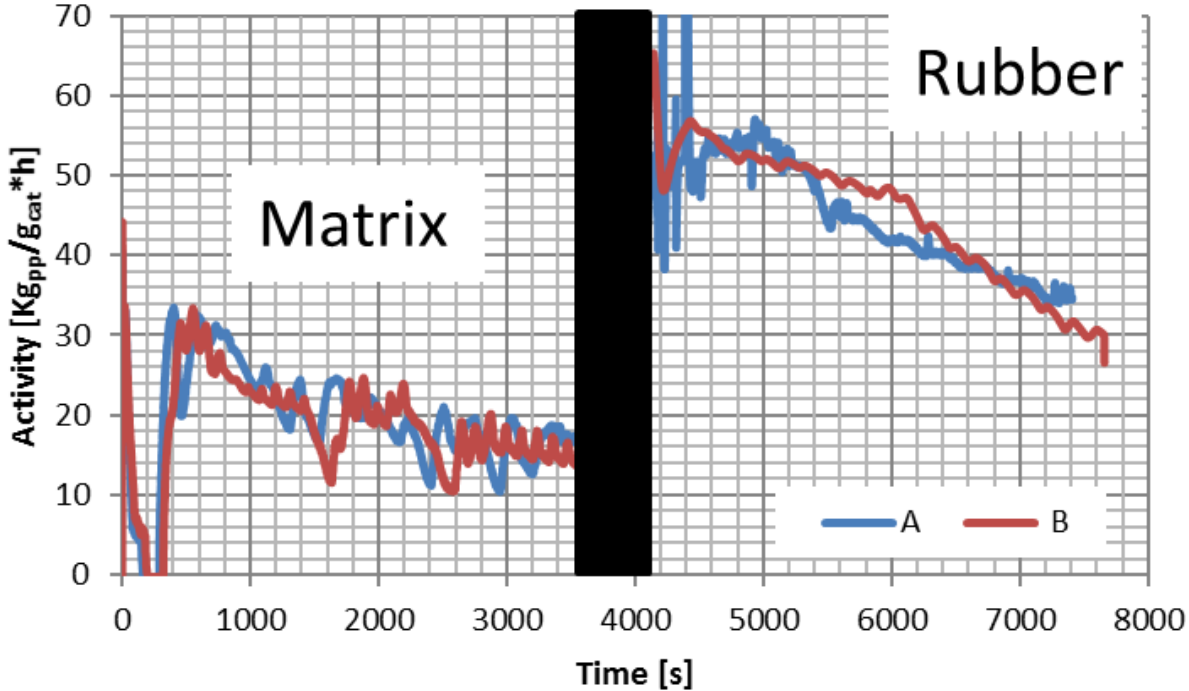
Figure 26: Copolymerization reproducibility (matrix phase at 70°C 20bar and 1%H2 and rubber phase at 70°C, 21 bar and 25/75 mol ratio ethylene/propene)

4.6 Experimental Plan

- Establishing activity level and reproducibility for both catalyst A in gas phase polymerization and catalyst B in bulk-phase polymerization.
- For both catalysts screening of effect of prepoly conditions on activity and bulk density in homopolymerization.
- External prepolymerizations under defined conditions.
- Homopolymerizations with defined prepolymers – activity and morphology.
- Heterophasic copolymerizations with defined prepolymers - activity, morphology and comonomer incorporation.

5 Polymer characterization

5.1 Polymer samples

Morphology of the polymer samples were studied to analyze the effect of prepolymerization and homopolymerization settings into the gained iPP and furthermore in the rubber phase. Mercury porosity measurements were performed by industrial partners and the Department for Industrial Chemistry at University of Halle. Scanning Electron Microscopy (SEM) and Differential Scanning Calorimetry (DSC) were performed by an industrial partner and the Department for Physics at University of Halle. MFR, FTIR, particle size distribution and bulk density were performed at the Department for Polymer Reaction Engineering at University of Halle

5.2 Crystallinity

The polymer melting temperature was determined from the peak of the differential scanning calorimeter (DSC) curve, measured with a Perkin-Elmer (mod. DSC-2) apparatus. DSC measurements were made at a heating rate of 10°K/min. The samples were melted at 200°C, then cooled down to -80°C and subsequently heated back to 200°C. The crystallinity of the polymer was calculated from the heat of fusion values, using the following equation:

$$X_{DSC} = \frac{\Delta H_m}{\Delta H_{\infty}} \cdot 100 \ [\%] \tag{21}$$

Where, ΔH_m, is the heat of fusion of the sample as determined from the DSC curve, and ΔH_{∞} is the literature reference is used for 100% crystalline polypropylene [117] melting heat (207 J/g for polypropylene). Crystallinities for

homopolymers are in a range from 42% to 53%. Figure 27 shows a DSC curve for a homopolymer sample.
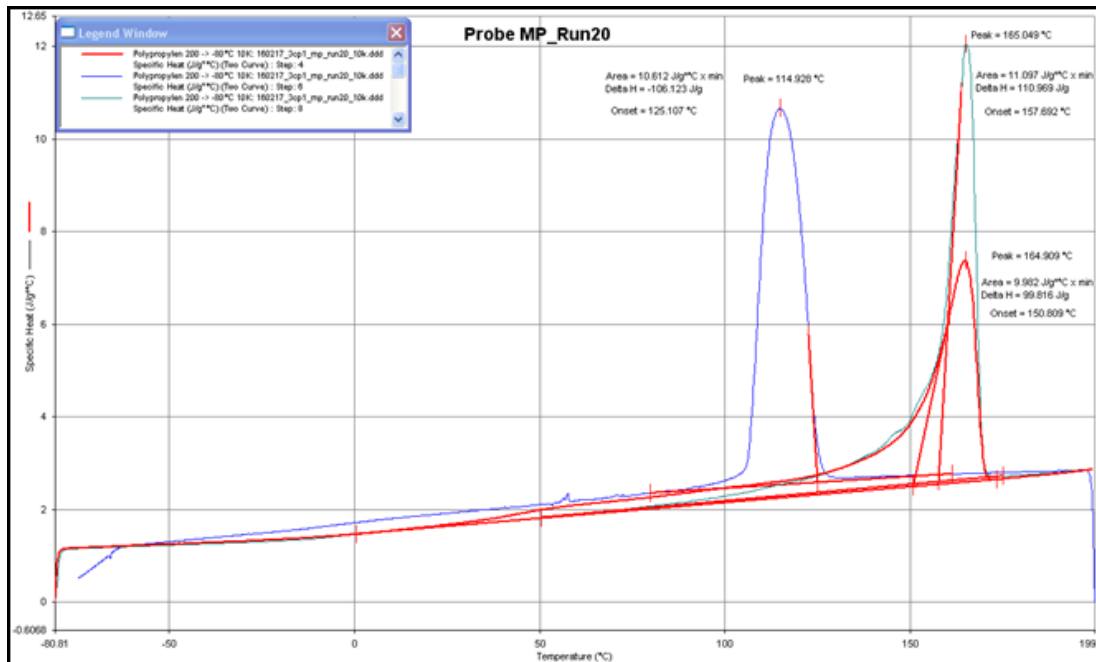
Figure 27: DSC curve for iPP

5.3 Porosity

Porosity of the obtained powders was studied by Hg-porosity at the chemistry department of the University Halle and both industrial partners facilities. Range of the measurement pressure were from low (p=0-4bar) to high pressure (p = 4-4000 bar). For all 3 machines pore sizes under 4 nm or over 1mm cannot be detected.

At high pressures the polymer will be compressed and will affect final results of total porosity. Due to the uncertainties of the measurement, particularly at the range of measurement only results of University of Halle will be take in account. The porosities measured are in the range of 1% to 35 vol%.

5.4   Melt Flow Index (MFI)

A well-known technic used to acquire information about the molecular properties of polyolefins is the melt flow index (MFI). MFI relate as a proportional of molecular weight of polypropylene (higher MFR, lower molecular weight). In this work, a CSI – 127 MF micro-melt flow setup was used to measure MFI of PP at 230ºC and using standard weight of 2.16 kg.

5.5   Bulk density

Bulk density (BD) of polymers is defined as the mass of a packed powder bed within a certain volume [10] [3]. Bulk density is influenced by many factors such as density, porosity but also particle size and particle size distribution. -, Bulk density is an easy accessible measurement and allows for comparison of similar particle populations first conclusions on morphology - in general a low bulk density correlates to high porosity, where as a high bulk density correlates to low porosity and dense compact particles.

The bulk density was determined using a standardized method of weighing a known volume of loosely packed polypropylene powder. The set-up consists of a supported funnel, placed on a receiver. About 10 g powder is poured through the funnel into the receiver which is a cylinder with a precisely known volume of 41,52 cm^3. Excess of powder is removed and the filled cylinder is weighed. The bulk density can be indicated in gram polymer per liter resp. kilograms per cubic meter.

$$\rho_{bulk} = \frac{m_{powder}}{V_{container}} [Kg/m^3]$$
(22)

5.6 Scanning electron microscope

Particle morphology was also studied by electron microscopy. At the department of Physics of Martin-Luther-University, a SEM microscope type JSM6300 was used. The polymer samples were prepared by the application of a thin layer of gold (at 50 mA, 150s) to make the sample conductive and thus visible to the equipment. Afterwards the samples were studied in vacuum. The diverse levels of magnification can range from 1mm up to 3 nm. Particles from 100 μm up to 700 μm were measured during this study. SEM micrographs are valuable for showing cracks, voids, and the presence of pores. Nevertheless, it should be noticed that for interpretation of SEM micrographs sample statistics have to be take into account – by SEM typically only a small population is being analyzed.

5.7 Ethylene content in rubber

Ethylene and propylene are given into the reactor during the copolymerization. Consumption rates of each monomer can be calculated as long as monomer composition and pressure in the reactor are constant. In this case, the monomer feed equals its consumption.

For this work different monomer ratios were tested, which will lead into different copolymer compositions. As the monomer feed ratio is equal to the copolymer composition (at isotherm, isobaric conditions with constant comonomer composition), copolymers with middle to high monomer incorporation ratios of ethylene in the rubber phase were polymerized.

6 Sorption measurements

In order to study the effect of particle morphology, additional sorption experiments with selected polymer samples have been performed.

6.1 Experimental setup high pressure sorption balance

For sorption measurement, an existing high-pressure sorption balance has been used in this work (Figure 28)

Figure 28: High pressure sorption balance

6.1.1 Measurement principle and setup

The polymer sample is placed in the sample holder in the pressure cell. Polymer samples are either in the form of membranes or powder. The load of the sample holder is transferred via a magnetic suspension coupling (type Rubotherm GmbH, Bochum) to an analysis balance (type Mettler-Toledo AT261, sensitivity: 10 µg) standing above.

The mass-uptake is monitored, from the sorbed mass in steady-state, equilibrium solubilities can be obtained, from the slope of the mass-uptake, conclusions on the rate of mass-transfer can be drawn.

Temperature of the pressure cell is controlled by a thermostat. The measurement cell can be pressurized by a manifold.

The sorbent is supplied by a heated feed tank and a pressure control valve. Pure gases as well as gas mixtures can be prepared for sorption measurements. The whole setup is connected to vacuum, nitrogen and a purge line. Measurement data (pressure, temperature, weight) is collected by a computer with a data acquisition software.
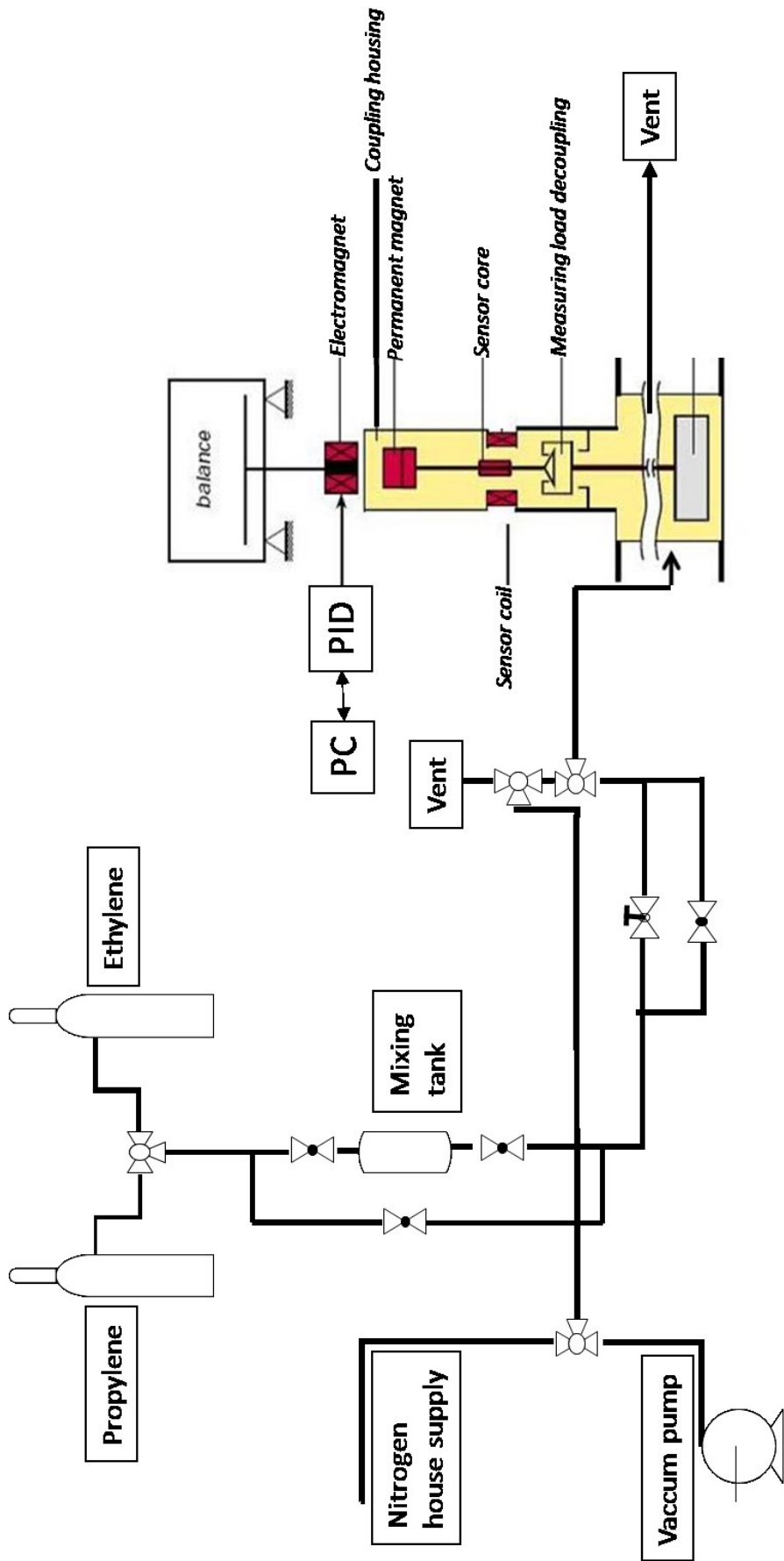
Figure 29: Flow sheet of the magnetic sorption balance

6.1.2 Buoyancy Force correction

On the sample, buoyancy force is acting. Hence even when pressurizing with a non-sorbing inerts, the shown mass is changing with pressure. For quantitative analysis of the sorption measurements this effect of buoyancy force needs to be compensated. Mathematically can this be expressed as:

$$m_{sorbed} = m_{balance} + V_{sc+s} * \rho_{NIST} \; [g] \tag{23}$$

For compensation, both the volume of the sample with sample holder and the density of the sorbent at measurement conditions is needed. The needed volumes have been determined by blank measurements with nitrogen, for the densities of propene and ethylene at 70°C, a two parameter virial-equation and data available from NIST have been used:

$$\rho_{NIST} = \cfrac{1}{\cfrac{R \cdot T}{p \cdot M} + \cfrac{F}{M} + \cfrac{G \cdot p}{M}} \; [g/m^3] \tag{24}$$

With:

$$F = K_1 * T + K_2 \; [m^3/mol] \tag{25}$$

This equation can describe with a small error experimental density data over the mentioned temperature and pressure range when the following constants are used:

	K_1	K_2	G
	[m³·mol⁻¹·K⁻¹]	[m³·mol⁻¹]	[m⁴·s²·mol⁻¹·kg⁻¹]
propylene	$3,7 \cdot 10^{-6}$	$-1,48 \cdot 10^{-3}$	$-5,02 \cdot 10^{-11}$
ethylene	$8,21 \cdot 10^{-7}$	$-3,85 \cdot 10^{-3}$	$-1,79 \cdot 10^{-12}$

The accuracy of the fit for both ethylene and propylene was satisfying for a pressure range between 0 and 25 bar and a temperature of 70°C. The literature data plotted on fitting function curve of propylene and ethylene can be seen as function of pressure in Figure 30:
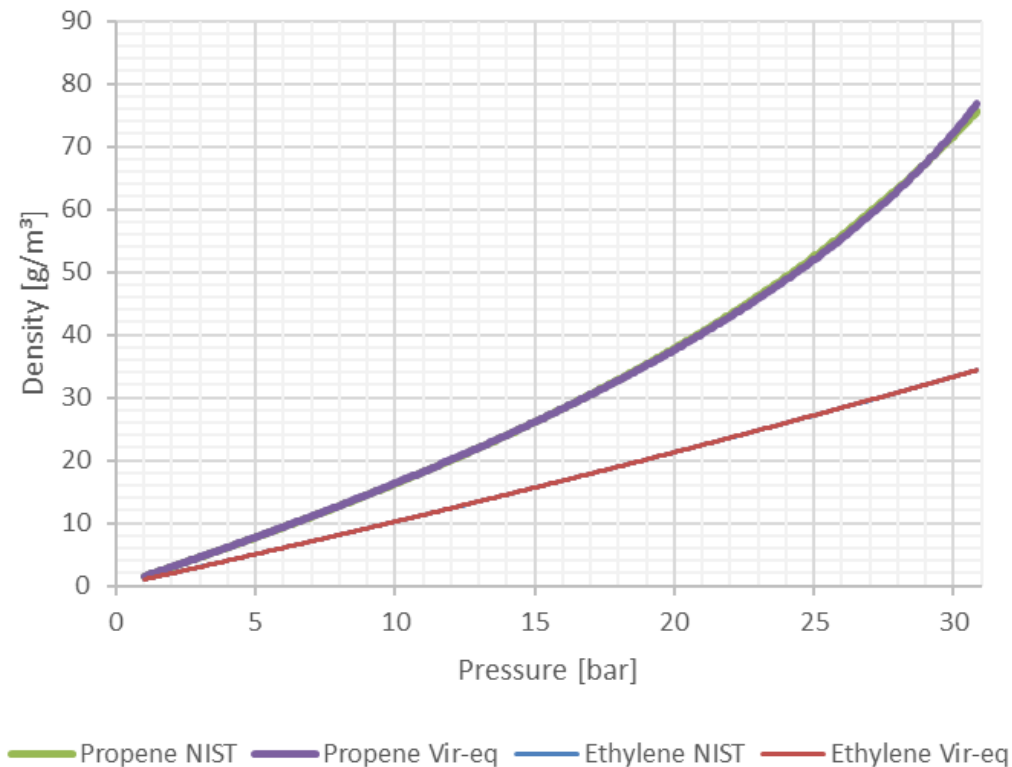
Figure 30: Fitting function curve of propylene and ethylene

The effect of the buoyancy force on the raw data and the effectiveness of the buoyancy force correction can be seen in Figure 31 (for blank measurements with nitrogen at different pressures).
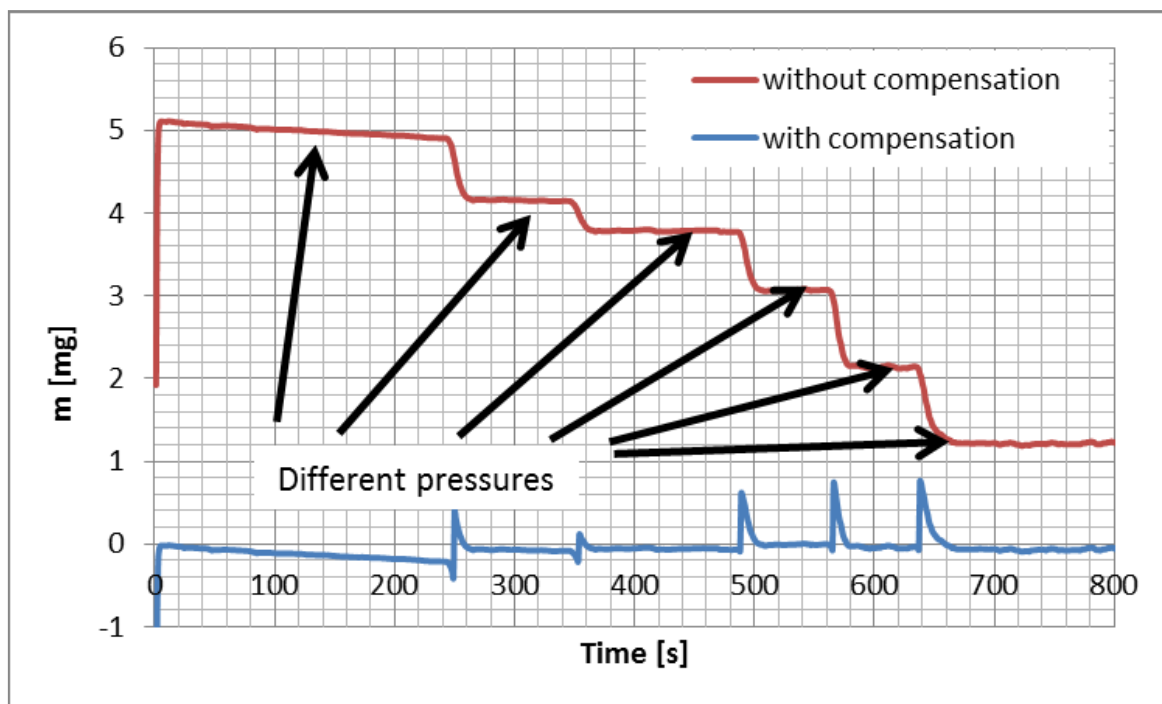
Figure 31: Example for buoyancy force correction (blank measurements with Nitrogen at 70°C)

6.1.3 Operational procedure

Prior to the actual sorption measurements, approximately one gram of polymer (powder or film) is placed in the sample container hanging to the magnetic coupling in the high-pressure chamber. The chamber is heated to the measurement temperature and vacuum of 46 mbar is applied in order to remove all possible sorbed gases in the polymer powder. After reaching a constant mass a tare is applied to the balance and the mass container is moved from the zero position to the measuring position.

The penetrants either propylene or ethylene are fed using a needle valve to control the filling rate. The filling takes approximately few seconds. The pressurizing causes a temperature cooling inside the chamber up to 4°C. Due to the construction of the whole setup, the chamber is ensured to run at nearly constant temperature bath of 70°C. Approximately, after two minutes the penetrant temperature inside the chamber reaches isothermal conditions. During the measurement, the increase in weight is recorded by the data-acquisition system.

6.1.4 Sample preparation

For measuring sorption on polymer powders no further preparation was needed. For sorption experiments on polymer films, these were prepared with the following procedure:

➤ The hot press Specac, (Figure 32) is heated up to 180°C for homopolymer and 200°C for copolymer.
➤ After reaching the setting point a small amount of sample will be heated for 10 minutes without any pressure to ensure complete melting of the sample.
➤ Afterwards a pressure around 10 tons was applied for 7 minutes.
➤ Finally, the films were taken out of the press and cooled down by water for 5 minutes to room temperature.

Figure 32: Powder press for film fabrication

The exact thickness is measured prior experiment with a caliper. Depending on the ring thickness, the thickness of the films can be varied. For this work, most

of the films had a thickness of 0.7 mm. Since very small amounts of powder are needed for a film, four films in a stack were pressed to increase the experimental sample mass thus reducing the experimental error.

6.1.5 Average deviation and reproducibility of the magnetic sorption balance

The stability and error of the balance were tested through a metallic piece into the chamber. Reproducibility was achieved due to repetition of four sorption experiments for the same sample. In Figure 33 a metallic piece was placed in the sample container and propylene was injected. After a certain time, the stability of the balance reading and its corresponding buoyancy correction.
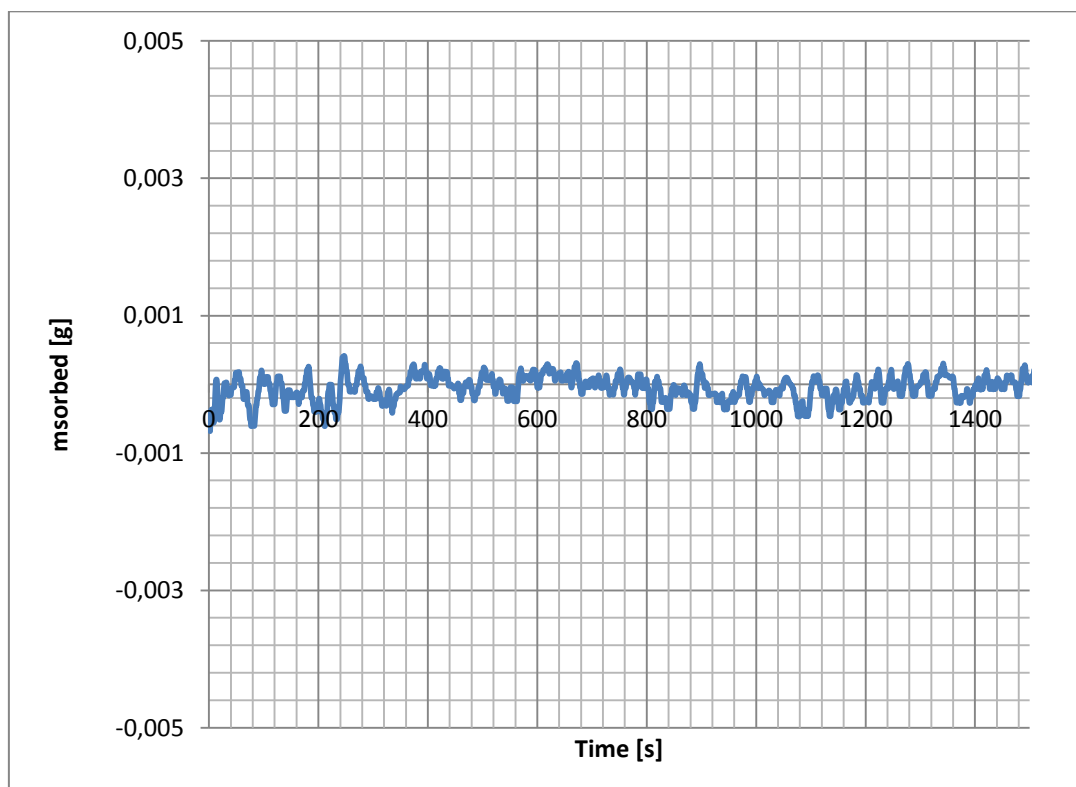
Figure 33: Average deviation during a sorption measurement

The result of this test proved that error is from +/-2.99x10^{-4} g. The differences can be attributed to the uncertainty in the corresponding steps and calculations required to determine the buoyancy correction, and temperature changes inside the chamber during the stabilization time to reach the desired pressure.

The reproducibility of sorption experiments was also tested. Figure 34 shows the sorption curves of the same polymer powder measured four times. It can be observed that both sorption rate (slope of the curve) and sorption equilibrium m_{eq} is similar.
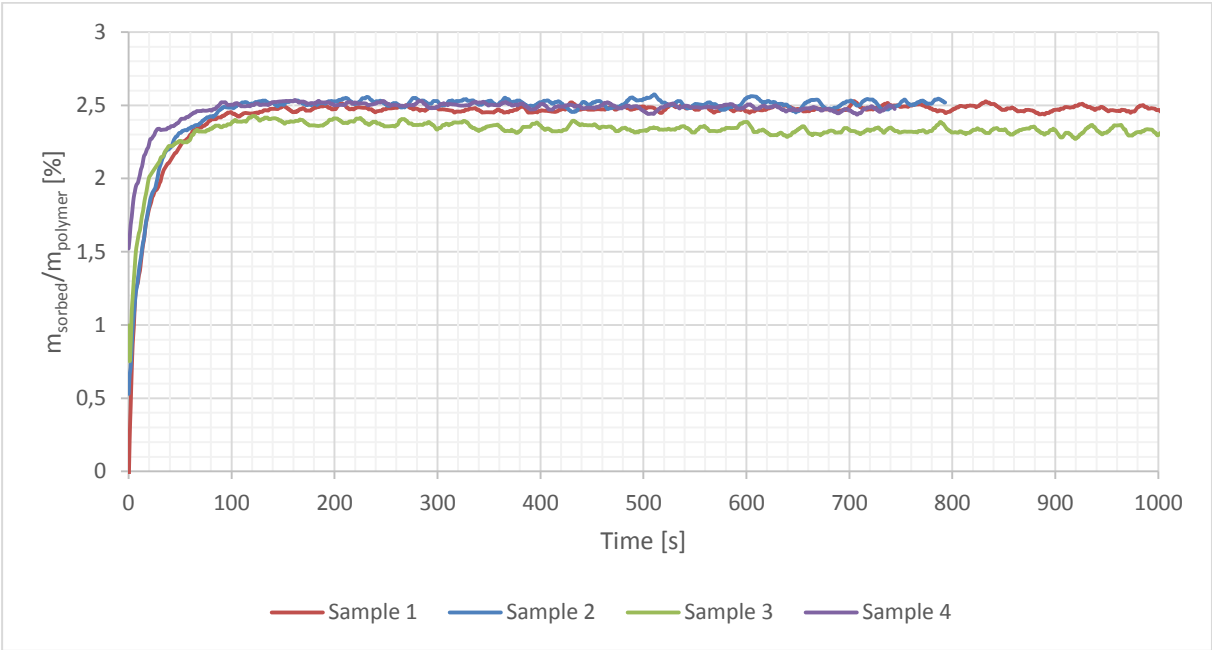
Figure 34: Reproducibility of sorption measurements for homopolymer (70°C, 11 bar, propylene).

7 Experimental results

7.1 Optimization reproducibility and activity

7.1.1 Gas-phase polymerizations with catalyst A

Reference polymerization data for catalyst A in gas phase polymerization at 70°C, 20 bars and 1 mol-% H_2 and DIDPMS as donor was indicated to be around 20 $Kg_{pp}/(g_{cat}*h)$.

The reference activity of was initially not reached (procedure with in-situ prepolymerization). In order to improve activity, the level of TEA was increased, in order to raise the scavenge potential against impurities while keeping the Si/Ti ratio constant. The amount of aluminum alkyle had to be slightly increased to Al/Ti = 260. With this ratio, reproducible results on reference activity level of is 21 $Kg_{pp}/(g_{cat}*h)$ could be reached. Further increase in TEA lead to an increase in MFI (transfer reactions), for all further experiments an Al/TI ratio of 260 was used.
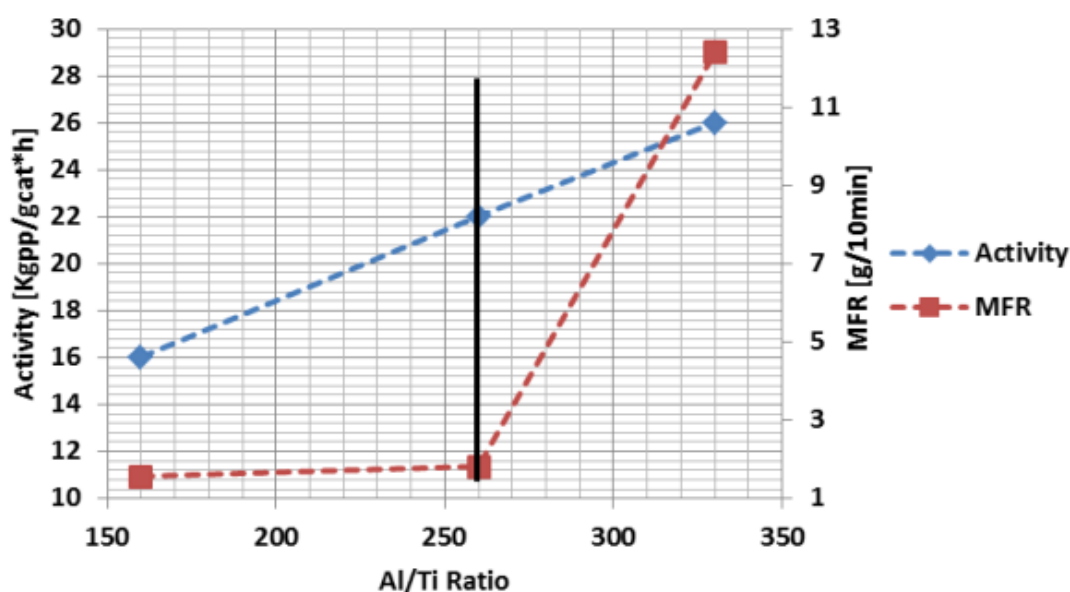
Figure 35: Effect of Al/Ti ration on activity and MFI

All matrix polymerizations were performed for 1 hour at isothermal and isobaric conditions.

To demonstrate reproducibility of the procedure and results, six experiments at same settings were repeated. Figure 36 shows the activity profiles of these homopolymerizations. Activity is only valid when setting points are reached and constant. Therefore, filling up, stabilization and heating should be reached as fast as possible (t<500).
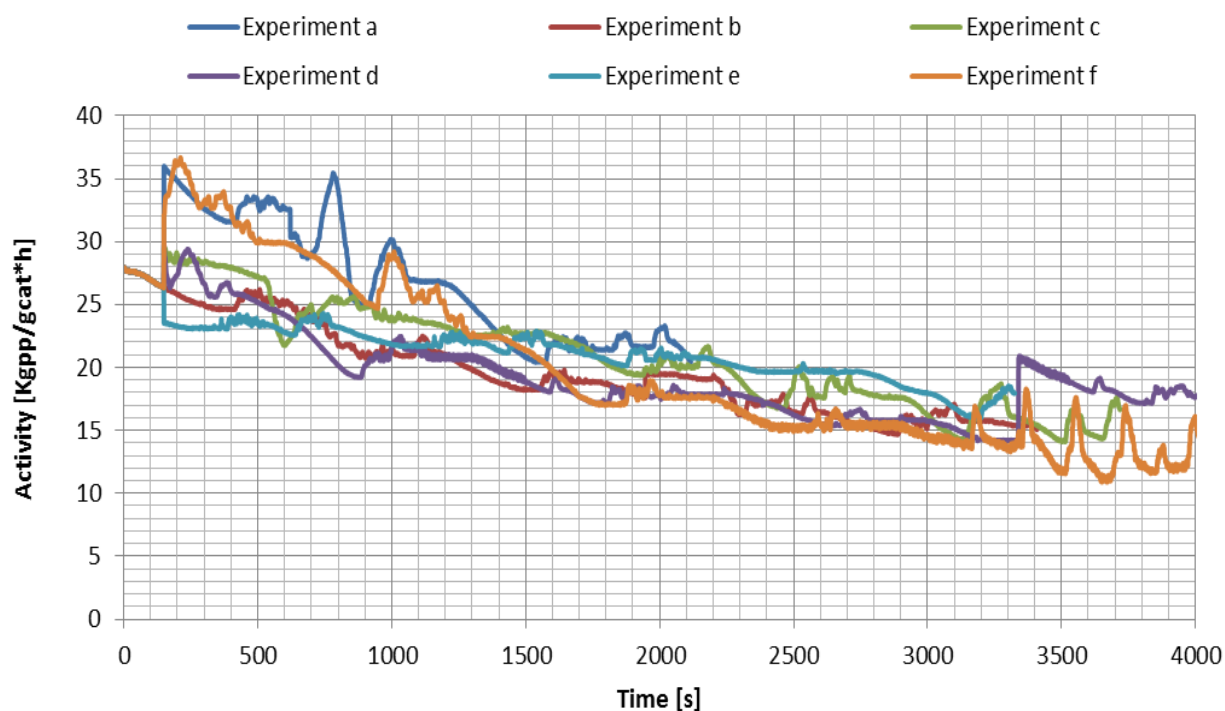
Figure 36: Reproducibility of A catalyst at 70°C, 20bar and 1 mol-% Hydrogen

Approximately 8 to 12 mg catalyst were used for all experiments. Average activities were in range from 20 to 25 $Kg_{pp}/(g_{cat}*h)$.

7.1.2 Catalyst B in bulk polymerizations

For catalyst B in bulk-phase polymerization at 80°C, 39 bar pressure and 3 mol-% hydrogen, a reference activity of approx. 45 $Kg_{pp}/(g_{cat}*h)$ was indicated. An Al/Ti ratio of 250 and Dicyclopentyl dimethoxy silane (DCP) with an Al/Do ratio of 10 as a donor was recommended. Table 2 shows the setting for the first experiments with catalyst B and Figure 37 shows the obtained average activity after one hour homopolymerization.

Table 2 : Reproducibility catalyst B

	T [°C]	p[bar]	cat	m_{cat}	TEA [ml]	Cocat [ml]	Name cocat	Prepo [min]	H2 [%]	Activity $[Kg_{pp}/g_{cat}*h]$	Bulk density $[kg/m^3]$
1	80	39	B	4,35	0,0832	0,0041	DCP	10	2	43	378
2	80	39	B	6,2	0,118	0,0059	DCP	10	2,01	49	359
3	80	39	B	5,1	0,097	0,0049	DCP	10	2,05	48	363
4	80	39	B	5,5	0,101	0,0055	DCP	10	1,9	45	361
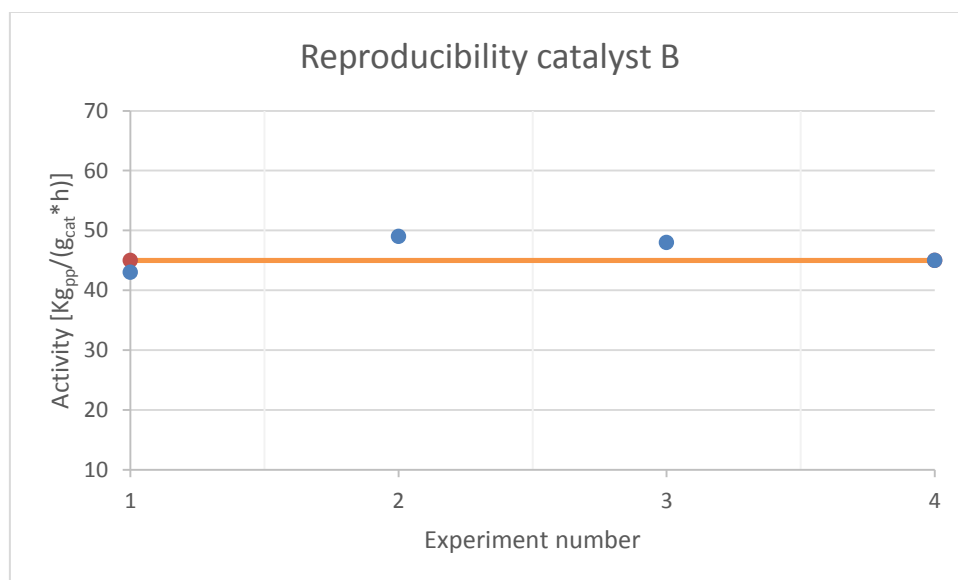
Figure 37 : Average activity for reproducibility (cat B)

7.2 Screening of prepoly settings on activity and morphology

In a broad screening study, for both catalysts A and B the conditions in homopolymerization and prepolymerization were systematically varied. The target was to identify how particle morphology can be adjusted while maintaining a good activity level.

For all experiments the procedures with in-situ prepolymerization (see chapter 4.5.2 for gas-phase polymerization and chapter 4.5.3 for bulk polymerization) were used. As fast indication for particle morphology, bulk density was measured after the homopolymerization stage.

The following variations were done:

- No prepoly step, direct catalyst injection at homopolymerization conditions.
- Prolonged prepoly of 20 min.
- Prepoly with more hydrogen present.
- Prepoly temperature.
- Prepoly with some ethylene (1 or 5 mol-%) present.
- Gas / Bulk phase conditions.
- Injection solution (oil/heptane/dry).

Table 3 and Table 4 summarize the most representative experiments for catalyst A and B.

7.2.1 Results Catalyst A

Table 3: Overview of experiments with catalyst A

Polymerization		Prepoly	Homopolymerization			Bulk density	Avg. Activity
Run	Type	Conditions	T [°C]	p [bar]	H_2 [mol%]	[kg/m³]	[kg_{pp}/g_{cat}*h]
20	**Gas**	**standard***	**70**	**20**	**1**	**476**	**22**
59	Gas	Hydrogen during matrix	70	20	1	465	23
24	Gas	no prepoly	70	20	1	462	16,6
59	Gas	Injection with heptane	70	20	1	456	17
26	Gas	standard*	60	20	1	452	16
34	Gas	standard*	70	15	1	448	15,3
35	Gas	standard*	80	15	1	448	20,6
46	Bulk	standard* bulk	80	36	1	441,2	29,14
27	Gas	standard*	90	20	1	440	29,6
53	Gas	prepoly at 19°C	70	20	1	440	24
21	Gas	standard*	70	25	1	440	25
52	Gas	prepoly at 45°C	70	20	1	431	16
45	Bulk	standard* bulk	70	30	1	429,8	25,32
42	Gas	long prepoly	70	20	1	428	20
36	Gas	1 mol% C_2	70	20	1	420	22
48	Bulk	no prepoly	70	30,4	1	418,3	23
41	Gas	3 mol% H_2	70	20	3	418	26
49	Bulk	standard* bulk	70	30,4	0,3	415,7	19
37	Gas	5 mol% C_2	70	20	1	385	26,8
60	Gas	Dry injection	70	20	1	373	7
50	Bulk	5 mol% C_2	70	30	1	230,7	50

For catalyst A, the applied standard procedure (30°C prepolymerization temperature, 70°C matrix temperature, 20 bar and 1 mol-% hydrogen) gives the highest bulk density of 476 kg/m³ and an activity of about 22 $Kg_{pp}/(g_{cat}*h)$.

Completely omitting the prepolymerization step slightly reduced bulk density and significantly reduces polymerization activity.

Varying prepolymerization time and temperature did not change bulk density drastically, but had some effect on resulting activity, with slightly higher activities at mild prepolymerization temperature. A row of experiments having different prepolymerization temperatures were achieved. Activity results after the matrix polymerization showed a maximum of activity by having between 27°C and 35°C during the prepolymerization.

Varying prepolymerization time and temperature did not change bulk density drastically, but had some effect on resulting activity, with slightly higher activities at mild prepolymerization temperature. Optimizing the prepolymerization temperature revealed a maximum of activity for prepolymerization temperatures between 27°C and 35°C.

In the standard procedure, oil is used for catalyst injection. Replacing oil by heptane for catalyst injection did not modify the morphology but led to less activity – most likely due to traces of impurities in heptane. Dry injection of the catalyst powder had a remarkable influence on powder morphology and activity, most likely due to overheating activity of the catalyst decreased dramatically.

Variation of the amount of hydrogen as chain transfer agent did not influence bulk density for catalyst A.

Clearly the highest impact on bulk-density could be seen via addition of ethylene into to the prepolymerization step. Addition of 5 mol-% ethylene in the prepoly-step decreases bulk density in case of gas-phase polymerization down to 385 kg/m³ while keeping activity on a high level of 26 $Kg_{pp}/(g_{cat}*h)$.

Also for bulk polymerizations, presence of ethylene in the prepoly stage significantly reduced bulk density for catalyst A from about 440 kg/m³ to 230 kg/m³ for prepoly with 5 mol-% ethylene being present.

7.2.2 Results Catalyst B

Table 4: Overview of experiments with catalyst B

Polymerization		Remarks	Homopolymerization			Bulk density	Avg. Activity
Run	Type		T [°C]	p [bar]	H_2 [mol%]	[kg/m³]	[kg_{pp}/g_{cat}*h]
15	Gas	comparasion with Cat A	70	20	1	421	29,9
19	Gas	prepo temp 40°C	70	27,5	1	418	27,9
20	Gas	no hydrogen	80	27,5	0	417	10,8
9	Gas	Reproducibility gas	70	20	1	413	29
16	Gas	standard*	60	20	1	404	25,3
18	Gas	prepo temp 40°C	80	27,5	1	400	37,2
5	Bulk	8%mol hydrogen	80	39	8	393	65
17	Gas	standard*	80	20	1	380	34,3
13	Bulk	Change of donor (dipdms)	80	39	3	379	46
2	Bulk	Reproducibility bulk	80	39	3	378	43
23	Gas	standard	80	27	1	373	40
10	Bulk	1%mol H2	80	38	1	368	39,6
4	Bulk	Reproducibility bulk	80	39	3	363	48
21	Gas	5%mol hydrogen	80	27,5	5	363	20,6
22	Gas	2,5%mol hydrogen	80	27,5	2,5	361	26,7
3	Bulk	Reproducibility	80	39	3	359	49
8	Bulk	Temp effect	60	30	3	359	30
1	Bulk	Standard Bulk	80	39	3	342	46
11	Bulk	19°C Prepo	80	38	3	341	32,27
7	Bulk	5%mol C2 during prepoly	80	39	3	277	68
6	Bulk	no prepo bulk	80	39	3	252	19,6

For the catalyst B at standard conditions (Al/Ti ratio of 250, Dicyclopentyl dimethoxy silane (DCP) with an Al/Do ratio of 10 as a donor, bulk polymerizations at 80°C, 39 bars pressure and 3 mol-% H_2 applying a prepolymerization step) were achieved.

The bulk density is with 350-380 kg/m³ somewhat lower compared to the catalyst A in gas-phase polymerization. The catalyst B was also tested in gas-phase polymerization and gives with around 30 $Kg_{pp}/(g_{cat}*h)$ reasonable, but significantly lower polymerization activities compared to bulk-phase polymerization. This is to some extend expected, since in bulk polymerization the monomer concentration is higher.

The reaction phase (bulk or gas-phase) is one of the factors affecting powder morphology most for catalyst B. Bulk-phase polymerization in general leads to visibly larger particles compared to gas-phase polymerization, which is in line with the higher activities observed. For catalyst B, the bulk density is for bulk-phase polymerization in general lower compared to gas-phase polymerization. Omitting the prepoly step again leads to substantially lower activities and lower bulk density.

A series of experiments in the gas phase were carried out to determine the effect of hydrogen on the morphology and activity (Table 4 run 20 to 23). Abstinence from hydrogen will significantly reduce activity. Increasing the concentration of hydrogen during matrix polymerization will increase the average activity. This increase reaches up to a maximum at 1-2 mol-% hydrogen and then decrease again at higher concentrations. Bulk density does not change significantly with hydrogen concentration.

As observed for catalyst A, also for catalyst B, the largest impact on bulk density can be seen with addition of ethylene to the prepoly step. By addition of 5 mol-% ethylene to the prepoly step, bulk density of the polymer after matrix polymerization can be reduced down to 277 kg/m³ while maintaining a high activity of 68 $Kg_{pp}/(g_{cat}*h)$.

7.3 Morphological Characterization

For a deeper morphological characterization, selected samples were analyzed by:

- Hg porosimetry
- N2 absorption
- Electron microscopy SEM/TEM
- Sorption measurements

N_2 absorption measurements (BET-method) at the institute for industrial chemistry of Halle University unfortunately did not lead to analyzable results.

Hg porosity measurements were carried out for selected samples, see Table 5:

Table 5: Comparison of the measurements Halle vs Industry laboratories

Number	Comment	Average Pore diameter [µm]	Porosity [%]	Bulk Density [g/cm3]
37	GP, prepoly 5% Ethylene	0,97	24	0,385
41	3% Hydrogen	4,9	14	0,418
48	No prepo Bulk	0,5	20	0,418
49	0,3% Hydrogen Bulk	4,2	34	0,415
50	5% Ethylene Bulk	2,1	50	0,23
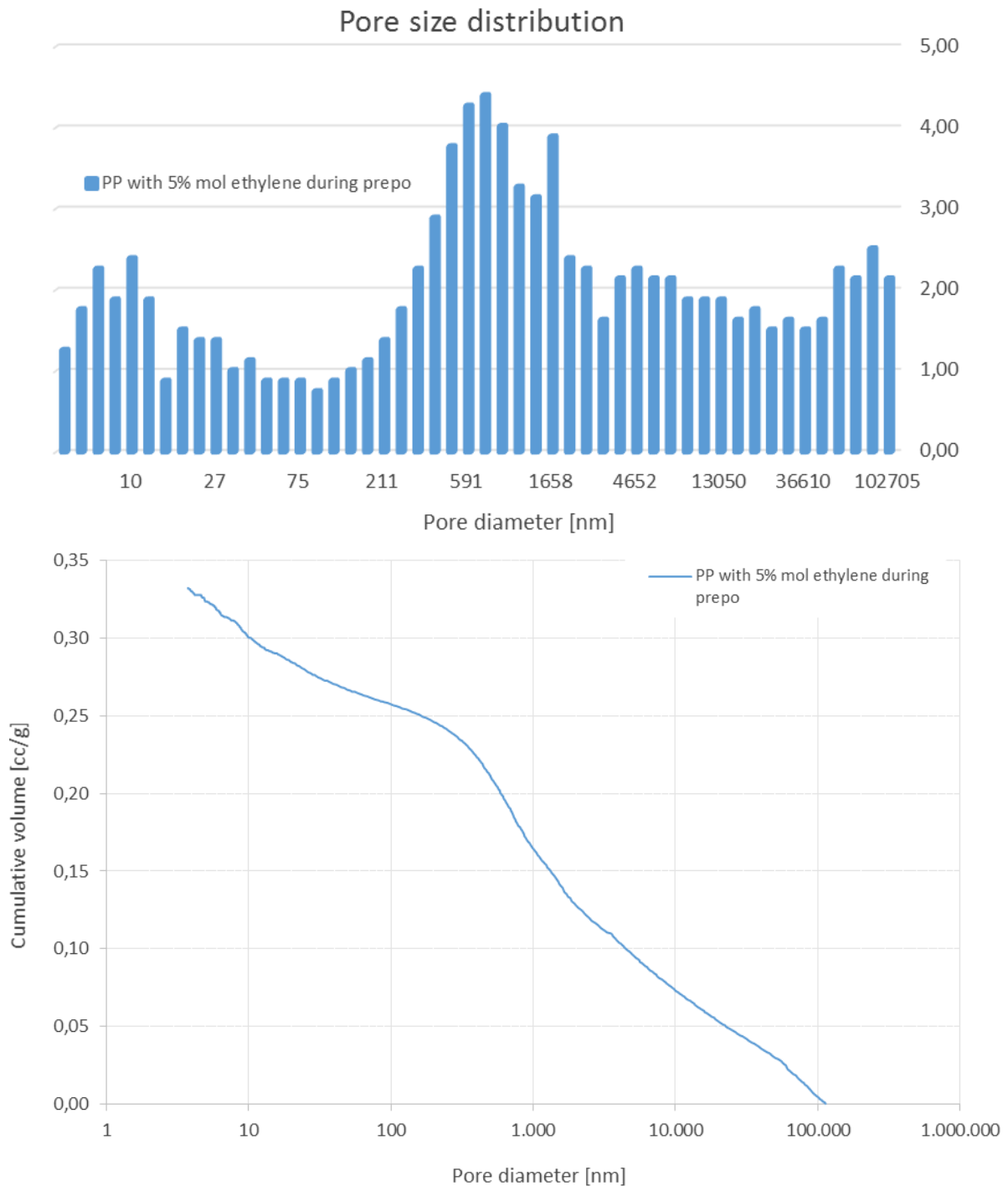
Figure 38: Pore size distribution by Halle (sample PP37)

An example for the pore size distribution of sample 37 (gas-phase polymerization with catalyst A, in-situ-prepolymerization with 5 mol-% ethylene) can be seen in Figure 38. A peak of the pore size distribution can be found at approx. 700 nm.

Even though the absolute numbers for porosity depend on the porosity equipment and measurement procedure applied, in particular the measurement range, and cannot be taken as absolute measurement, qualitative comparisons between different samples are possible.

As an example, porosity measurements are compared with the corresponding bulk densities for different samples in Table 6 and Figure 39.

Table 6: Influence of different parameters on the bulk density during bulk reaction

Run	Comentar	Polymerization type	Average pore	Total cumulative	Bulk density	Total porosity (%)
24	just prepo	gas	138,06	0,1937	462	17,64
20	standard	gas	162,29	0,1656	476	14,26
48	no prepo	bulk	436,5	0,2742	418	20,96
37	5%C2	gas	971,34	0,3322	385	24,777
50	5%C2	bulk	2104	0,9765	230	48

It is possible to correlate bulk density with average pore diameter and porosity, as can be seein Figure 39.

For instance, sample PP20 (standard phas-phase polymerization with prepoly step) has the highest bulk density, but also the lowest porosity of the studied samples. On the other hand, samples PP 37 (gas-phase polymerization with ethylene present during prepoly) and PP 50 (bulk-phase polymerization with ethylene present during prepolymerization) Hg-porosity measurments confirm the finding of bulk density measurements, that addition of ethylene during prepoly step has a strong effect o particle morphology. Formation of pores and porosity increases strongly.
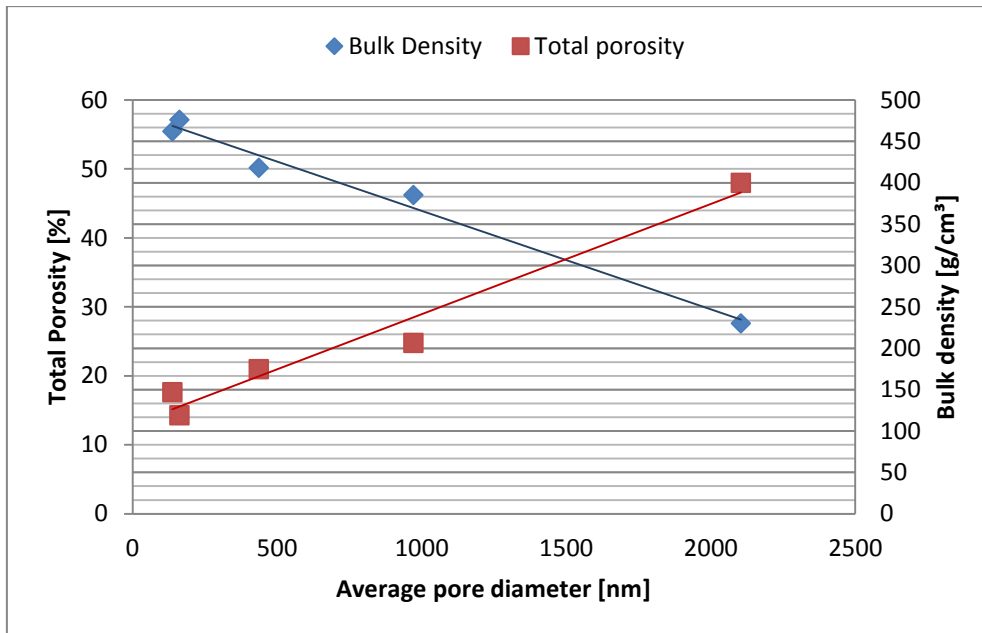
Figure 39: Influence of pore diameter on the bulk density and total porosity

In addition, electron microscopy images of the selected powder samples were taken in order to study particle morphology from a qualitative point of view. These images are shown in Figure 40.
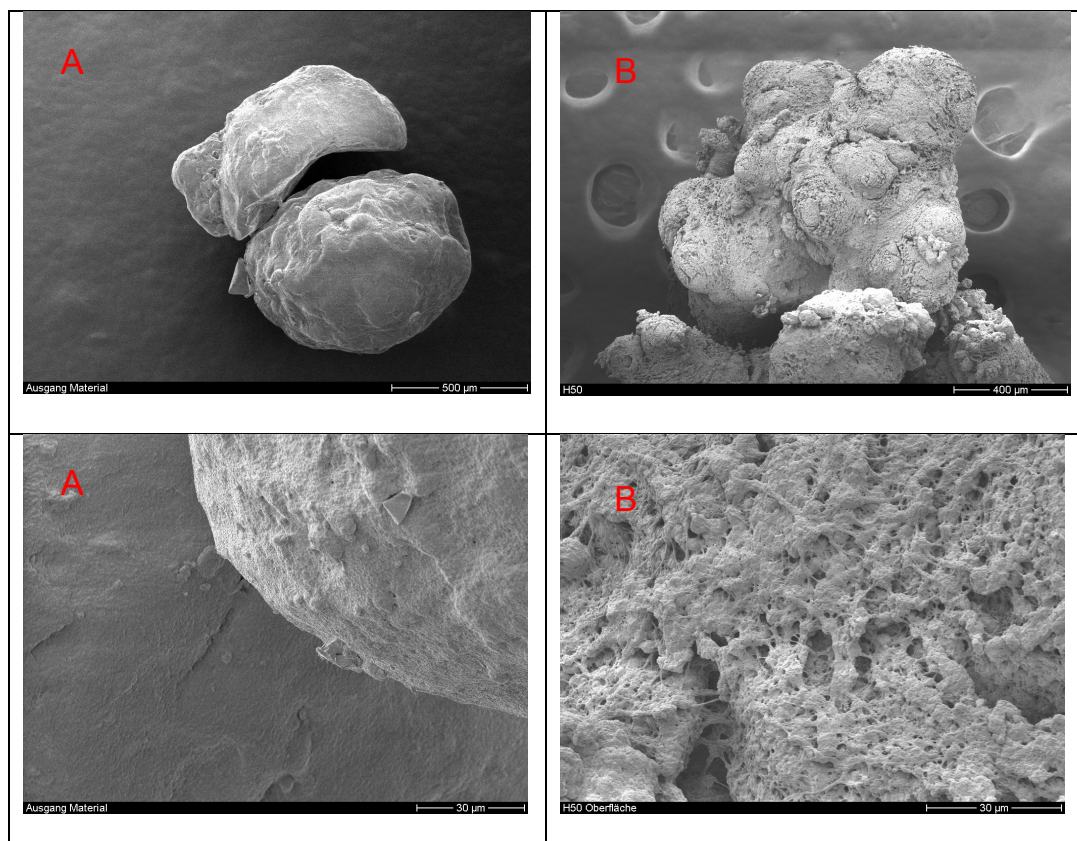
Figure 40: SEM Micrographs of the surface of PP samples A) PP20 (standard procedure) B) PP50 (5% ethylene).

The images above show two different PP samples. Images denoted with "A" correspond to sample PP20, a gas-phase polymerization of catalyst A with standard-prepoly conditions. The images denoted "B" correspond to sample PP 50, a bulk-phase polymerization of catalyst A with ethylene being present during prepolymerization. The upper micrographs exhibit the particle at higher scale and the lower micrographs are a zoom-in of the surface.

The two samples show certain roughness on the surfaces. The micrographs "A" exhibit a more compact surface compared to micrograph "B", which shows much more pores on the outer surface, which is in line with the results of porosity measurements.

To conclude the screening studies, the impact of prepolymerization conditions on activity and particle morphology has to be noted. For both catalysts A and B in both polymerization processes studied, -gas-phase polymerization and bulk phase polymerization- the most efficient measure to reduce bulk density and increase particle porosity while maintaining high activity is addition of a small amount of ethylene in the prepolymerization step.

7.4   External Prepolymerization

The in-situ-prepolymerization procedure has two major shortcomings:

1) Transient heating up period from prepoly- to main polymerization in this heating-up stage, polymerization conditions are not constant and undefined. The exact degree of prepolymerization is not known.

2) The carry-over from ethylene from prepolymerization to main polymerization cannot be avoided, the amount of unreacted ethylene and its impact on matrix polymerization is not known.

In order to overcome these problems, a new procedure with external prepolymerization was applied, details of the procedure can be found in chapter 4.5.4)

7.4.1 Reproducibility of external prepolymerization

In order to confirm both the obtained morphological modifications as well as the external prepolymerization procedure, reproducibility must be ensured. The following figure shows the reproducibility of the external prepolymerization in the 0.25-liter calorimeter with catalyst A. Prepolymerization temperature was 25°C, 15 to 25 mg catalyst were used per experiment, no hydrogen but 5 mol-% ethylene were applied, the prepolymerization was run for 10 minutes. The obtained degree of prepolymerization is consistent and reproducible.
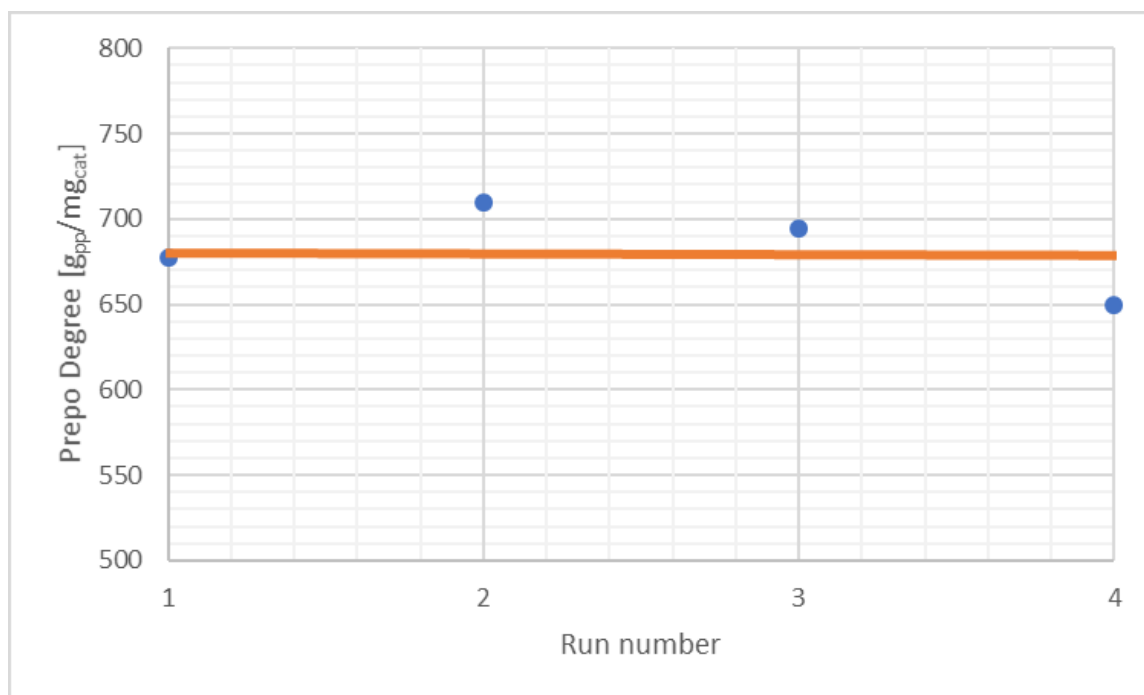
Figure 41: Prepolymer reproducibility in the 0.25-liter calorimeter

As it can be seen the external prepolymerization is within the frame of typical experimental errors constant. For all four reproducibility runs, prepolymerization degrees between 650 and 710 g/g were reached.

7.4.2 External prepolymerization with different ethylene content

For a systematic study of the impact of ethylene during prepolymerization on particle morphology, a series of experiments with different ethylene content in the prepoly step was performed. The ethylene content was varied from 0 to 10 mol-% ethylene. Table 7 shows the obtained results for the catalyst A and catalyst B.

Table 7: External prepoly with different ethylene content

Catalyst	C_2 conc. [mol%]	T_{prepo} [°C]	m_{cat} [mg]	TEA [ml]	Donor [ml]	m_{powder} [g]	Prepo Degree %
A	1,25	25-28	19,0	0,368	0,016	8,7	458
A	2,5	25-28	13,0	0,248	0,011	7,0	538
A	5	28-30	12,4	0,237	0,010	8,4	677
A	10	30-35	20,0	0,382	0,017	14,1	705
B	1,25	25-28	26,0	0,497	0,025	12,0	462
B	2,5	25-28	10,0	0,191	0,009	4,6	460
B	5	28-30	6,2	0,118	0,006	4,3	694
B	10	30-35	8,0	0,153	0,007	6,0	750

In this type of pre-reactions a Al/Ti = 260 ratio and a Al/Do = 10 ratio was used. As it can be seen the ethylene concentration raises the degree of prepolymerization (DP). This is expected as ethylene raises the polymerization activity.

Unfortunately, at high concentrations of ethylene the released heat cannot be compensated and the reactor temperatures raised up to 35°C. Both the increased catalyst activities and the increasing temperature led to relatively high degrees of polymerization. For industrial applications, the degree of prepolymerization should be lower. Therefore, polymerization temperature was reduced to 10°C and the prepolymerization time was reduced to 7 minutes.

Due to these two changes the degree of prepolymerization was constant between 300 and 600 (Table 8). It is also remarkable to notice that high ethylene concentrations during the prepolymerization must be carefully cooled down. A temperature difference between outside and inside temperature of 10°C is common by concentrations of 5 mol-% and higher.

Table 8: Improved external prepoly with different ethylene content

Catalyst	C$_2$ conc. [mol-%]	T$_{prepo}$ [°C]	m$_{cat}$ [mg]	TEA [ml]	Donor [ml]	m$_{powder}$ [g]	Prepo Degree %
A	1,25	20-25	10	0,191	0,008	4,7	470
A	2,5	20-25	8,1	0,155	0,006	3,5	432
A	5	15-25	5,2	0,099	0,004	2,6	500
A	10	15-25	5,3	0,01	0,004	2,5	472
B	1,25	20-25	15	0,287	0,014	6,3	420
B	2,5	20-25	10	0,191	0,009	3	300
B	5	15-25	11,4	0,218	0,01	5,6	491
B	10	15-25	7,5	0,143	0,007	4,5	600

7.4.3 Morphology prepolymer

In order to study particle morphology of the prepolymer; SEM micrographs of prepolymer of both catalysts were taken (Figure 42 and Figure 43).
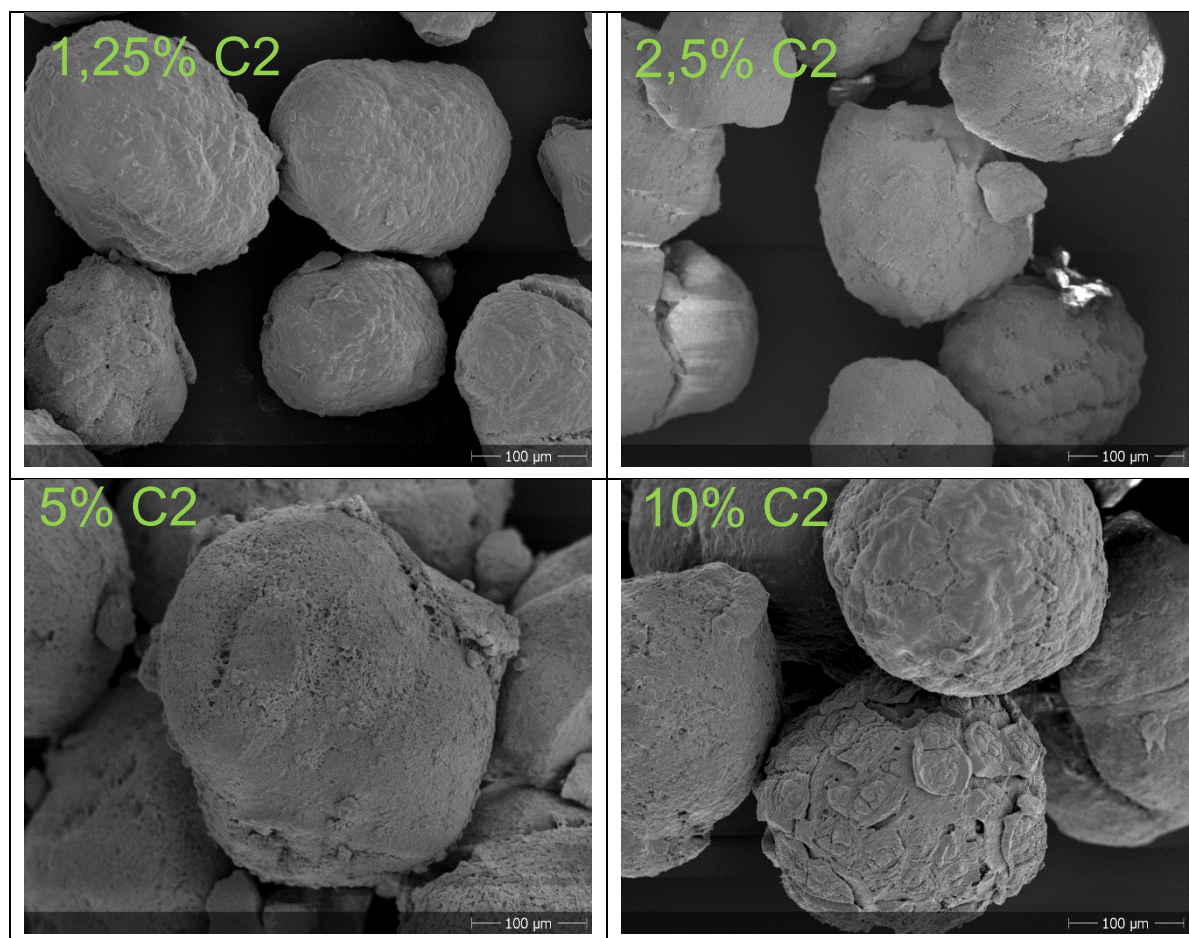
Figure 42: SEM Micrographs of prepo-powder with adjusted morphology (catalyst A)
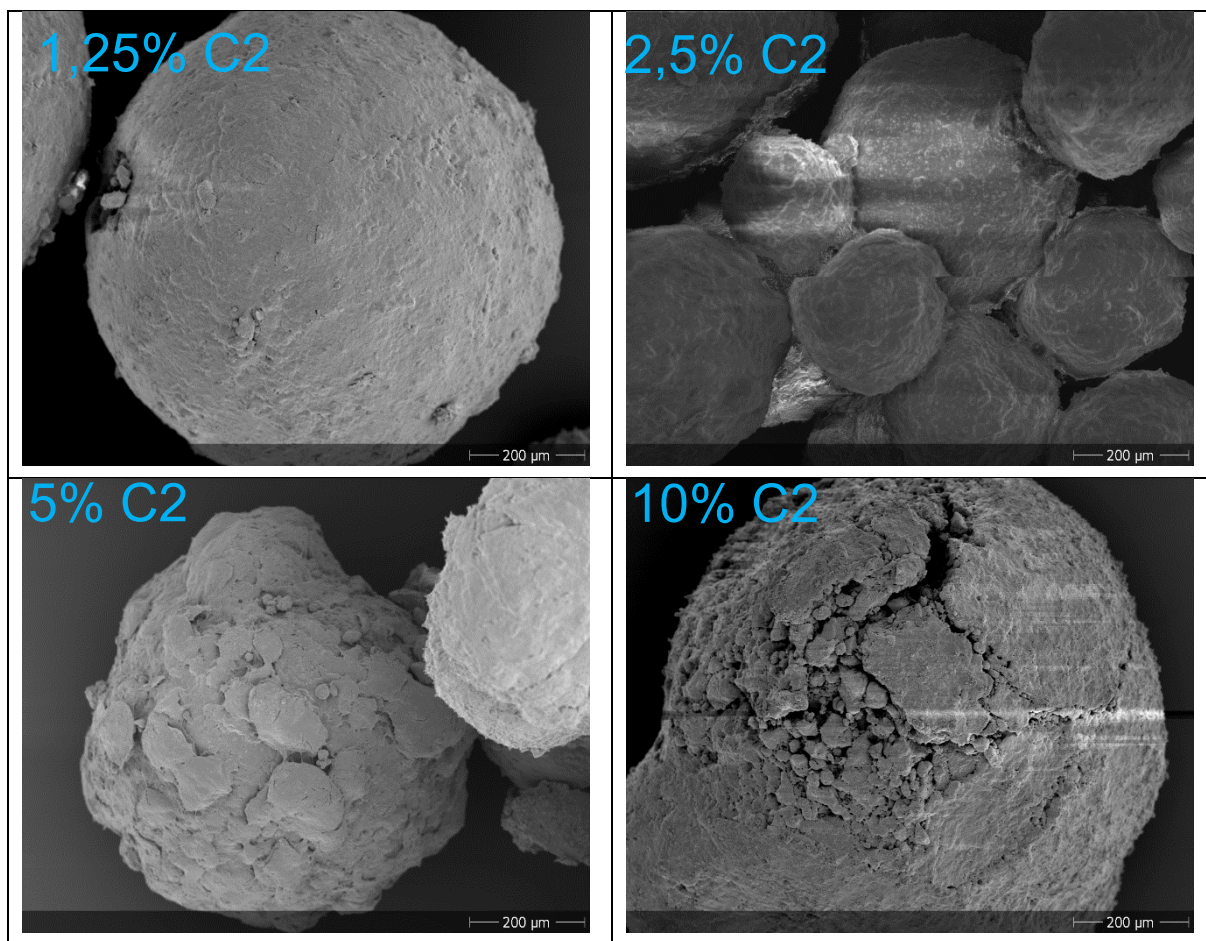
Figure 43: SEM Micrographs of prepo-powder with adjusted morphology (catalyst B)

For the catalyst A the prepolymerized catalyst has a diameter of around 100 µm. This size remains constant independent of the concentration of added ethylene during the prepolymerization. The powder obtained has a spherical shape. For the case of 1.25 mol-% the effect of ethylene during prepolymerization is barely measurable.

Morphological changes on the surface of the prepo-powder are noticeable from a concentration of 5 mol-% or higher. In these cases, the surface is more porous and some cracks are visible.

In case of catalyst B, particle size of the prepolymer powder varies with ethylene content between 300 and 600 µm. The higher the ethylene content the larger the particle size, this is probably related to the increase in productivity resp. degree of prepolymerization. Comparable to catalyst A, the surface of the prepo-powder is for catalyst B visually influenced at concentrations higher than 5 mol-% ethylene.

7.5 Homopolymerization with modified prepolymerized powder

After inert recovery of the prepolymers described in chapter 7.4, these prepolymers were tested in homopolymerization. For homopolymerizations of these prepolymers, the procedures described in chapter 4.5.5 (gas-phase polymerization) and 4.5.6 (bulk phase polymerization) were used.

In contrast to the runs with in-situ prepolymerization described in chapter 7.2, the procedure with external prepolymerization ensures that there is no carry-over of ethylene from the prepolymerization to the main stage polymerization.

In the following, the obtained results for catalyst kinetics and morphology in homopolymerization as function of ethylene content in the prepolymerization will be discussed.

7.5.1 Kinetics and bulk density

The results for activity and bulk density of gas-phase homopolymerizations at 70°C, 20 bar and 1 mol-% hydrogen as function of ethylene content in the prepolymer can be seen in Figure 44 (for catalyst A) and Figure 45 (for catalyst B)
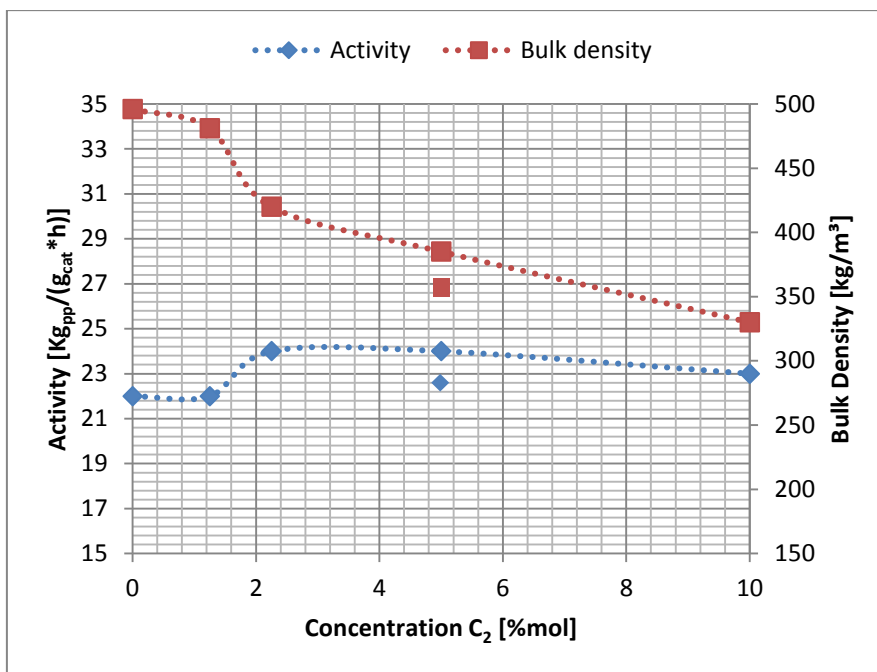
Figure 44: Effect of ethylene in external prepoly on gas-phase polymerization (Catalyst A)
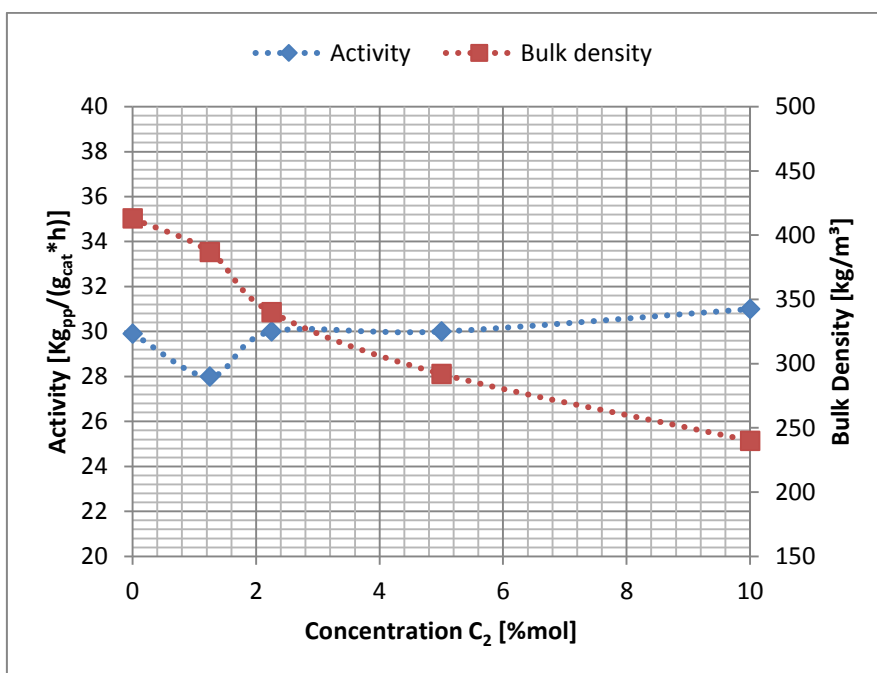
Figure 45: Effect of ethylene in external prepoly on gas-phase polymerization (Catalyst B)

For both catalysts activity in the gas phase remains nearly constant (20 to 25 $Kg_{pp}/(g_{cat}*h)$ for catalyst A and 27 to 32 $Kg_{pp}/(g_{cat}*h)$ for catalyst B), but bulk density reduces significantly with increasing ethylene content, for catalyst A from

around 500 kg/m³ for prepolymer without ethylene to about 340 kg/m³ for prepolymer with 10 mol-% ethylene. For catalyst B, the reduction in bulk density is similar, from about 420 kg/m³ for prepolymer without ethylene to 240 kg/m³ for prepolymer with 10 mol-% ethylene.

In addition, bulk phase polymerizations were carried out with prepolymers with different ethylene content of both catalysts A and B. Bulk phase reaction conditions were 80°C, 39 bars and 3 mol-% hydrogen. In Figure 46 the results are shown for catalyst A in Figure 47 for catalyst B:
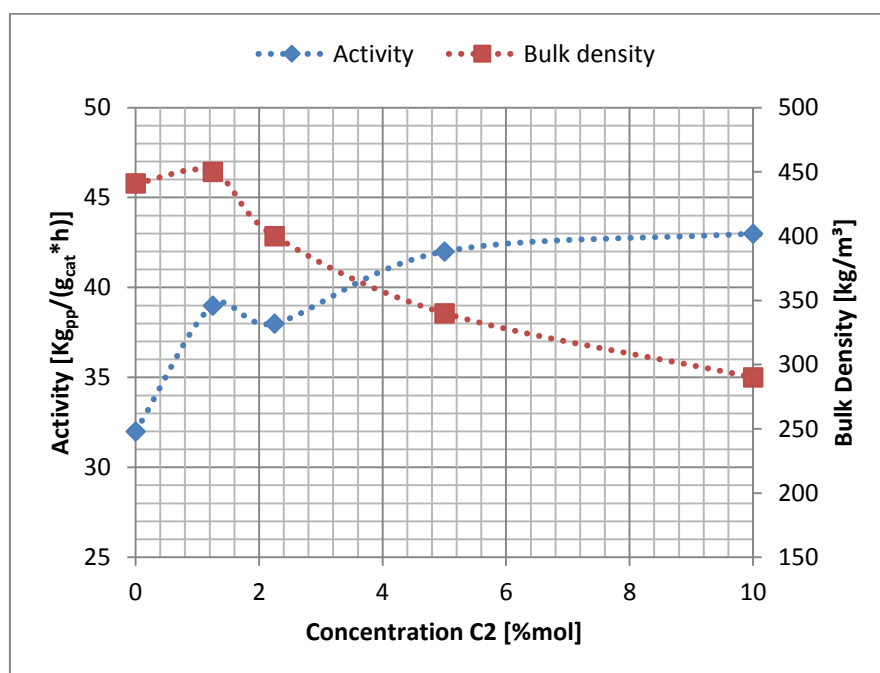
Figure 46: Effect of ethylene in external prepoly on bulk-phase polymerization (Catalyst A)
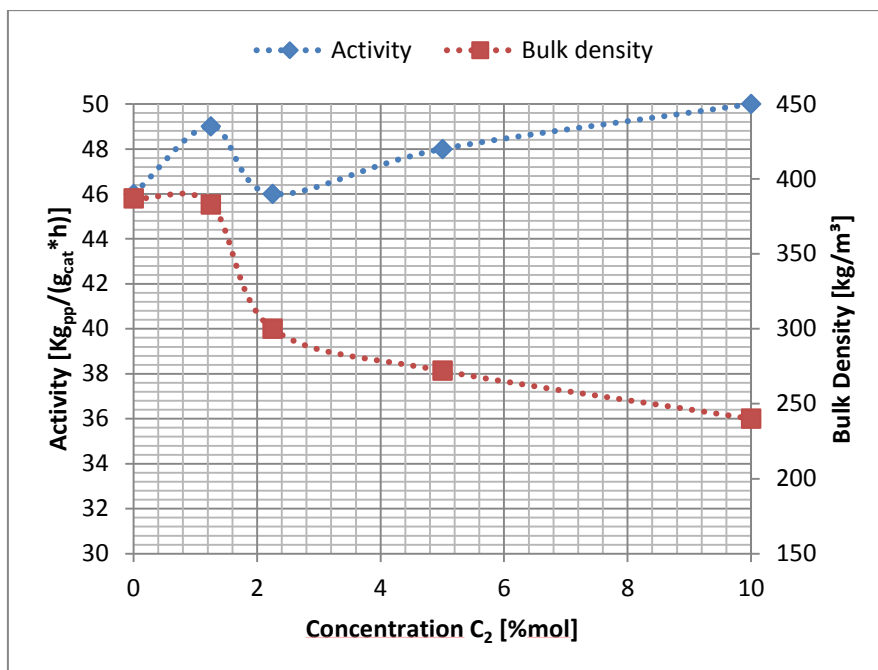
Figure 47: Effect of ethylene in external prepoly on bulk-phase polymerization (Catalyst B)

In bulk phase reactions, for catalyst A a slight increase of activity with increasing ethylene content in the prepolymer is noticed. For catalyst A, activity in bulk phase conditions increased from 32 $Kg_{pp}/(g_{cat}*h)$ for prepolymer without ethylene to about 42 $Kg_{pp}/(g_{cat}*h)$ for prepolymer with 10 mol-% ethylene.

For the catalyst B, observed activities were within the frame of experimental error nearly constant with 46 to 50 $Kg_{pp}/(g_{cat}*h)$ for all ethylene contents in the prepolymer.

For both catalysts, bulk density was significantly reduced for ethylene contents in the prepolymer of 2.5 mol-% or more. For catalyst A, bulk density reduces from about 440 kg/m³ for prepolymer with 2.5 mol-% ethylene or less to about 300 kg/m³ for prepolymer with 10 mol-% ethylene.

For catalyst B, bulk density reduces from about 400 kg/m³ for prepolymers with low ethylene content of 2.5 mol-% or less to about 240 kg/m³ for prepolymers with 10 mol-% ethylene.

Table 9 summarizes the highest and lowest bulk densities measured.

Table 9: Bulk density decrease through ethylene in der prepo

	Ethylene during prepo	
Cat-phase	0% C2	10% C2
A-Gas	496	330
B-Gas	413	240
A-Bulk	441	290
B-Bulk	387	240

The obtained results for homopolymerizations both in gas-phase and in bulk phase polymerization with prepolymers of both catalysts clearly confirms the results of the screening study in chapter 7.2. Addition of ethylene during prepolymerization is an effective handle to reduce bulk density without compromising activity.

7.5.2 Morphological characterization

SEM micrographs polymer after homopolymerization stage can be seen in Figure 48.
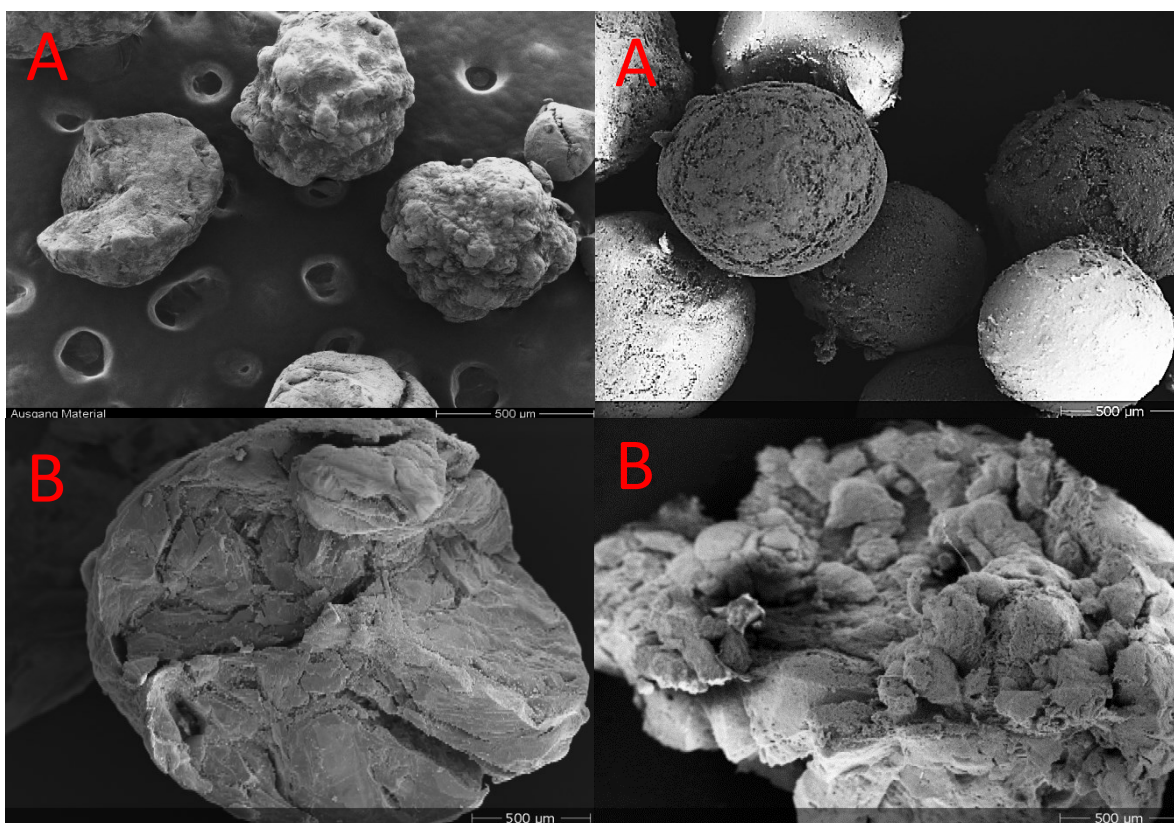
Figure 48: Effects of the settings on the morphology of polypropylene: Left side up: Polypropylene at 70°C, 20 bar and 1 mol-% H_2 (Catalyst A), Right side up: Polypropylene with 10 mol-% C_2 (Catalyst A), Left side down: Polypropylene at 80°C, 39 bar and 1 mol-% H_2 (Catalyst B), Right side down: polypropylene with 10 mol-% C_2 (Catalyst B)

The texture of the selected samples surfaces differed. The surface of the particles became rougher with more ethylene content during the prepolymerization. Samples without ethylene exhibit a more compact form and smaller pores, while samples with ethylene during the prepolymerization seem to be larger and more porous.

For selected samples, Hg-porosity measurements were carried out. Table 10 summarizes the measured pore volumes and porosities of the measured homopolymer samples. The given numbers cannot be seen as absolute values since these strongly depend in measurement conditions, but comparisons between different samples are clearly possible.

In line with the bulk density measurements, there is the clear trend that addition of ethylene during prepolymerization leads to increase of porosity. Furthermore, porosity of PP obtained through gas-phase polymerization is higher compared to bulk-phase polymerization.

One reason for the differences between bulk- and gas-phase polymerization might be the different concentration ratios between propene, ethylene and hydrogen in bulk- and gas-phase polymerization, i.e. the obtained MFR's are in bulk polymerization much lower compared to gas-phase polymerization.

The differences in polymer properties in turn might influence rearrangement during particle-growth and hence particle morphology. On the other hand, differences in particle temperature, especially at the beginning of the reaction, between bulk polymerization and gas-phase polymerization might influence morphology generation.

Table 10: Hg-Measurement of iPP with adjusted morphology

Catalyst	C2 Conc. [mol-%]	Phase	V_{tot} [cm³/g]	Porosity [%]
A	0	Gas	0,59	12
A	5	Bulk	0,63	14,8
A	10	Bulk	0,73	22
A	5	Gas	1,08	21,1
A	10	Gas	1,42	29,5

Catalyst	C2 Conc. [mol-%]	Phase	V_{tot} [cm³/g]	Porosity [%]
B	0	Bulk	0,65	10
B	5	Bulk	0,69	18,1
B	10	Bulk	0,7	24
B	5	Gas	0,93	23,6
B	10	Gas	1,04	37

The standard procedures without ethylene during the prepolymerization produce iso-PP with the smallest porosity. Both catalysts have porosity between 10 and 13% independent of the phase conditions during the matrix polymerization.

With the addition of ethylene during the prepolymerization, also the porosity rises significantly. For catalyst A, the porosity was twice higher and for catalyst B almost 4 times higher. As discussed in chapter 7.3, bulk density is inversely proportional to porosity. As the porosity rises, also the available volume throughout the pores will increase and correlates to small bulk densities.

The pore size distribution of the standard procedure and the samples with highest porosity for catalyst A and catalyst B are shown in Figure 49 and Figure 50.
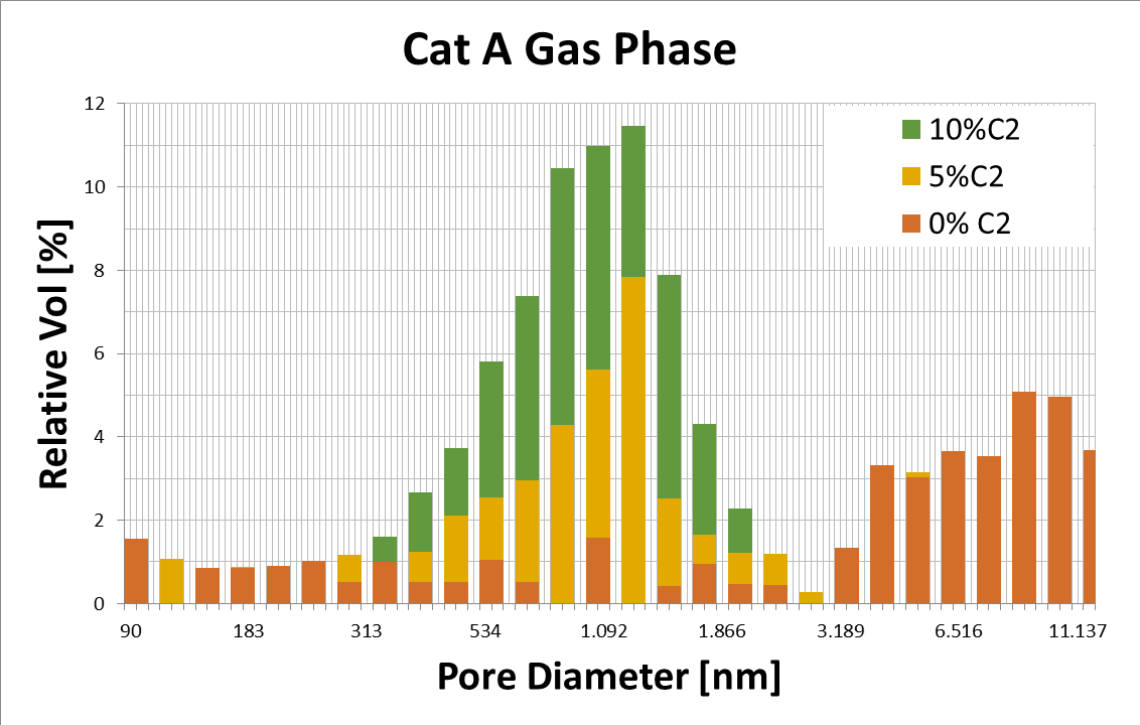
Figure 49: Pore size distribution by adding ethylene during the prepolymerization (Catalyst A)
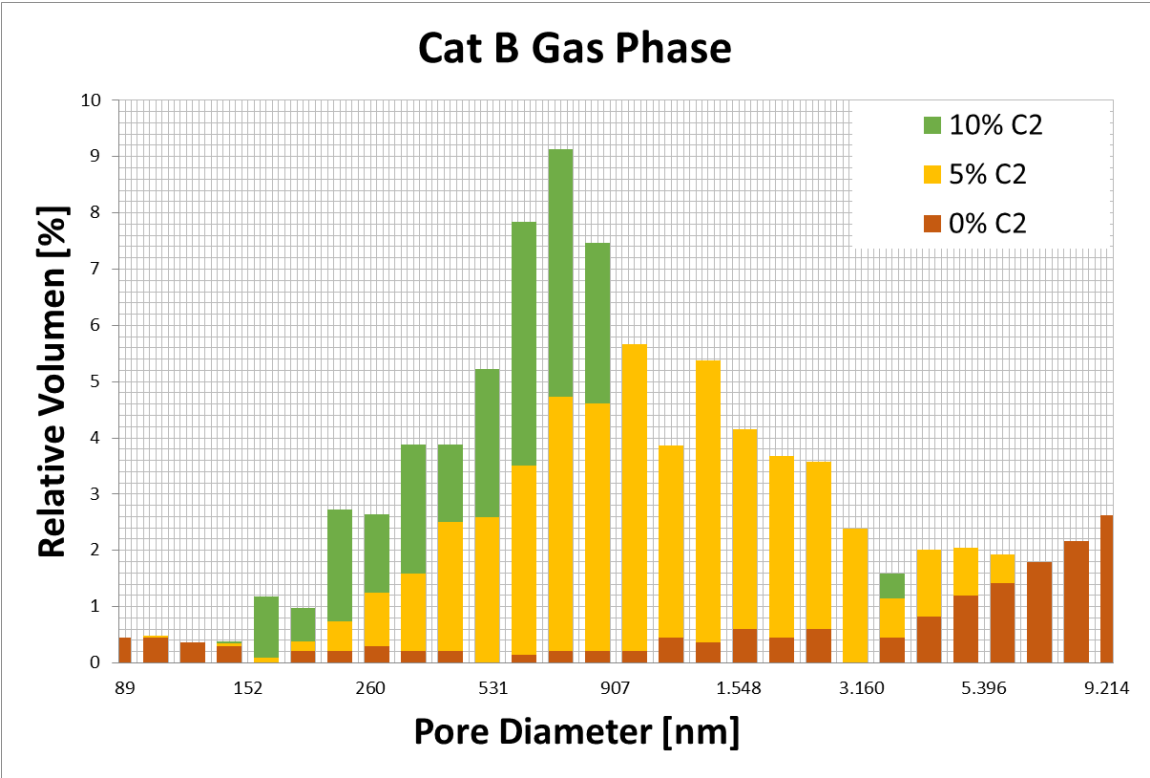
Figure 50: Pore size distribution by adding ethylene during the prepolymerization (Catalyst B)

It is cleary visible, that with increasing ethylene content in the prepolymer, the matrix polymer shows a shift of the pore size distribution to lower pore sizes.

7.5.3 Differential scanning calorimetry (DSC)

To ensure that crystallinity of the homopolymer was not affected by adding ethylene during the prepolymerization, DSC measurements were performed.

Catalyst	C2 Conc. [mol-%]	Phase	ΔH [J/g]	Crystallinity [%]
A	0	Gas	91,08	44
A	5	Bulk	103,707	50,1
A	10	Bulk	103,707	50,1
A	5	Gas	105,984	51,2
A	10	Gas	99,36	48

Catalyst	C2 Conc. [mol-%]	Phase	ΔH [J/g]	Crystallinity [%]
B	0	Gas	107,847	52,1
B	5	Bulk	102,672	49,6
B	10	Bulk	112,608	54,4
B	5	Gas	97,29	47
B	10	Gas	97,497	47,1

For catalyst A, crystallinity is between 44% and 51%. Polymers produce with catalyst B show slightly higher crystallinities compared to catalyst A. For both cases, bulk phase reactions produce PP with slightly higher crystallinity than gas phase polymerization. Addition of ethylene during prepolymerization doesn't show a significant influence on crystallinity of the matrix polymers.

7.5.4 Sorption measurements

The influence of the morphology modifications by prepoly conditions on the resulting mass-transfer has been studied following the approach introduced by Kröner [115]:

From given polymer samples, sorption measurements with both a compressed film and porous powder are carried out. From the film measurements with known morphology effective diffusion coefficients are determined. From the powder sorption measurements effective diffusion length are determined, using the diffusion coefficient from the film measurements. Target was to study how this effective diffusion length can be adjusted by prepoly conditions.

Since particle porosity influences mass transfer, pore-free PP films were prepared as described in chapter 6. Sorption experiments were carried out using the sorption balance illustrated in chapter 6 and the effective diffusion coefficient was determined as explained in chapter 6.1.3. As the thickness of the films remains constant, effective diffusion coefficient of the measured material equals the slope of the sorption measurement. No polymer swelling was assumed due to its small effect on the effective diffusion coefficient.

In Figure 51 the normalized sorption curves of propylene for polymer films (catalyst A and B with 10 mol-% ethylene during the prepolymerization) and the calculated curves from Crank's model, by using the half of the film thickness as parameter l, are shown:
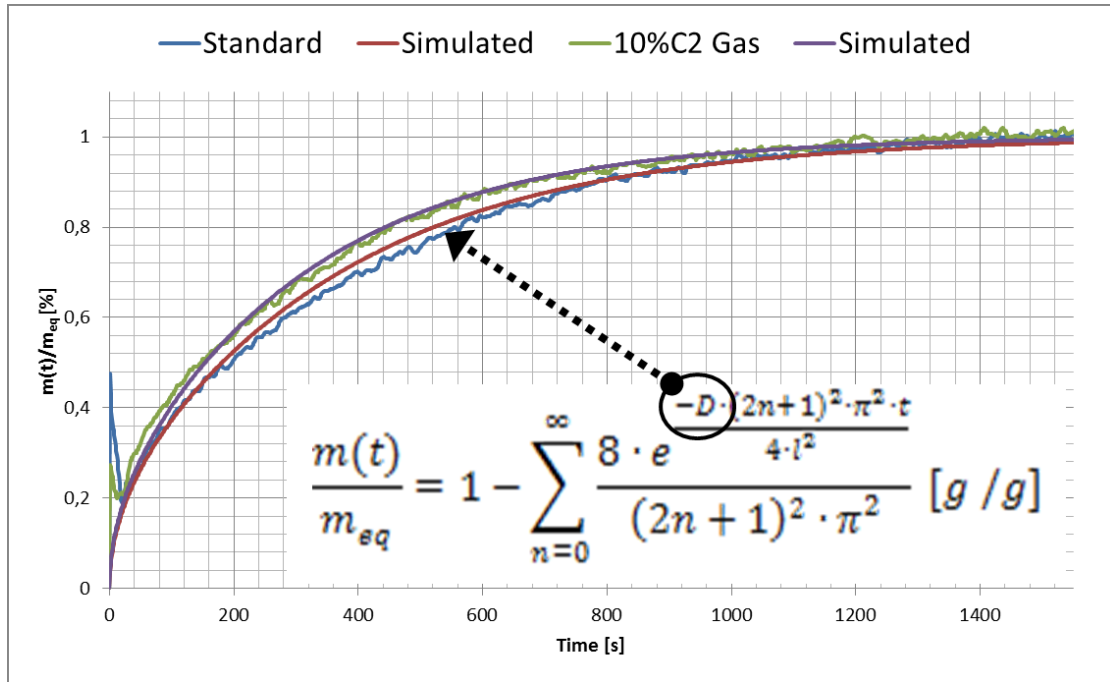
Figure 51: Estimation of diffusion coefficient for iso-PP films (70°C, 11bar, propylene)

The measured values and the simulated slopes through crank's mass transfer solution fit with each other. Due to gas filling, only values after 50 seconds are considered.

An overview of the effective diffusion coefficients determined is given in Table 11.

Table 11: Effective diffusion coefficients for samples with adjusted morphology

A cat		Propene	Ethylene
Name	Thickness [µm]	D_{eff} [10^{-11} m²/s]	D_{eff} [10^{-11} m²/s]
Standard	600	9	9,54
5% C2 Gas	664	8,31	8,57
10% C2 Gas	687	6,53	6,66
5% C2 Bulk	696	6,41	8,65
10% C2 Bulk	691	6,09	7,11

B cat		Propene	Ethylene
Name	Thickness [µm]	D_{eff} [10^{-11} m²/s]	D_{eff} [10^{-11} m²/s]
Standard	732	6,32	
5% C2 Gas	685	7,37	8,78
10% C2 Gas	665	7,59	6,93
5% C2 Bulk	736	5,57	8,44
10% C2 Bulk	752	7,17	8,57

The resulting films have an average thickness of 0,69 mm; the exact thickness is measured prior experiment with a digital measuring slide The determined effective diffusion coefficients for propylene D_{eff} are for all samples in between 6,09 to 9 x 10^{-11} m² s^{-1}, which is in the range of literature values.

After obtaining the diffusion coefficients, sorption measurements were carried out with powder samples. In Figure 52 and Figure 53 the normalized sorption curves for propylene in matrix polymers made of prepolymers with different ethylene content are shown.
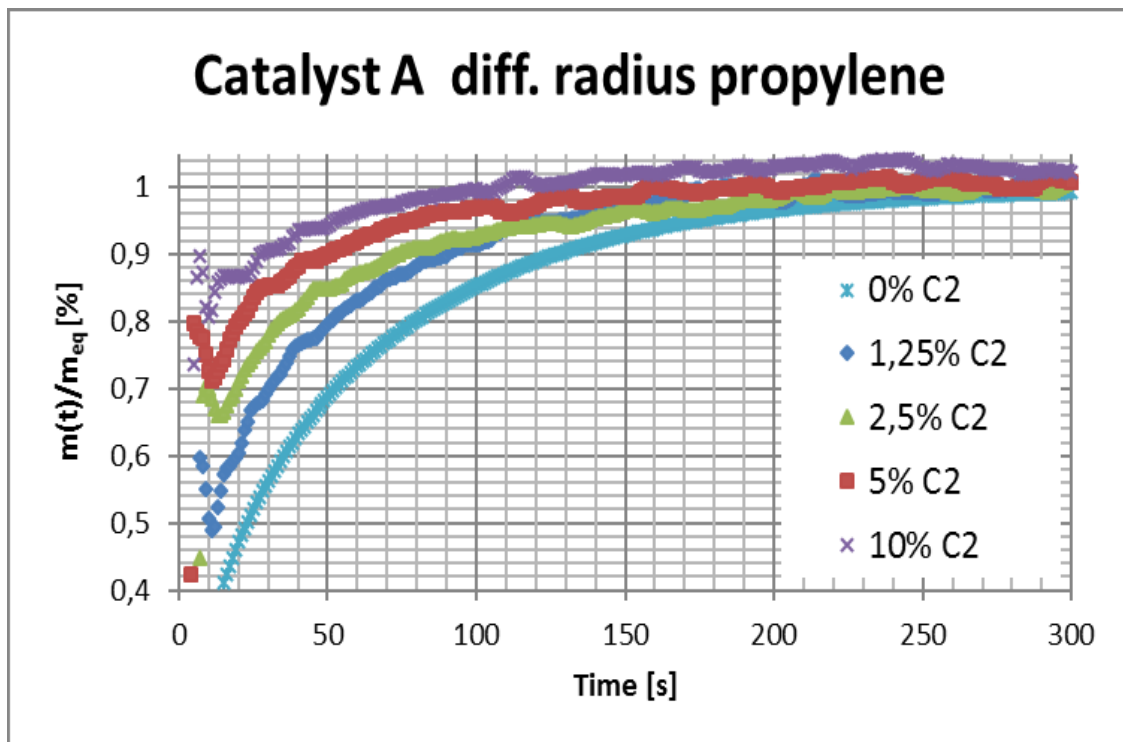
Figure 52: Sorption measurement for samples with ethylene during prepolymerization (70°C; 12 bar, propylene, catalyst A)
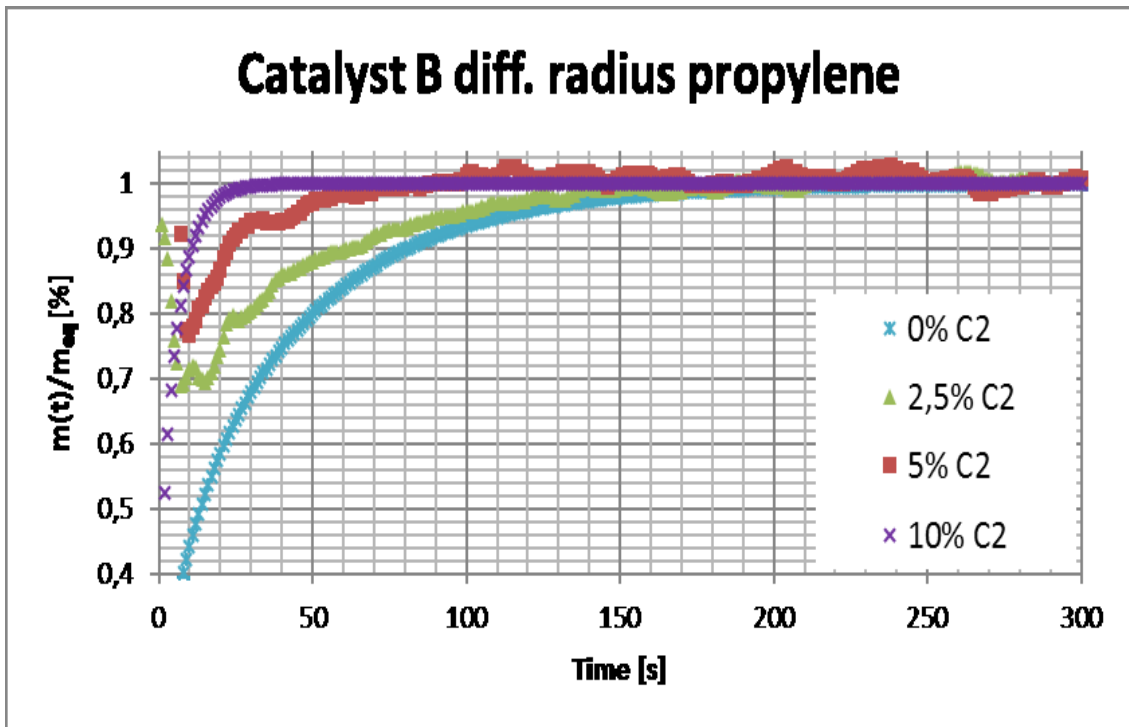
Figure 53: Sorption measurement for samples with ethylene during prepolymerization (70°C; 12 bar, propylene, catalyst B)

Already from the sorption curves it is clearly visible, that the samples with ethylene during the prepolymerization are faster in steady state, which means that mass-transfer is faster.

As described in chapter 6, using the effective diffusion coefficient derived from film measurements (Table 11), using Crank's solution of the diffusion equation for a sphere, the effective diffusion length can be determined.

The determined effective diffusion length are summarized in Table 12 :

Table 12: Effect of C2 during prepolymerization on the effective length of diffusion determined following the approach of Kröner [98]

	Diffusion radius [µm]			
	Cat A		Cat B	
C2[mol-%]	Bulk phase	Gas phase	Bulk phase	Gas phase
0		260	220	
1,25	350	220	195	160
2,5	280	190	180	120
5	250	180	120	100
10	250	150	80	80

The effective diffusion length is for prepoly without ethylene in the range of 260 µm (catalyst A) resp. 220 µm (catalyst B).

The diffusion length is in general lower for catalyst B compared to catalyst A and in gas-phase polymerization it is lower compared to bulk polymerization, which is both in line with bulk-density measurements.

With addition of ethylene in the prepolymerization, the effective diffusion length is effectively reduced, in case of catalyst A in gas-phase polymerization down to 150 µm, in case of gas-phase polymerization of catalyst B down to 80 µm.

The effect of this reduction in diffusion length on polymerization behavior will be discussed in chapter 8.3.

7.6   Results Copolymerization stage

In the sections above, it could be shown that particle morphology can be controlled by adjusting of prepolymerization conditions, in particular ethylene concentration during prepolymerization.

In order to see the impact of matrix morphology on the rubber incorporation, heterophasic copolymerizations were carried out according to the procedure described in chapter 4.5.7.

7.6.1 Effect of pressure and monomer composition on activity

The activity in the copolymerization stage depends strongly on pressure and monomer composition.

For an initial screening of activity, heterophasic copolymerizations were carried out for both catalyst A and B with a standard matrix polymer prepared by the following procedure:

- In-situ prepolymerization without ethylene at T = 25°C, p = 11 bar, for 10 minutes.
- Matrix polymerization in gas-phase at T = 70°C, p= 20 bar, H2 = 1 mol-% for 1 h.
- Gas-phase copolymerizations at T = 70°C, pressures between 11 and 21 bar, gas compositions between 25 and 75 mol-% ethylene and 1 h.

Average activities for catalyst A and B in the copolymerization are shown in Figure 54.
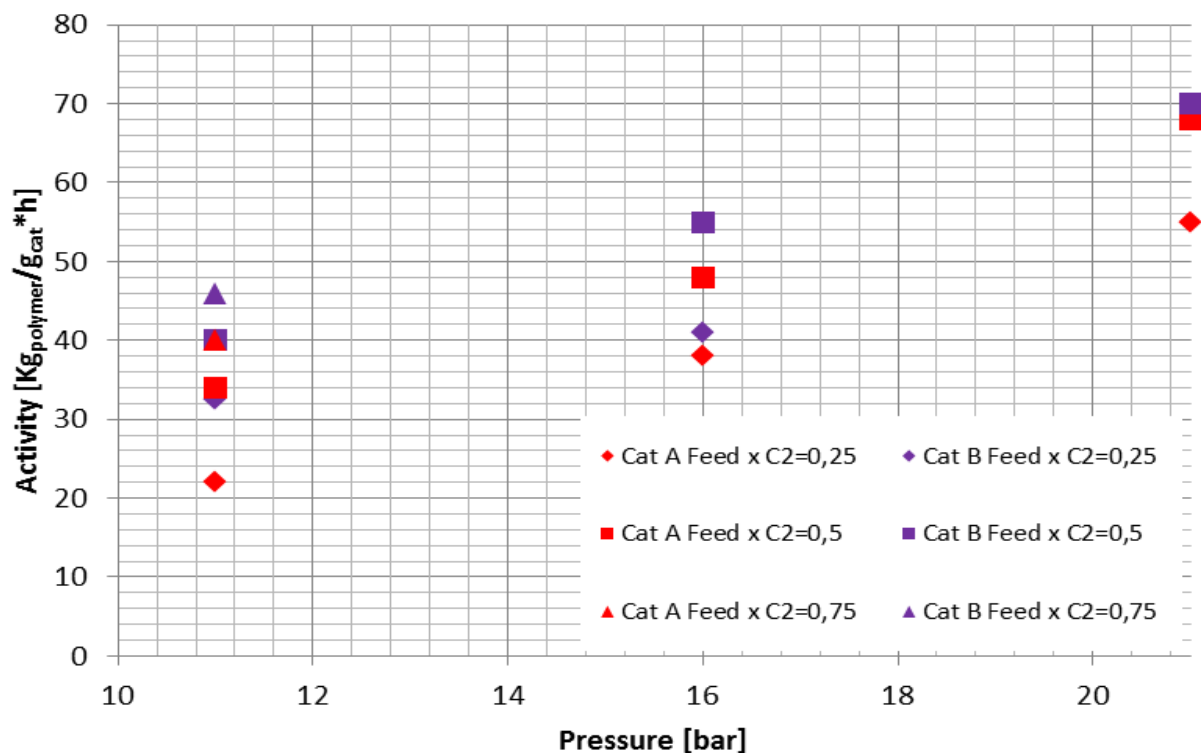
Figure 54: Average activities for copolymerizations with catalyst A and B.

High activities up to 70 $Kg_{pp}/(g_{cat}*h)$ have been observed, the magnitude measured activities agree with literature values [115]. Not surprisingly, activities increase with increasing pressure and increasing ethylene content in the gas-phase. Activity of catalyst B was higher than catalyst A. The observed reaction rates are on the boundary of the possible cooling capacity of the used reactor, temperature differences between thermostat and reactor of up to 25°C were measured.

7.6.2 Effect of prepolymers with adjusted morphology on activity in heco stage

In chapter 7.5.1 it was described, that the prepolymers with adjusted morphology had no or only minor effect on the polymerization rate in homopolymerization.

In order to check the influence on activity in the heco-stage a corresponding series of experiments were made

- External prepolymerizations with 0 to 10 mol-% ethylene in order to adjust particle morphology.
- Matrix polymerization for catalyst A and catalyst B at T = 70°C, p = 20 bar, H2 = 1mol-%
- Copolymerization at T= 70 p= 16 bar C2/C3 = 0,25 and 0,5 mol-%

Unexpectedly, for both catalysts A and B, activity in heco-stage decreases with increasing ethylene content in the prepolymer.

For catalyst A, activity in heco-stage at p = 16 bar, T = 70°C, C2/C3 = 0,5 mol-% decreases from 48 $Kg_{pp}/(g_{cat}*h)$ for prepolymers without ethylene to 28 $Kg_{pp}/(g_{cat}*h)$ for prepolymers with 10 mol-% ethylene. For catalyst B, activity in heco stage at the same settings decreases from about 55 $Kg_{pp}/(g_{cat}*h)$ to 32 $Kg_{pp}/(g_{cat}*h)$.

To verify this decrease on the activity another row of experiments at p = 16 bar, T = 70°C, C2/C3 = 0,25 mol-% was achieved. In this case, activity of catalyst A went from 38 $Kg_{pp}/(g_{cat}*h)$ to 24 $Kg_{pp}/(g_{cat}*h)$. For catalyst B a decrease from 44 $Kg_{pp}/(g_{cat}*h)$ to 27 $Kg_{pp}/(g_{cat}*h)$ was measured.

The observed average activities are depicted in Figure 55:
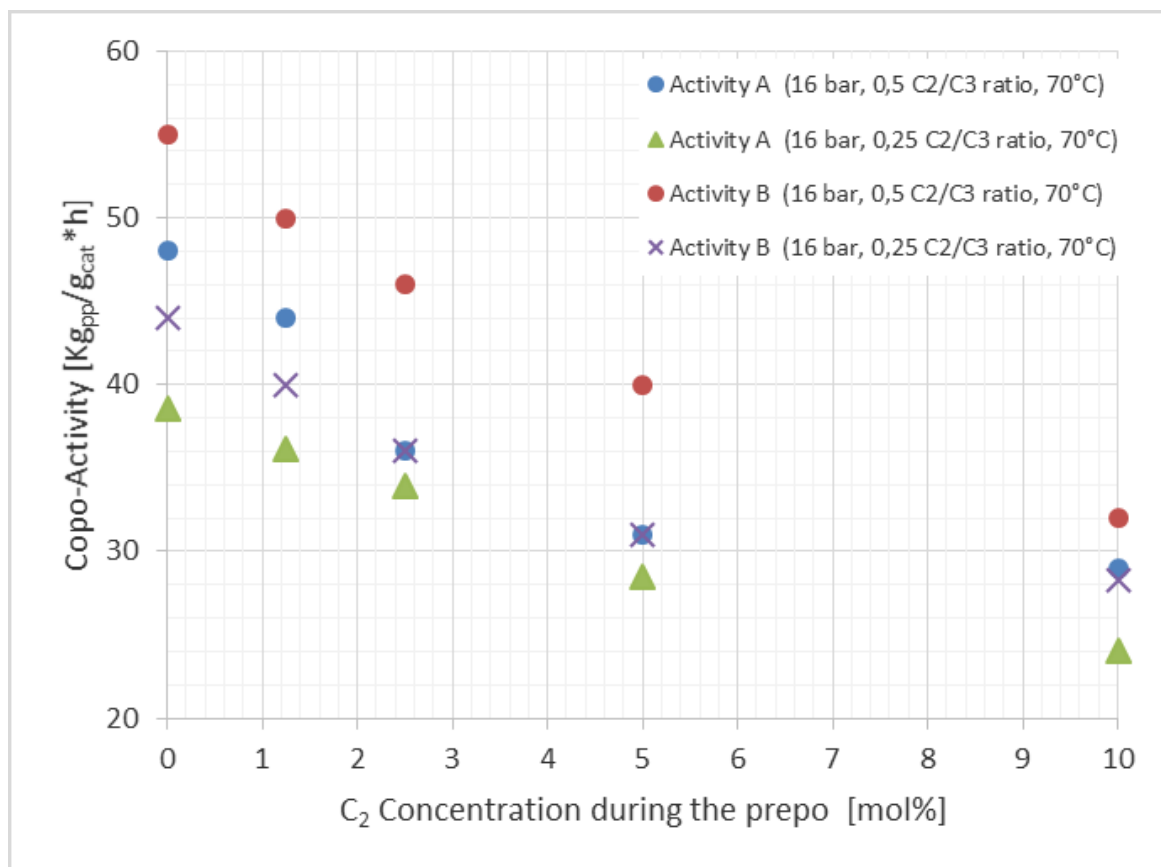
Figure 55: Copolymerization's activity with and without ethylene during the prepolymerization

Surprisingly, there is a clear and strong influence of ethylene content during prepolymerization on polymerization activity during copolymerization. For both catalysts studied, activity during copolymerization step drops with increasing ethylene concentration during prepolymerization.

Some potential reasons for this phenomenon could be the activation and subsequent deactivation of active center specific for ethylene already during prepolymerization step, but this should be studied further.

7.6.3 Ethylene incorporation

The ethylene incorporation behavior can be studied via plotting the ethylene content in the polymer versus the monomer composition.

For the two catalysts A and B at standard conditions -without ethylene in the prepolymerization stage- the incorporation behavior has been studied via:

- In-situ prepolymerization without ethylene at T = 25°C, p = 11 bar, for 10 minutes.
- Matrix polymerization in gas-phase at T = 70°C, p= 20 bar, H2 = 1 mol-% for 1 h.
- Gas-phase copolymerizations at T = 70°C, pressures between 11 and 21 bar, gas compositions between 25 and 75 mol-% ethylene and 1 h.

The resulting ethylene incorporation is depicted in Figure 56.
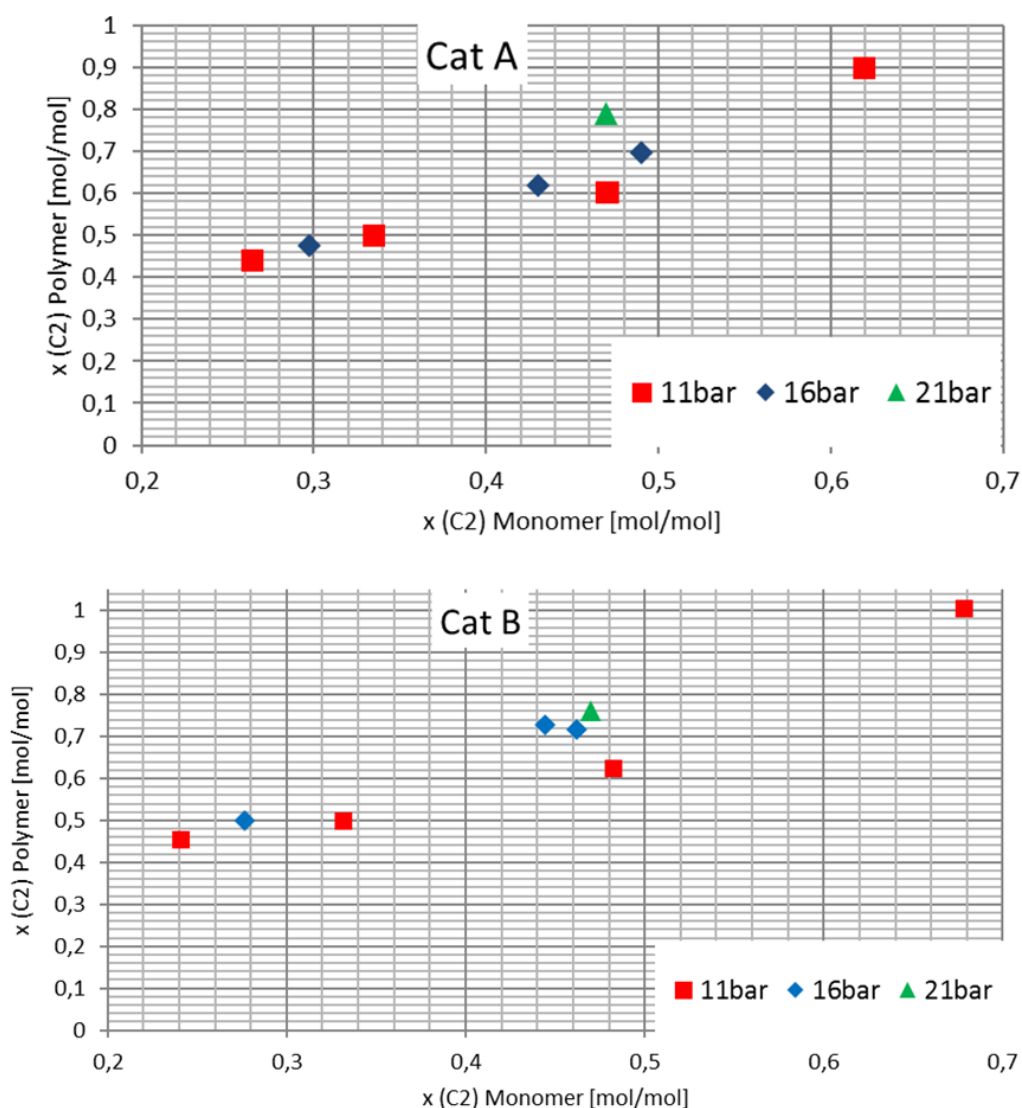
Figure 56: Monomer concentration ratios vs. copolymer incorporation ratios for catalyst A and B (no ethylene during the prepolymerization)

In general, ethylene incorporation is for catalyst B slightly higher compared to catalyst A.

There is a slight tendency for increased ethylene incorporation at higher pressures. This might be related to phase equilibria or mass-transfer effects.

According to previous studies of Kröner [115] and others, in the heco-stage there is a diffusion limitation for ethylene.

With increased porosity resp. reduced diffusion length, this diffusion limitation should decline, resulting in a higher ethylene incorporation. In order to check this hypothesis, a series of copolymerizations with prepolymers with adjusted morphology was carried out.

For the two catalysts A and B with adjusted morphology the ethylene incorporation in heco-stage was studied the following way;

- External prepolymerizations with 0, 1,25, 2,5, 5 and 10 mol-% ethylene, T = 25°C and 8 minutes
- Matrix polymerization in gas-phase at T = 70°C, p = 20 bar, H2 = 1 mol-% for 1 h.
- Gas-phase copolymerizations at T = 70°C, p = 16 bar, gas compositions between 25 and 60 mol-% ethylene and 1 h.

The resulting ethylene incorporation is depicted in Figure 57.
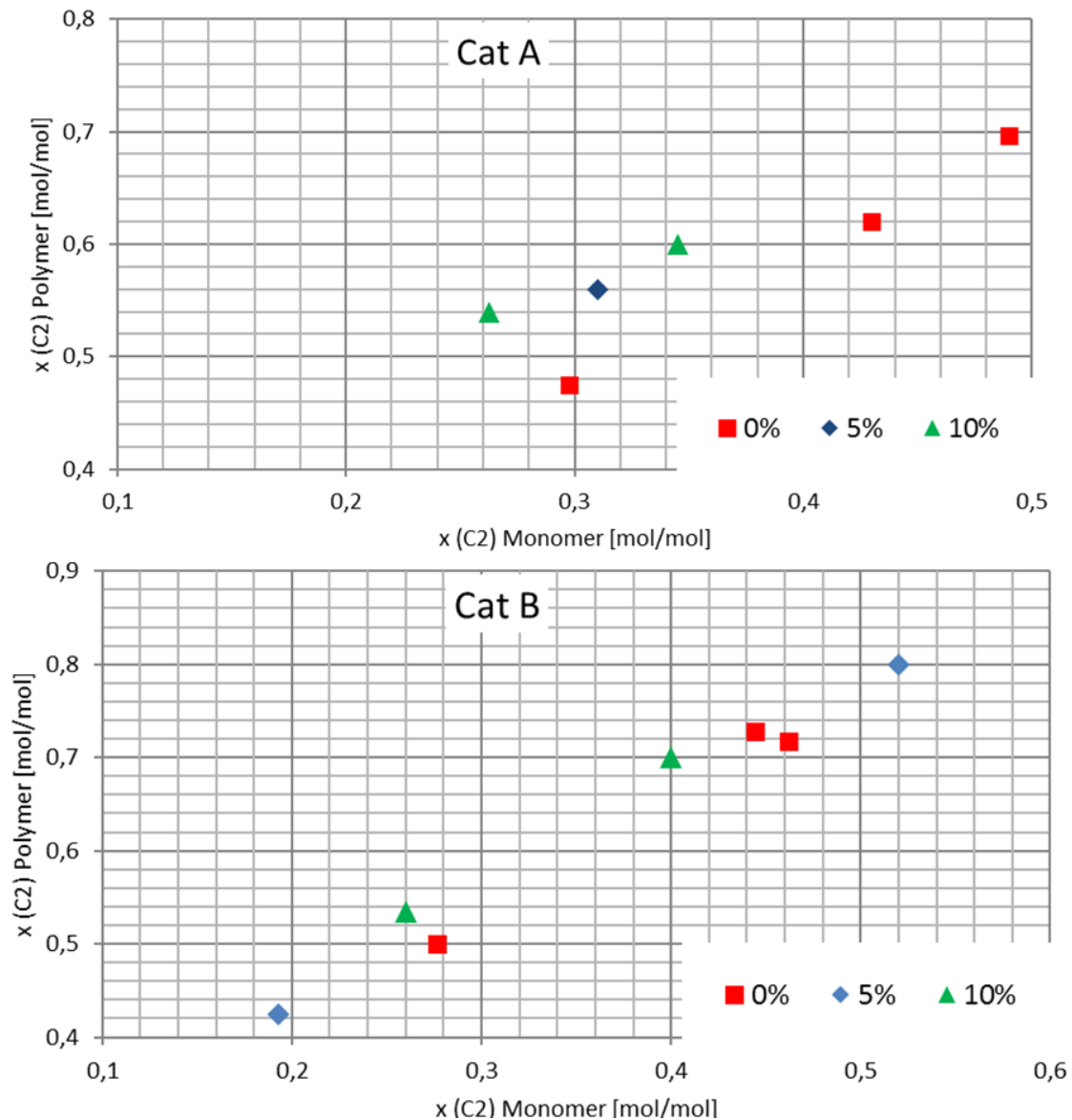
Figure 57: Monomer concentration ratios vs. copolymer incorporation ratios for catalyst A and B with adjusted morphology

Especially for catalyst A, the prepolymers with ethylene present show – compared to the standard prepolymerization without ethylene- a higher ethylene incorporation in the rubber stage. For a feed of 30 mol-% ethylene, the incorporation increases for prepolymers with adjusted morphology from about 48 mol-% to 55 mol-%.

This might be attributed to better mass-transfer due to reduced diffusion length and due to lower mass-transfer restrictions due to lower polymerization rate in case of adjusted morphology prepolymers.

7.6.4 Morphological characterization

In Figure 58, bulk densities before and after hecopolymerization are depicted as function of ethylene content during prepolymerization. Copolymerization conditions (pressure, temperature and ratio C_2/C_3) were kept constant at 16 bar and 70°C and 50/50.
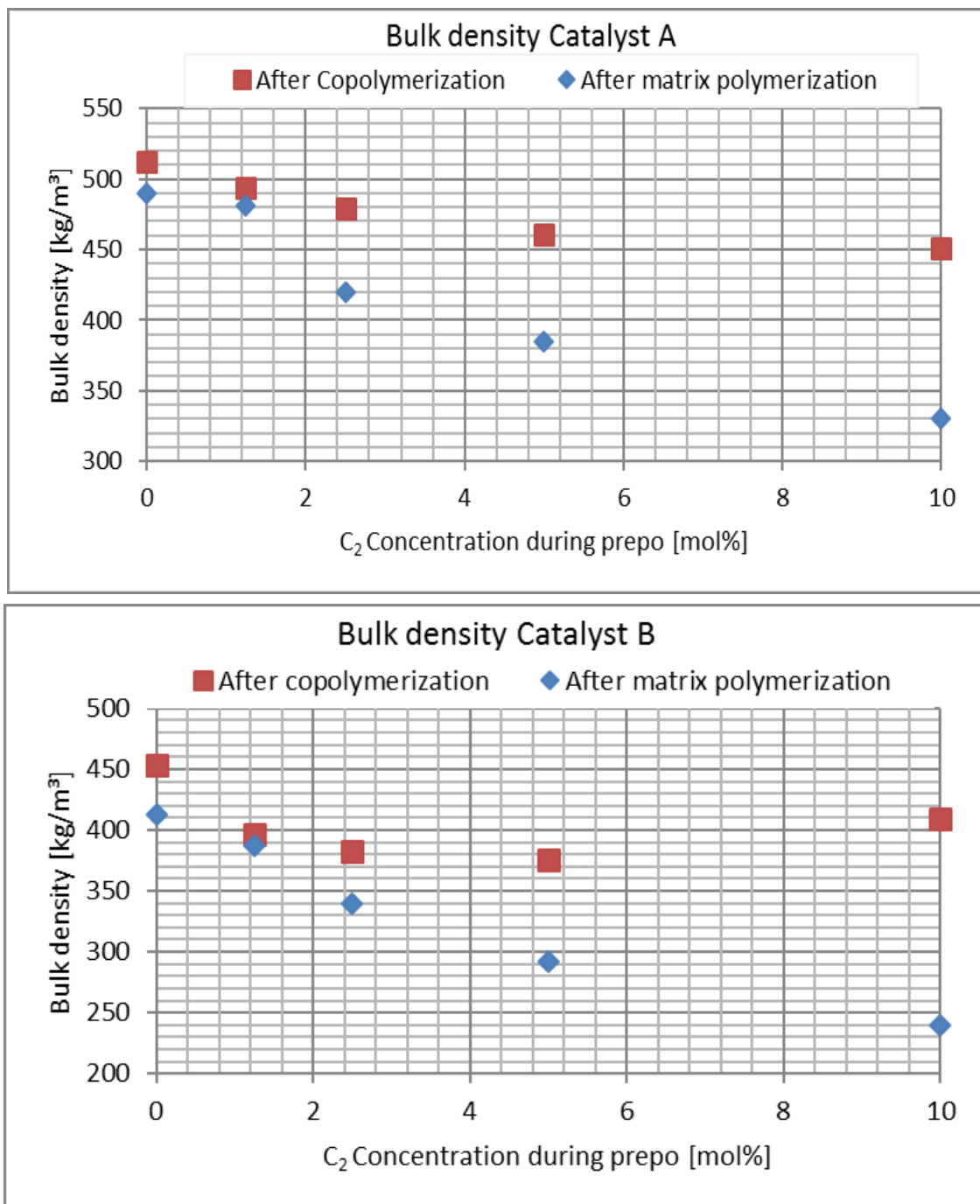
Figure 58: Comparison of the bulk densities after matrix polymerization (70°C, 20bar 1 mol-% hydrogen) and after copolymerization step (70°C, 16 bar, C_2/C_3= 50/50)

As expected, during heco-step pores are effectively filled and bulk density increases. For samples with ethylene present in prepolymerization, the final bulk density is lower, potentially leaving room for more rubber incorporation.

The evolution of the particle morphology for catalyst A and catalyst B with prepoly in bulk phase at 25°C and 8 minutes; matrix stage at 70°C, 20 bar and 1 mol-% H_2 and rubber stage at 70°C, 16 bar and 50 mol-% C_2 is shown in Figure 59 and Figure 60:
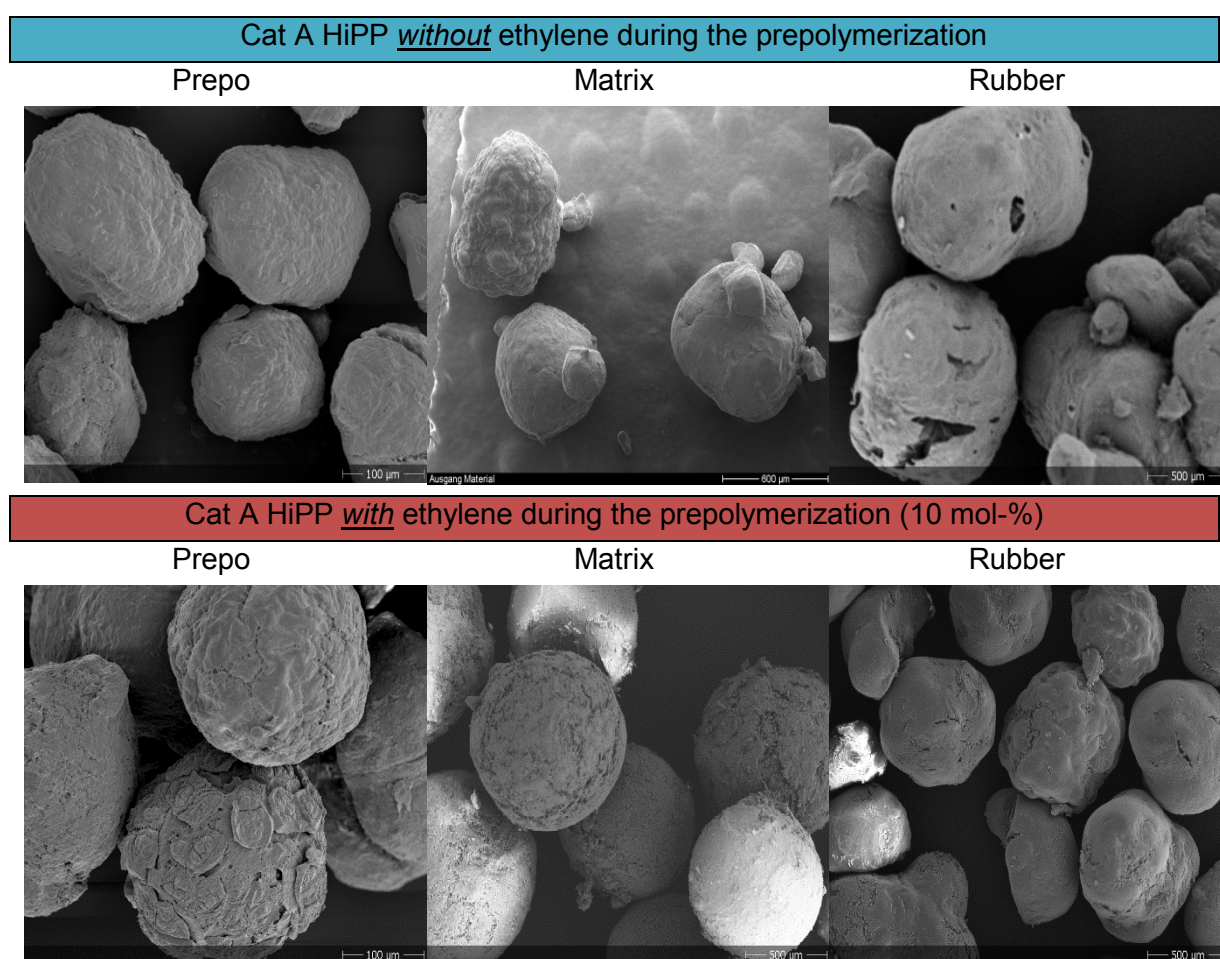
Figure 59: SEM micrographs of catalyst A at prepo, matrix and rubber stage

Cat B HiPP *without* ethylene during the prepolymerization		
Prepo	Matrix	Rubber

Cat B HiPP *with* ethylene during the prepolymerization (10 mol-%)		
Prepo	Matrix	Rubber
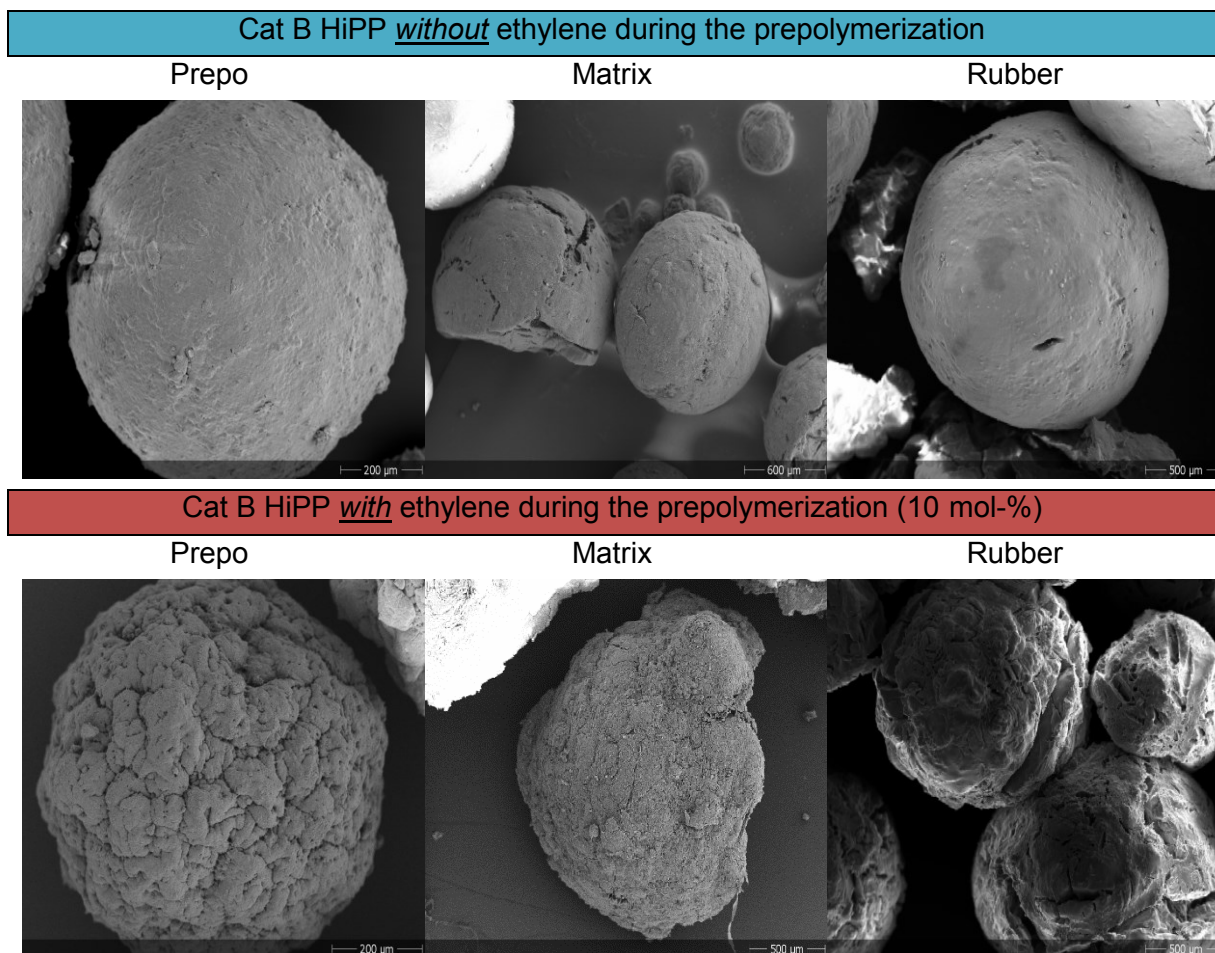
Figure 60: SEM micrographs of catalyst B at prepo, matrix and rubber stage

Figure 59 and Figure 60 show some remarkable differences between the samples with and without ethylene in all polymerization stages. The micrographs exhibit a compact surface with small pores for the samples without ethylene. Compared to samples with ethylene which have much more pores on the outer shell. Also, it can be clearly seen that the porosity after the homopolymerization is bigger than after the copolymerization.

Also polymer samples after the heco-stage were analyzed by Hg-porosimetry.

The samples (catalyst A) analyzed contained from 0 mol-% to 10 mol-% ethylene during the prepolymerization. Matrix gas-phase polymerization settings were at 70°C, 20 bar, 1 mol-% hydrogen and 1 hour. The copolymerization was achieved at 70°C, 16 bar a C2/C3 ratio of 50 and the time was kept constant at one hour. The pore size distributions gained from the Hg-Porosity measurements are displayed in Figure 61.
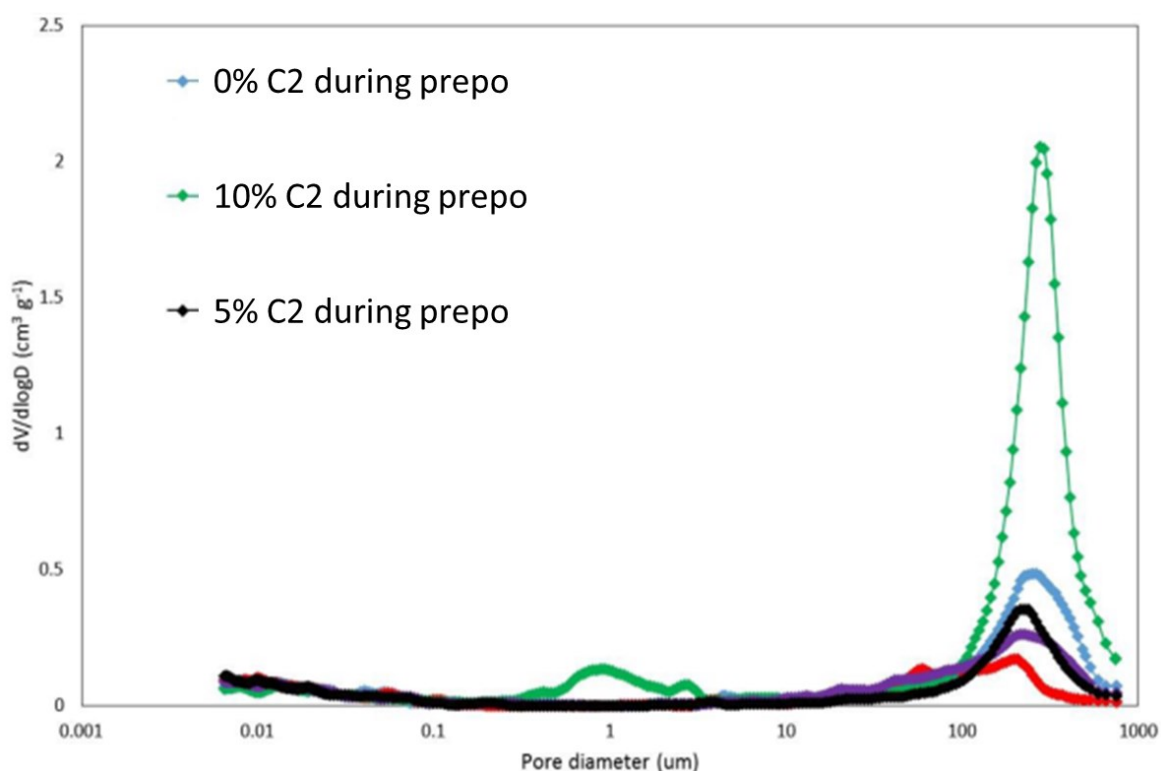
Figure 61: Differential pore size distributions of HiPP samples

All pore size distributions show a similar contribution of pores ranging from approx. 100 – 800 µm, which should be attributed to *intra*-agglomerate (or *inter*-primary particles). For samples with high ethylene concentration during the prepolymerization *inter*-particle porosity was also detected. The modes and intensities of these distributions vary among the samples.

The pore size distribution of the sample with 10 mol-% ethylene concentration during the prepo (Figure 61 green line) displays some additional porosity ranging from approx. 0.4 – 4 µm, and this contribution of pores should be attributed to *intra*-particle porosity suggesting that these particles are porous whereas the other samples do not display porous particles.

The pore size distribution of the sample with high ethylene concentration during the prepo shows a broader distribution of *inter*-primary particle pores, as pores as small as approx. 10 µm are present. This broader distribution could also tentatively be explained by a more heterogeneous particle size distribution, or a more heterogeneous *intra*-agglomerate pore size distribution.

The fact that the distributions of all samples have not returned to baseline level around approx. 6 nm should thus be attributed to compression rather than that these pores are present in the samples. All porosity < 0.1 µm should therefore be ignored.

8 Parameter study on the effect of length scale of diffusion

One of the principal objectives that were set in this project was to establish relationships between reaction conditions, particle morphology, process kinetics and mass transfer of high impact polypropylene during the whole reaction progress.

For this objective, a broad experimental study was conducted through measurements of activity, morphology and sorption kinetics as function of reaction conditions.

In previous studies, it was concluded, that while there is there is no or only minor mass-transfer limitation for propylene, there is a significant mass-transfer limitation for ethylene during the in rubber-stage copolymerization [115].

In this study, means for systematic adjustment of particle morphology have been developed and the corresponding impact on mass-transfer kinetics has been studied. By use of ethylene in the prepolymerization step, bulk density can be reduced significantly and mass-transfer can be intensified, expressed via a reduction of the effective length scale of diffusion.

In the following chapter, the impact of this intensified mass-transfer on the balance of reaction and diffusion and -as a consequence- on ethylene incorporation during the rubber step shall be studied in form of a parameter study applying the particle model developed by Kröner [115].

8.1   Particle model developed by Kröner

From previous studies [36] [37] [50] [63] [65] it is known, that neither a polymeric flow nor a multigrain-type of particle model can describe experimental mass-transfer data on polyolefin particles correctly.

Kröner [98] concluded on the basis of electron microscope images and sorption data, that domains of fused micrograin clusters are the relevant domain for sorption of monomers in polypropylene particles.
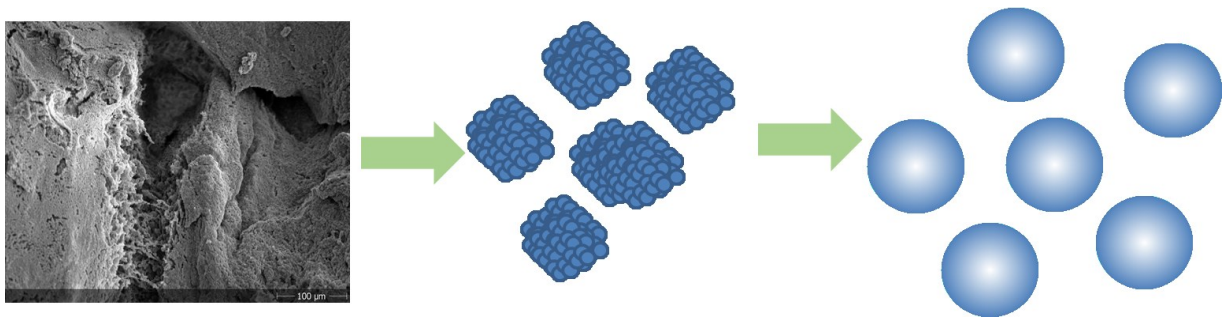
Figure 62 : Morphological concept for powder mass-transfer model

Kröner determined the size of these micrograin cluster from sorption data and provided for the studied catalyst system an empirical correlation for the micrograin cluster size as function of yield [98].

In the model, multigrain clusters are described as spherical, quasi-homogeneous, pore-free domains. Mass-transfer in the domains is described by diffusion applying diffusion coefficients derived from film measurements [115].

For description of the polymerization, Kröner uses a two-site model with the following kinetic scheme [115]:

<u>Site 1:</u>

Initiation: $Ti + TEA \rightarrow Ti^*$ Rate not considered, assumed to be very fast (!)

Chain start: $Ti^* + C3 \rightarrow P_{C3,1}^*$ Rate not considered, assumed to be very fast (!)

Propagation: $P_{C3,n}^* + C3 \rightarrow P_{C3,n+1}^*$ $r_1 = kp_{C3,C3,1} \cdot c_{C3} \cdot c_{P^*,C3,1}$

                  $P_{C3,n}^* + C2 \rightarrow P_{C2,n+1}^*$ $r_2 = kp_{C3,C2,1} \cdot c_{C2} \cdot c_{P^*,C3,1}$

                  $P_{C2,n}^* + C2 \rightarrow P_{C2,n+1}^*$ $r_3 = kp_{C2,C2,1} \cdot c_{C2} \cdot c_{P^*,C2,1}$

                  $P_{C2,n}^* + C3 \rightarrow P_{C3,n+1}^*$ $r_4 = kp_{C2,C3,1} \cdot c_{C3} \cdot c_{P^*,C2,1}$

Deactivation: $P_{C2,n}^* + C3 \rightarrow D_{n+1}$ $r_5 = kdes_1 \cdot c_{C3} \cdot c_{P^*,C2,1}$

                  $P_{C3,n}^* + C3 \rightarrow D_{n+1}$ $r_6 = kdes_1 \cdot c_{C3} \cdot c_{P^*,C3,1}$

<u>Site 2:</u>

Initiation: $Ti + TEA \rightarrow Ti^*$ Rate not considered, assumed to be very fast (!)

Chain start: $Ti^* + C2 \rightarrow P_{C2,1}^*$ Rate not considered, assumed to be very fast (!)

Propagation: $P_{C2,n}^* + C2 \rightarrow P_{C2,n+1}^*$ $r_7 = kp_{C2,C2,2} \cdot c_{C2} \cdot c_{P^*,C2,2}$

                  $P_{C2,n}^* + C3 \rightarrow P_{C3,n+1}^*$ $r_8 = kp_{C2,C3,2} \cdot c_{C3} \cdot c_{P^*,C2,2}$

                  $P_{C3,n}^* + C3 \rightarrow P_{C3,n+1}^*$ $r_9 = kp_{C3,C3,2} \cdot c_{C3} \cdot c_{P^*,C3,2}$

                  $P_{C3,n}^* + C2 \rightarrow P_{C2,n+1}^*$ $r_{10} = kp_{C3,C2,2} \cdot c_{C2} \cdot c_{P^*,C3,2}$

Deactivation: $P_{C2,n}^* + C3 \rightarrow D_{n+1}$ $r_{11} = kdes_2 \cdot c_{C3} \cdot c_{P^*,C2,2}$

                  $P_{C3,n}^* + C3 \rightarrow D_{n+1}$ $r_{12} = kdes_2 \cdot c_{C3} \cdot c_{P^*,C3,2}$

                  $P_{C2,n}^* + C2 \rightarrow D_{n+1}$ $r_{13} = kdes_3 \cdot c_{C2} \cdot c_{P^*,C2,2}$

                  $P_{C3,n}^* + C2 \rightarrow D_{n+1}$ $r_{14} = kdes_3 \cdot c_{C2} \cdot c_{P^*,C3,2}$

Kröner [98] has determined for a similar ZN catalyst the following values:

Table 13: Estimated kinetic rate constants

	Site 1	Site 2
x_{active} [Ti*/Ti]	0,08	$1 \cdot c_{ethylene}$
kp_{C3C3} [l/mol/s]	5400	23.000
kp_{C2C2} [l/mol/s]	320.000	47.000
r_{C3}	0,05	0,09
r_{C2}	8,6	90
k_{des} [l/mol/s]	$1,7 \cdot 10^{-4}$	$2,3 \cdot 10^{-3}$

Site 2 is activated by ethylene and is therefore only active in copolymerization stage. As example, for the monomers in the micrograin clusters, the following material balance results:

$$\frac{\partial c_M}{\partial t} = \frac{D_{M,eff}}{(1 - \Phi_c)} \cdot \left(\frac{\partial^2 c_M}{\partial r^2} + \frac{2}{r} \cdot \frac{\partial c_M}{\partial r} \right) + R_M \qquad (26)$$

More details on mathematical formulation of the model and its derivation can be found in [115].

8.2　Model adaptions

The empirical correlation for the size of the micrograin clusters as function of yield was derived by Kröner for another ZN-catalyst system and hence cannot be used as such in this study.

Kröner used for size of the micrograin clusters as function of yield a cubic correlation of the following form:

$$r_{sorb} = (Ax^3 + Bx^2 + x + C) * 10^{-6} \, m \qquad (27)$$

This correlation was adapted to the experimental determined sorption lengths after matrix stage (see chapter 7.5.4)

Of course it is not possible to determine a three parameter formula from just one measurement. The only modified parameter was the parameter "C", assuming that development of sorption length in general occurs in a similar way as determined by Kröner. This is a strong and critical simplification, but should be adequate for description of the real situation at the end of the matrix stage and the beginning of the heco-stage. For deeper studies, more experimental studies on development of the sorption length during the course of reaction have to be carried out.

The resulting modified correlations for the size of the micrograin clusters is plotted in (Figure 63).
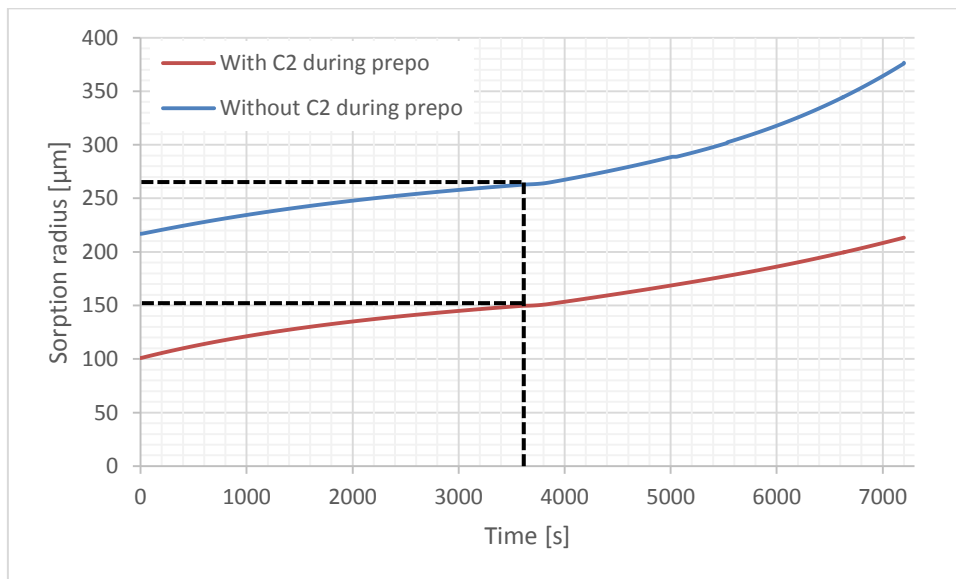
Figure 63: Growth of sorption radius for Catalyst A (matrix phase at 70°C, 20 bars, 1%-mol H$_2$ and 1 hour. Heco-phase at 70°C, 16 bar and 50/50 C2/C3 molar ratio for one hour)

Table 14: Modified parameter "C" for the development of sorption length.

	parameter C [µm]	r$_{diff}$ (1h) [µm]
prepoly without C2	190	260
prepoly with 10 mol.-% C2	90	150

8.3 Simulation study

Using the adapted kinetic models described, a parameter variation to test the impact of the modified morphology has been carried out.

For this purpose, the conditions with highest difference in ethylene incorporation depending on prepolymerization conditions observed experimentally, that is catalyst A, heco-polymerization at 70°C, 16 bars pressure and 30 mol-% ethylene, see Figure 57, chapter 7.6.3 have been used.

Carrying out the simulations for the two discussed cases (prepolymerization without ethylene and prepolymerization with 10 mol.-% ethylene) using the modified correlation for the size of the micrograin clusters depicted in Figure 64, the following activity-time plots are obtained:
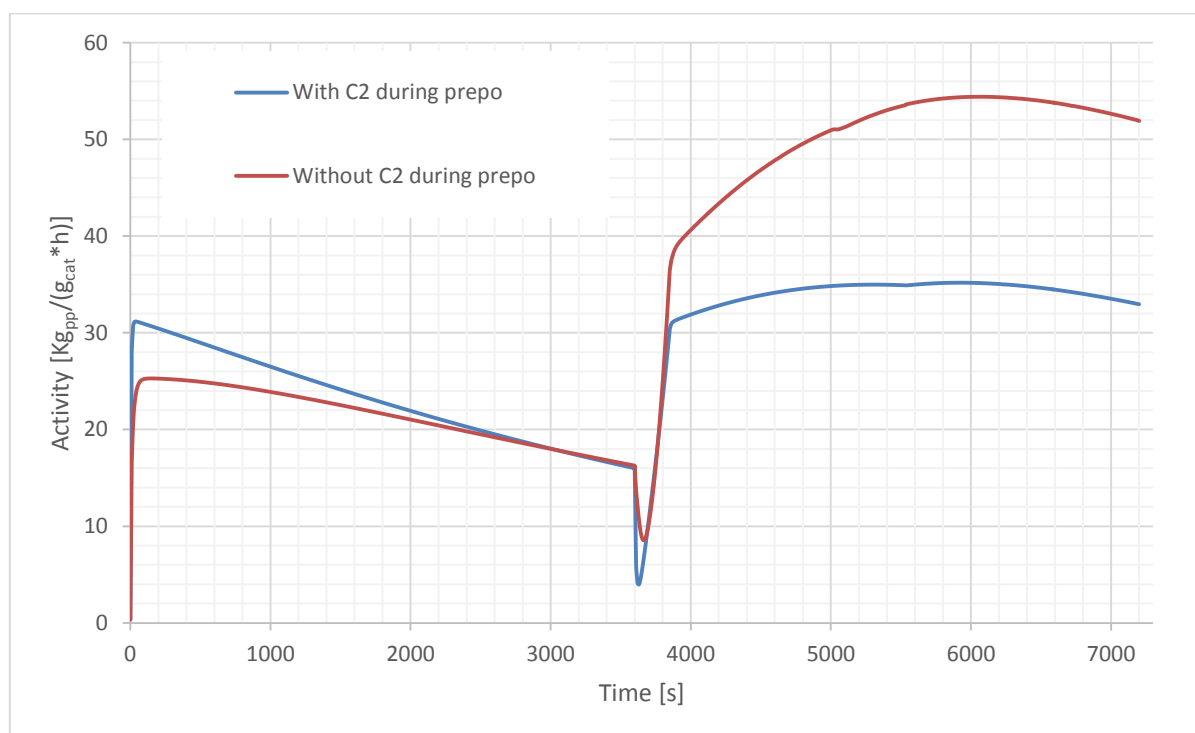
Figure 64: Activity-time for simulation catalyst A (matrix phase at 70°C, 20 bars, 1%-mol H2 and 1 hour. Heco-phase at 70°C, 16 bar and 50/50 C2/C3 molar ratio for one hour)

For the prepolymerization without ethylene (plot in red), activity during homopolymerization drops from about 25 $Kg_{pp}/(g_{cat}*h)$ to 18 $Kg_{pp}/(g_{cat}*h)$ and

increases during heco-stage up to 55 $Kg_{pp}/(g_{cat}*h)$. An ethylene incorporation of 47 mol.-% during heco-stage is calculated.

The simulation results fit surprisingly well to the experimental results, especially considering that literature data for the kinetic constants has been used without further parameter adaption.

For the same conditions, but prepolymerization with 10 mol.-% ethylene, activities (plot in Blue in Figure 64) drop to about 30 $Kg_{pp}/(g_{cat}*h)$, see Figure 55 in chapter 7.6.2.

One potential explanation for this finding is that site 2 is already activated in the prepolymerization step and hence undergoes –in contrast to the prepolymerizations without ethylene- already deactivation during the matrix-stage.

The effect of reduced activity is resembled in the simulations by a reduced fraction of active Titanium. x_{active} has been adopted in order to meet the experimental observed activities of about 30 $Kg_{pp}/(g_{cat}*h)$.

Ethylene incorporation in this conditions increases to 55 mol.-%.

This increase in calculated ethylene incorporation is in line with the experimental findings in Figure 57, chapter 7.5.4.

For further discussion of these interesting findings, effectiveness factors for ethylene during heco-polymerization have been calculated for the two discussed cases, see Figure 65.
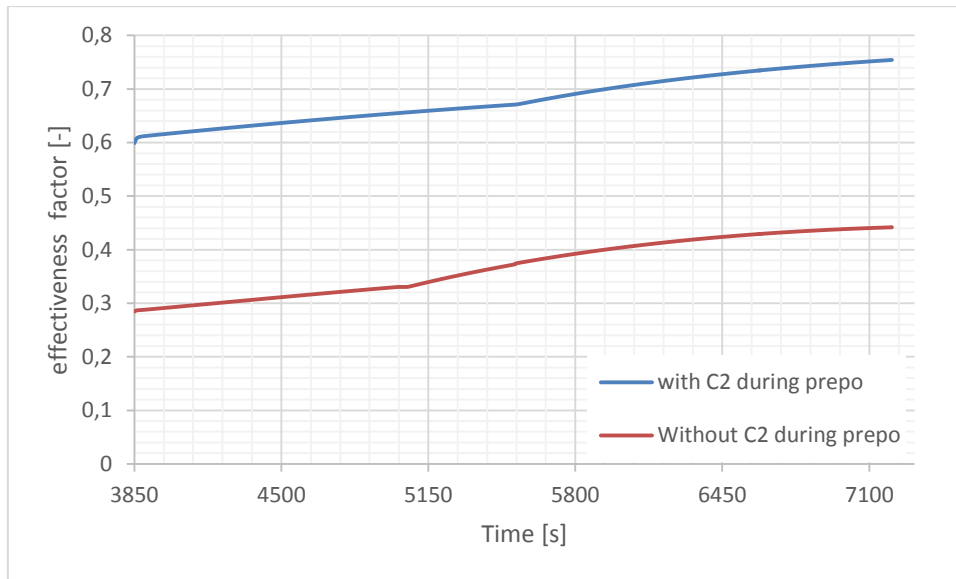
Figure 65: Comparison effectiveness factor for ethylene for both simulation (prepoly without C2 (red) and prepoly with 10 mol.-% C2 (blue)).

For prepolymerization without ethylene, the effectiveness factor for ethylene during the heco stage are in between 30 and 40%, that means the average ethylene concentration in the micrograin clusters is between 30 and 40% of the equilibrium concentration at reaction conditions – the actual ethylene concentration during heco stage is significantly affected by mass-transfer restrictions.

For prepolymerizations with 10 mol.-% ethylene –and therefore much reduced micrograin cluster size, see Figure 63- the effectiveness factors for ethylene during heco stage are in between 60 and 75%, which is much larger compared to the prepolymerization without ethylene. The actual ethylene concentration during heco stage is much closer to equilibrium concentration.

The effectiveness factor is both influenced by the micrograin cluster size and also the reaction rate. The lower the micrograin cluster size, the larger the mass-transfer, the higher will be the effectiveness factor. The lower the polymerization rate, the lower the mass-transfer restriction will be, the higher the effectiveness factor will be.

In case of prepolymerization with 10 mol-% ethylene, both micrograin cluster size is reduced and also reaction rate in heco-stage is reduced.

In order to separate this two influences some additional simulations with reduced sorption lengths but high activities (realized by increased fraction of active sites) in the heco stage has been performed and following results have been obtained (Table 15)

Table 15: Activity, Ethylene incorporation and effectiveness factors for different sorption radii

r_{diff} [µm]	Heco-activity [$Kg_{pp}/(g_{cat}*h)$]	Effectiveness factor [-]	X_{c2} [mol-%]	x_{active} [Ti*/Ti]
260	49	0,3-0,45	47	1
150	30	0,6-0,7	55	0,1
150	48	0,5-0,6	60	1

As can be seen the reduction in diffusion lengths already alone leads to significant increase in the effectiveness factor.

It can be concluded, that ethylene incorporation during heco-stage is significantly affected by mass-transfer restrictions. The reduction of micrograin cluster size as relevant sorption length by addition of ethylene during the prepoly step helps to intensify mass-transfer and thus to increase the actual ethylene concentration during heco-stage, which in turn helps to better exploit the catalyst capabilities for ethylene incorporation.

9 Summary and discussion of the results

This work focuses on study on how to control and modify particle morphology during the multistage-stage production process of heterophasic polypropylene materials. Furthermore, the impact of adopted particle morphology on the behaviour in the polymerization process in terms of process kinetics and mass-transfer has been studied.

Morphology, kinetics and mass transfer characteristics were studied for two industrial ZN catalysts. Polymerizations were divided into three steps: prepolymerization, matrix and rubber phase. Prepolymerizations and matrix polymerizations in the bulk phase were executed batch wise, while rubber and matrix polymerizations in the gas phase were performed semi batch wise.

Initially, reaction conditions and experimental procedures were optimized in order to establish reproducibility and reference activity levels. After reproducibility and reference activity had been reached for both catalysts, a broad experimental screening on the effect of homopolymerization conditions and prepolymerization conditions on particle morphology was carried out. The target was to identify how particle morphology can be adjusted while maintaining a good activity level.

The experimental results clearly show that a prepolymerization step is essentially required. Omitting the prepolymerization step leads to significant reduction of polymerization activity. For both polymerization systems studied, the most efficient measure to adjust morphology while maintaining high activity is addition of a small amount of ethylene in the prepolymerization step.

Samples with ethylene being present in the prepoly step clearly show an increased porosity, reduced bulk density and rougher surface. To confirm these results, additional series of external prepolymerizations in a 250 ml reaction calorimeter have been performed. The external prepolymerizations allow to fully decouple prepolymerization and matrix stage conditions. In particular, carry-over of any ethylene from prepoly to matrix stage can be completely avoided. Prepolymerization degrees increase with higher ethylene concentrations. After some optimization prepolymerization degrees in between 400 to 600 g_{pp}/g_{gcat}

were obtained. All prepoly-powders were recovered under inert conditions in a glove box.

Matrix phase polymerizations with prepoly powder were carried out in both bulk and gas phase. In both cases, reference activity level and reproducibility have again been reached with this new procedure for both catalyst systems. For gas-phase polymerizations at 70°C, p = 20 bars and 1 mol-% hydrogen, catalyst activity remains nearly constant (20 to 25 $Kg_{pp}/g_{cat}/h$ for catalyst A and 27-32 $Kg_{pp}/g_{cat}/h$ for catalyst B). For bulk phase polymerizations at 80°C, 39 bars and 200 mmol hydrogen, for catalyst A, catalyst activities in the range of 30 to 37 $Kg_{pp}/g_{cat}/h$ and 43-48 $Kg_{pp}/g_{cat}/h$ for catalyst B are obtained.

With addition of ethylene in the prepoly step, bulk density of the matrix polymer is significantly reduced. For catalyst A in gas phase polymerization, bulk density reduces from about 500 kg/m³ for prepoly without ethylene to about 340 kg/m³ for prepolymerizations with 10 mol-% ethylene. For bulk phase polymerization with catalyst A, the bulk density is in general a bit lower, but the same trend is observed, a reduction in bulk density from about 450 kg/m³ for prepoly without ethylene to 300 kg/m³ for prepolymerizations with 10 mol-% of ethylene. For catalyst B, addition of ethylene in the prepoly step reduces the bulk density from about 400 kg/m³ for prepolymerization without ethylene to about 250 kg/m³ for prepolymerizations with 10 mol-% ethylene, for both gas-phase and bulk-phase matrix polymerizations.

Correspondingly, with increasing ethylene content in the prepolymerization step, porosity is increasing. The pore size distribution -measured by Hg-porosity measurements- is shifting to smaller pore sizes. Electron microscope images taken show for samples with ethylene in the prepolymerization step a rougher surface and an increased fraction of visible cracks and pores. DSC results do not show any significant differences in terms of crystallinity for the samples with different ethylene content in the prepolymerization step.

One potential explanation approach for this strong effect of ethylene in the prepolymerization step on particle morphology are differences in the rearrangement of micrograins and micrograin clusters in the macroparticle due to different viscoelastic material properties of the prepolymers produced. Also differences in the reaction conditions during prepolymerization might play a role.

To quantify mass-transfer rates, sorption measurements have been performed with the produced powders in a high-pressure sorption balance. Diffusion coefficients and sorption radii were determined following the approach introduced by Kröner [115].

First sorption experiments with different samples revealed a significant reduced effective diffusion length for samples with ethylene being present in the prepolymerization step compared to standard homopolymerization samples. Effective diffusion coefficients were around $9 \cdot 10^{-11}$ m²/s while sorption lengths dropped from 260 μm (for prepolymerization without ethylene) to 150 μm (prepolymerization with 10 mol-% ethylene) for catalyst A and from 220 μm (prepolymerization without ethylene) to 80 μm (prepolymerization with 10 mol.-% ethylene) for catalyst B.

By having iPP with an adjusted morphology and reduced sorption length, the production of ICPs using in situ polymerization of propene with ethylene-propene rubber (EPR) was the second focus of this research. Settings such as pressure, ethylene/propene ratio and indeed initial morphology were systematically varied.

Copolymerization time was maintained constant at 1 hour. As expected, for both catalysts, the average activity increases with increasing pressure and ethylene content in gas-phase. As expected, during heco-step pores are effectively filled and bulk density increases. For samples with ethylene present in prepolymerization, the final bulk density is lower, potentially leaving room for more rubber incorporation. Hg-Porosity measurements showed also a decrease of the porosity compared to homopolymer.

While ethylene in the prepolymerization step had only a minor effect on catalyst activity in the homopolymerization step, a surprisingly strong effect of ethylene in the prepolymerization step on catalyst activity in heco-stage was observed.

For catalyst A, activity in heco-stage (p = 16 bar, T = 70°C, C2/C3=50:50 mol/mol) drops from 48 Kg_{pp}/g_{cat}/h for prepolymers without ethylene to 28 Kg_{pp}/g_{cat}/h for prepolymers with 10 mol-% ethylene. For catalyst B, activity in heco stage at the same conditions decreases from about 55 Kg_{pp}/g_{cat}/h (prepolymer without ethylene) to 32 Kg_{pp}/g_{cat}/h (prepolymer with 10 mol-% ethylene).

One explanation attempt for this surprising finding might be that -in case of prepolymerization with ethylene- the ethylene-specific active site already is activated during the prepoly step and undergoes subsequent deactivation, while in case of prepolymerization without ethylene this activation and deactivation of the ethylene specific site just starts during heco-stage.

There is a tendency, that for polymers with ethylene being present during prepoly, the ethylene response in heco-stage is slightly improved, this might be attributed to improved mass-transfer rates. This effect was most pronounced for catalyst A, heco-polymerizations at 70°C, 16 bars and 30 mol-% ethylene, where ethylene incorporation increased from 48 mol-% (prepolymers without ethylene) to 55 mol-% (prepolymer with 10 mol-% ethylene).

In order to study these finding further, a simulation study using the micrograin-cluster model proposed by Kröner was performed. The correlations for micrograin cluster size were adapted to the experimental results for sorption length determined in this work.

With the adapted model and the kinetic parameters determined by Kröner for another catalyst, the experimental results for catalyst A, prepolymerization without ethylene, gas-phase polymerization in homo- and heco-stage can be surprisingly well described, both in terms of activity and ethylene incorporation. The efficiency factor for ethylene during heco-polymerization is in between 0,3 and 0,45, indicating a severe mass-transfer limitation for ethylene, which is in-line with earlier results of Kröner.

Applying now the same model for prepolymers with 10 mol-% ethylene and a corresponding lower diffusion radius and correcting for the lower activity observed by adjusting the fraction of active Titanium of site 2, the experimentally observed activities can be resembled. For these conditions, the simulation also shows the experimentally observed higher ethylene incorporation. Further analysis reveals that in these conditions, the effectiveness factor for ethylene in the heco-stage is with 0,6 to 0,7 substantially higher, indication a lower degree of mass-transfer limitation compared to the prepolymerization without ethylene.

It can be concluded, that ethylene incorporation during heco-stage is significantly affected by mass-transfer restrictions. The reduction of micrograin cluster size as relevant sorption length by addition of ethylene during the prepoly

step helps to intensify mass-transfer and thus to increase the actual ethylene concentration during heco-stage, which in turn helps to better exploit the catalyst capabilities for ethylene incorporation.

10 Table of symbols

Abbreviations	Description
AFM	Atomic force microscope
Al/Ti or Al/Do	Alumina/Titan or Alumina/Donor ratio
BD	Bulk Density
C2 or C2H4	Ethylene
C3 or C3H6	Propylene
Copo	Copolymerization
DP or PD	Prepolymerization degree
DSC	Differential scanning calorimetry
DCP	Dicyclopentyl(dimethoxy)silane
DIPDMS	Diisopropyl-dimethoxy silane
EPR	Ethylene-Propylene-Copolymer-Rubber
FTIR	Fourier transform infrared spectroscopy
Heco	Heterophasic copolymerization
hiPP	High impact Polypropylene
MGM	Multi grain Model
MFR or MFI	Melt flow rate (index)
μ-GC	Micro Gas Chromatograph
PB	Polybutadien
PE	Polyethylene
PP	Homo Polypropylene
iPP / isoPP	Homo Polypropylene
$P^*_{x,n}$	Growing chains with terminating unit x and chain length n
Prepo	Prepolymerization
SEM	Scanning Electron Microscopy
TEA	Triethylalumina
TEM	Transmission Electron Microscopy
Ti	Titanium
Ti*	Activated Titanium
ZN	Ziegler-Natta

Capital Letters	Description	Unit
A	Area	m^2
A_1	Deviation parameter (Stern)	-
A_2	Temperature parameter (Sanchez-Lacombe)	K
A_3	Pressure parameter (Nakamoto)	bar
B_1	Deviation parameter (Stern)	-
B_2	Concentration parameter (Sanchez-Lacombe)	-
B_3	Pressure parameter (Nakamoto)	1/bar
C	Concentration of the penetrant dissolved	$mol/l_{amorphous}$
C_H'	Langmuir sorption capacity	$mol/l_{amorphous}$
$D_{0,i}$	Pre-exponential diffusion factor	m^2/s
D_{eff}	Effective diffusion coefficient	m^2/s
D_i	Diffusion coefficient of component i	m^2/s
E_d	Activation energy of diffusion	J/mol*K
E_p	Energy of permeation	J/mol*K
F	First virial coefficient	m^3/mol
G	Second virial coefficient	$(m^4 \cdot s^2)/(mol*kg)$
H_i	Henry constant	bar
H_i^*	Modified Henry constant	$mol/l_{amorphous}/bar$
ΔH_m	Heat of fusion	J/g
ΔH_{oo}	Literature reference 100% crystalline	J/g
ΔH_R	Heat of reaction	J/mol*K
ΔH_s	Enthalpy of sorption	J/mol*K
K_1	Empirical constant (virial equation)	$m^3/mol/K$
K_2	Empirical constant (virial equation)	m^3/mol
MW_i	Molecular weight of component i	g/mol
N	Number of clusters	-
$\dot{N}_i$	Mole flow of component i	mol/s
P	Stirring power	W
R	Universal gas constant	J/K/mol
RC	Rubber content	wt%
S_c	limiting value of penetrant solubility	$mol/l_{amorphous}/bar$
T	Temperature	K
T_{crit}	Critical temperature	K
T_{glas}	Glas transition temperature	K

	Volume of the cluster	m^3
V	Volume of the cluster	m^3
$V_{PP,amorphous}$	Volume of the amorphous homopolymer	m^3
V_R	Reaction volume in a cluster	m^3
$\Delta V_{swelling}$	Volume increase due to swelling	m^3
X_{DSC}	Crystallinity of the polymer from DSC	%

Small Letters	Description	Unit
a_i	Activity of component i	-
b	Adjustable pressure affinity parameter	1/bar
c_i	Concentration of component i	mol/l
c_M	Concentration of monomer M	mol/l
cp_{PP}	Specific heat capacity Polypropylene	J/g/K
$cryst$	Crystallinity	g/g
d	Diameter	m
f_i^0	Standard fugacity of component i	bar
f_i^l	Fugacity of component i in vapour phase	bar
f_i^v	Fugacity of component i in vapour phase	bar
j_i	Mole flow density	mol/s/m^2
$kdes_i$	Deactivation rate constant number i	l/mol/s
$kp_{i,j,z}$	Propagation rate constant for chains with termination x, addition of monomer y and site species z	l/mol/s
l	Characteristic length of diffusion	m
$m_{balance}$	Sorbed mass (reading of the balance)	g
m_i	Mass of component i	g
m_{sorbed}	Sorbed mass (buoyoncy force corrected)	g
m_{eqq}	Sorbed mass at equilibrium	g
n_{Ti}	Moles of Titanium	mol
p	System pressure	bar
p_{crit}	Critical pressure	bar
p_{dev}	Pressure, untill error of Stern < 5%	bar
p_i	Partial pressure of component i	bar
p_i^{lv}	Partial pressure of component i	bar
$r_{cluster}$	Cluster radius	m
r_i	Reaction rate of reaction number i	mol/s

r_n	Normalized cluster radius	-
$r_{particle}$	Particle radius	m
r_s	Segment number	-
x_i	Mole fraction of component i	mol/mol

Greek Symbols	Description	Unit
α	Temperature independent constant	-
β	Adjusted empirical parameter	l/mol
γ_i	Activity coefficient of component i	-
ε	Porosity	m^3/m^3
$\eta_{eff,i}$	Effectiveness factor for component i	mol/mol
λ_i	Thermal conductivity of component i	W/m/K
ρ_i^x	Density of component i in phase x	kg/m^3
ϕ_c	Volume fraction of crystals	m^3/m^3
ϕ_{mon}	Volume fraction monomer	m^3/m^3
σ	Concentration dependence of solubility	l/mol
χ_{1p}	Flory Huggins interaction parameter	-
φ_i	Fugacity coefficient of component i	-
φ_i^{lv}	Fugacity coefficient of component i at vapour pressure	-

11   Literature and references

[1] Plastics Europe, "Plastics – the Facts 2016 An analysis of European plastics production, demand and waste data for 2015",**www.plasticseurope.org**

[2] Weekly resin report: PP, PE prices steady to higher across most commodity grades,**http://www.plasticstoday.com/resin-pricing/weekly-resin-report-pp-pe-prices-steady-higher-across-most-commodity-grades/167782636125048**.

[3] C. Hall, Polymer Materials: An Introduction for Technologists and Scientists, MacMillan Education, London, 1989

[4] R. A Phillips, M. D. Wolkowics, E. P. Moore, Jr., "Structure and Morphology'', Polypropylene Handbook, Hanser/Gardner Publications Inc., Cincinnati, 1996, 113

[5] G. Odian, Principles of Polymerization, John Wiley & Sons, 2004, 644-682

[6] J. Boor, "Ziegler-Natta Catalysts and Polymerizations", Academic Press, New York, 1979

[7] P. Kittilsen, T.F. McKenna, J. Appl. Polym. Sci., 2001, 82, 1047

[8] S. Job, C. Jan, P.J. Bosman, G. Weickert, K. Roel Westerterp, Liquid-phase Polymerization of Propylene with a Highly Active Ziegler–Natta Catalyst. Influence of Hydrogen, Cocatalyst, and Electron Donor on the Reaction Kinetics, Journal of Polymer Science Part A: Polymer Chemistry, 1999, 37.2, 32-219

[9] N. Farmer, Trends in Packaging of Food, Beverages and Other Fast-Moving Consumer Goods, Elsevier, 2013

[10] E. P. Moore, Jr., "Polypropylene Handbook", Carl Hanser Verlag, Munich Vienna New York, 1996, p. 149

[11] S. van der Ven, "Polypropylene and other Polyolefins", Elsevier, Amsterdam, 1990

[12] P. Galli, S. Danesi, T. Simonazzi, "Polypropylene Based Polymer Blends: Field of Application and New Trends", Polym. Eng. Sci., 1984, 24, 544

[13] K. Kutz, Applied Plastics Engineering Handbook: Processing, Materials, and Applications, 39, 784

[14] M. Caracotsius, Chemical Engineering Science 1992, 47, 2591-2596

[15] N. P. Khare, B. Lucas, K. C. Seavey, A. Sirohi, S. Ramanathan, S. Lingard, Y. Song, C.-C. Chen, Y. A. Liu, Industrial & Engineering Chemical Research 2004, 43, 884

[16] D. B. Malpass, I. Elliot, Introduction to Industrial Polypropylene: Properties, Catalysts, Processes, John Wiley & Sons, Hoboken, NJ, 2012 ISBN: 978-1-118-06276-0

[17] R. B. Lieberman, R. T. LeNoir, Manufacturing: Polypropylene Handbook, ed., E. P Moore, Jr., Hanser/Gardner Publications, Inc., Cincinnati, 1996, 287

[18] J.A. Debling, W.H. Ray, Heat and mass transfer effects in multistage polymerization processes-impact polypropylene. Ind. Eng. Chem. 1995, 34, 3466-3480

[19] N. Cheremisinoff, Handbook of Polymer Science and Technology, Volume 1

[20] P. Nicholas, Handbook of Polymer Science and Technology, 1

[21] E.L. Hoel, C. Cozewith, G. D. Byrne, AIChE J. 2006, 40, 1669

[22] T. F, McKenna, H. Benamouama, & R. Spitz. Mass transfer resistance in Ziegler-catalysed slurry phase polymerisation: A new look at reaction modelling. DECHEMA Monographien, 1995, 131, 223–234.

[23] M. P. McDaniel. Fracturing silica-based catalysts during ethylene polymerization. Journal of Polymer Science, Polymer Chemistry, 1981, 19, 1967–1976.

[24] J. B. P. Soares & A. E. Hamielec. Metallocene/aluminoxane catalysts for olefin polymerization. A review. Polymer Reaction Engineering, 1995, 3, 131–200.

[25] K. Soga, & T. Shiono, Ziegler–Natta catalysts for olefin polymerization. Progress in Polymer Science, 1997, 22, 1503–1546.

[26] A. E. Hamielec, & J. B. P. Soares. Polymerization reaction engineering—Metallocene catalysis. Progress in Polymer Science, 1996, 21, 651–706.

[27] W. Kaminsky, New polymers by metallocene catalysis. Macromolecular Chemistry and Physics, 1996, 197, 3907–3945.

[28] I. Urdampilleta, A. Gonzalez, J. Ruin, C. Cal, J. Asua, Morphology of High Impact Polypropylene Particles, Institute for Polymer Materials (POLYMAT), The University of the Basque Country, 1072, 20018 Donostia-San Sebastian

[29] T. McKenna, J. B. P.Soares, Single particle modelling for olefin polymerization on supported catalysts: A review and proposals for future developments, Chemical Engineering Science, Volume 56, Issue 13, 2001, 3931-3949.

[30] W. Geoffrey, R. Stefan, Catalysts for the Living Insertion Polymerization of Alkenes: Access to New Polyolefin Architectures Using Ziegler–Natta Chemistry. Angewandte Chemie, 2002, 41, 2236-2257.

[31] J. B. P. Soares, & A. E. Hamielec. Effect of hydrogen and of catalyst prepolymerization with propylene on the polymerization kinetics of ethylene with a non-supported heterogeneous Ziegler–Natta catalyst. Polymer, 1996, 37, 4599–4605.

[32] J.T.M. Pater, G. Weickert, W.P.M.van Swaaij, "Propene bulk polymerization kinetics: Role of prepolymerization and hydrogen", AIChE journal, 2003, 49, 180-193

[33] G. Weickert, G. B. Meier, J. T. M. Pater, & K. R. Westerterp. The particle as a microreactor: catalytic propylene polymerizations with supported metallocenes and Zielger–Natta catalysts. Chemical Engineering Science, 1999, 54, 3291–3296.

[34] M. Kakugo, H. Sadatoshi, M. Sakai,Yokoyama, Macromolecules, 1989, 22, 3172-3177

[35] S. W. Webb, W. C. Conner, & R. L. Laurence. Monomer transport influences in the nascent polymerization of ethylene by silica-supported chromium oxide catalyst. Macromolecules, 1989, 22, 1885–1894.

[36] S. W. Webb, E. L. Weist, M. G. Chiovetta, R. L. Laurence & W. C. Conner. Morphological influences in the gas phase polymerization of ethylene by silica supported chromium oxide catalysts. Canadian Journal of Chemical Engineering, 1991, 69, 665– 681.

[37] V. W. Buls, T. L. Higgins. A particle growth theory for heterogeneous Ziegler polymerization. Journal of Polymer Science: Part A-1, 1970, 8, 1037–1053

[38] C. W. Hock. How TiCl3 Catalysts Control the Texture of As-polymerized polypropylene. Journal of Polymer Science: Part A-1, 1966, 4, 3055–3064.

[39] Z. W. Wilchinsky, R. W. Looney, G. M. Tornquist. Dependence of polymerization activity on particle and crystallite dimensions in ball milled TiCl3 and TiCl3/AlCl3 catalyst components. Journal of Catalysis, 1973, 28, 351–367.

[40] Jr., J. Boor. Ziegler–Natta catalysts and polymerization. New York: Academic Press. 1979.

[41] L. Noristi, E. Marchetti, G. Baruzzi, P. Sgarzi. Investigation on the particle growth mechanism in propylene polymerization with MgCl2-supported Ziegler–Natta catalysts. Journal of Polymer Science: Part A: Polymer Chemistry, 1994, 32, 3047–3059.

[42] J. W. Begley, J. Polymer Sci., 1966, Part A-1, 4, 319

[43] W. R Schmeal, J. R. Street, AIChE Journal 1971, 17, 1188

[44] J. R. Crabtree, F. N. Grimsby, A. J. Nummelin, J. M. Sketchley, Applied polymer, 1973, Volume 17, Issue 3, 959–976

[45] G. Weickert, G. B. Meier, J. T. M. Pater, K. R. Westerterp, Chemical Engineering Science 1999, 54, 3291

[46] W. R. Schmeal, J. R. Street. Polymerization in expanding catalyst particles. A.I.Ch.E. Journal, 1971, 17, 1189–1197.

[47] W. R. Schmeal, J. R. Street. Polymerization catalyst particles: Calculation of molecular weight distribution. Journal of Polymer Science: Polymer Physics Edition, 1972, 10, 2173–2187.

[48] D. Singh, R. P. Merrill. Molecular weight distribution of polyethylene produced by Ziegler–Natta catalysts. Macromolecules, 1971, 4, 599–604.

[49] D. Singh, R.P. Merill, Macromolecules 1971, 4, 599

[50] Y. I. Yermakov, V. G. Mikhalchenko, V. S. Beskov, Y. P. Grabovskii, I. V. Emirova, Plast. Massy 1970, 9, 7

[51] S. Floyd, K. Y. Choi, T. W. Taylor, W. H. Ray, 1986, Volume 32, Issue 1, Pages 2935–2960

[52] F. Machado, T.F.L. McKenna, E.L. Lima, J.C. Pinto, In-Situ Preparation of Polypropylene / 1-Butene Alloys Using a MgCl2-Supported Ziegler-Natta Catalyst, Eur. Polym. J., 44, 1130-39

[53] J. Eric, Industrial & engineering chemistry product research and development, Nagel, 1980, 19, 3, 372 -379

[54] C. Martin, T.F. McKenna, Chem. Eng. J., 2002, 87, 89-99

[55] J. Crank, G. S. Park, „Diffusion in Polymers", Academic Press, London, 1968

[56] R. A. Hutchinson, W. H. Ray, Journal of Applied Polymer Science 1986, 34, 657-676

[57] M. A. Ferrero, M. G. Chiovetta. Catalyst fragmentation during propylene polymerization: Part I. The effects of grain size and structure. Polymer Engineering Science, 1987, 27(19), 1436–1447.

[58] M. A. Ferrero, M. G. Chiovetta. Catalyst fragmentation during propylene polymerization: Part II. Microparticle diffusion and reaction effects. Polymer Engineering Science, 1987, 27(19), 1448– 1460.

[59] M. A. Ferrero, M. G. Chiovetta. Catalyst fragmentation during propylene polymerization: Part III. Bulk polymerization process simulation. Polymer Engineering Science, 1991. 31(12), 886–903.

[60] M. A. Ferrero, E. Kol, R.Sommer, W. C. Conner. Characterization of the changes in the initial morphology for MgCl2-supported Ziegler–Natta

polymerization catalysts. Journal of Polymer Science Part A: Polymer Chemistry, 1992, 30, 2131–2141.

[61] F. Bonini, V. Fraaije, G. Fink. Propylene polymerization through supported metallocene/MAO catalysts: Kinetic analysis and modeling. Journal of Applied Polymer Science, 1995, 33, 2393– 2402.

[62] R. L. Laurence, M. G. Chiovetta. Heat and mass transfer during olefin polymerization from the gas phase. In: K. H. Reichert & W. Geisler (Eds.), Polymer reaction engineering: Influence of reaction engineering on polymer properties 1983, 74–111.

[63] M. G. Chiovetta. Heat and mass transfer during the polymerization of alpha-olefins from the gas phase, Ph.D. Dissertation, University of Massachusetts at Amhurst, 1983.

[64] Kittilsen, P., Svendsen, H., & McKenna, T. F. (2001). Modeling of transfer phenomena on heterogeneous Ziegler catalysts. IV. Convection effects in gas phase processes. Chemical Engineering Science, 56(13), 3997–4005.

[65] T. F. McKenna, H. Benamouama, R. Spitz. Mass transfer resistance in Ziegler-catalysed slurry phase polymerisation: A new look at reaction modelling. DECHEMA Monographien, 1995, 131, 223– 234.

[66] T. F. McKenna, D. Cokljat, R. Spitz. Heat transfer from heterogeneous catalysts: An exploration of underlying mechanisms using CFD. A.I.Ch.E. Journal, 1999, 45(11), 2392–2410.

[67] T. F. McKenna, D. Cokljat, R. Spitz., V. Mattioli, P. Wild. Heat and mass transfer during heterogeneously catalyzed olefin polymerisation. Paper 72e, pp. 210–218, Third annual polymer producers conference, A.I.Ch.E. Spring Meeting, Houston, 1999, TX, March 14–18.

[68] T.F. McKenna, R. Spitz, Cokljat, D. AIChE J 1999, 45, 2393.

[69] J. Kosek, F. Stepanek, M. Marek, Adv. Chem. Eng, 2005, 30, 137

[70] D.C. Bassett, Principles of Polymer Morphology, Oxford Science Publications, New York,1988

[71] J. A. Debling, J. J. Zacca, W. H. Roy, "Reactor Residence-Time Distribution Effects on the Multistage Polymerisation of Olefins. Multi-Layered Products: Impact Polypropylene", Chem. Eng. Sci., 1997, 52, 1969

[72] T. Simonazzi, G. Cecchin, S. Mazzullo, Outlook on Progress in Polypropylene Based Polymer Technology Prog. Polym Science 1991, 303.

[73] Z-q. Fan, Y-q. Zhang, J-t. Xu, H-t. Wang, L-x. Feng, "Structure and Properties of Polypropylene/poly (Ethylene-Co-Propylene) in-situ Blends Synthesized By Spherical Ziegler-Natta Catalyst'', Polymer, 2001, 42, 5559.

[74] M. Kakugo, H. Sadatoshi, J. Sakai, Morphology of nascent polypropylene produced by MgCl2 supported Ti catalyst, In Catalytic Olefin Polymerization, eds. T. Keii, K. Soga, Elsevier, Amsterdam, The Netherlands, 1990, 345-354

[75] P. Galli, J. Haylock. Continuing initiator system developments provide a new horizon for polyolefin quality and properties. Prog. Polym. Sci. 1991, 16, 443-462.

[76] P. Galli J, C. Haylock, T. Simonazzi, Manufacturing and properties of polypropylene copolymers, Polypropylene Structure, blends and composites, Springer, Dordrecht, 1-24

[77] M. Kakugo, M. Hashimoto, J. Isobata, Sumitomo's liquid-phase and gas-phase processes for polypropylene production. AIChE Annual Meeting, New York, U.S.A. 1987

[78] J.B.P Soares, A. E. Hamielec. Kinetics of propylene polymerization with non-supported heterogeneous Ziegler– Natta catalyst—Effect of hydrogen on rate of polymerization, stereoregularity, and molecular weight distribution. Polymer, 1996, 37, 4606–4616.

[79] M. Bartke, „Polymer Particle Growth and Process Engineering Aspects", Severn, J.R., Chadwick, J.C., "Tailor-Made Polymers", Wiley-VCH, 2008, 3 ISBN 978 3 527 31782-0.

[80] F.A.N Fernandes, L.M.F Lona, "Fluidized bed reactor for polyethylene production. The influence of polyethylene prepolymerization", Brazilian Journal of Chemical Engineering, 2000, 47, 163-170

[81] K. Chen, B. Lio, J.B.P. Soares "Effect of Prepolymerization on the Kinetics of Ethylene Polymerization and Ethylene/1-Hexene Copolymerization with a Ziegler–Natta Catalyst in Slurry Reactors", Macromolecuar Reaction Engineering, 2016, 10,5, 463-478

[82] US Pat. 5,106,804, 1992

[83] M. Kakugo, H. Sadatoshi, M. Yokoyama, K. Kojima, Macromolecules 1989, 22, 547

[84] T.F. McKenna, D. Bouzid, S. Matsunami, T. Sugano, Polym. Reac. Eng., 2003, 11, 177

[85] T.M.J. Pater, G. Weickert, W.P.M.V. Swaaj, J Appl Polym Sci 2003, 87, 1421.

[118] R. Huang, D. Liu, S. Wang, B. Mao, Macromol Chem Phys 2004, 205, 966.

[86] M. Kakugo, H. Sadatoshi, M. Yokoyama, K. Kojima, Macromolecules. 1989, 22, 547-551

[87] J.A Debling, W.H. Ray, Morphological development of impact polypropylene produced in gas phase with a TiCl4/MgCl2 catalyst.

[88] J.A, Debling, Modeling Particle Growth and Morphology Of Impact Polypropylene Produced In The Gas Phase, Ph.D.Thesis, University of Wisconsin 1997

[89] G. Cecchin, E. Marchetti, G. Baruzzi, Macromol. Chem. Phys., 2001, 202, 1987-1994

[90] D. Bouzid, T.F.L. McKenna, Macromol. Chem. Phys., 2006, 207, 13-19

[91] Y. Chen, W. Chen, D. Yang, Eur. Polym. J., 2007, 43 2999

[92] Y. Chen, W. Chen, D. Yang, J. Appl. Polym. Sci., 2008, 108, 2379

[93] Z. Fu, Y. Zhang, Z. Fan, J. Xu, J. Appl. Polymer. Sci., 2007, 103, 2075

[94] R. Li, X. Zhang, Y. Zhao, X. Hu, X. Zhao, D. Wang, Polymer, 2009, 5124.

[95] C. Tong, Y. Chen, Y. Chen, X. Zhang, D. Yang, J. Zhang, Polymer, 2008, 49, 2974

[96] A. Zubov, L. Pechackove, L. Sedar, M. Bobak, J. Kosek, Chem. Eng. Sci., 2010, 65, 2361

[97] M. Bobak, T. Gregor, B. Bachman,J. Kosek, Macromol. React. Eng., 2008, 2, 176

[99] C. E. Rogers, V. Stannett, M. Szwarc, Journal of Polymer Science 1960, 45, 61

[100] B. Freeman, Y. Yampolskii, I. P. John, Materials Science of Membranes for Gas and Vapor separation, Wiley & Sons, 2006

[101] Felder, Polymers Physical Properties, Academic Press, 1980

[102] H.Levine, Amorphous Food and Pharmaceutical Systems.

[103] M. Bartke, S. Kröner, A. Wittebrock, A. Reichert, K. Illiopoulus, I. Dittrich, C. Sorption and Diffusion of Propylene and Ethylene in Heterophasic Polypropylene Copolymers, 2007, Volume 259, Issue 1, 327–336

[104] C. George, S. Thomas, Transport phenomena through polymeric systems Prog polym Sci, 2001, 26, 985-1017

[105] D. W. van Krevelen, „Properties of Polymers ", Elsevier Scientific, Amsterdam, 1976

[106] S. A. Stern, J. T. Mullhaupt, P. J. Gareis, AIChE Journal 1969, 15, 64

[107] R. Hutchinson, and W. Ray, Journal of Applied Polymer Science, 1990, Vol. 41, 51–81

[108] P. J. Flory, Principles of Polymer Chemistry 1953, 511-584

[109] A. F. M. Barton, "CRC Handbook of Polymer–Liquid Interaction Parameters and Solubility Parameters", CRC Press: Boca Raton, 1990

[110] C. Nakamoto. T. Kitada. E. Kato Pressure dependence on the Flory-Huggins interaction parameter of poly (N-isopropylacrylamide) gels, Polymer Gels and Networks, 1996, Volume 4, Issue 1, Pages 17-31

[111] Y. Kamiya, T. Hirose, K. Mizoguchi, Y. Naito, Gravimetric study of high-pressure sorption of gases in polymers. 1986, Volume 24, Issue 7, 1525–1539

[112] E. L. Cussler, Diffusion Mass Transfer in Fluid Systems, 2009

[113] P. Neogi, Diffusion in Polymers, 1996

[114] R.E. Kesting, A.K. Fritzsche, Polymeric gas separation membranes, John Wiley & Sons, Inc, New York, 1993.

[98] T. Kröner, M. Bartke, Sorption of Olefins in High Impact Polypropylene – Experimental Determination and Mass Transport Modeling. Macromolecular reaction engineering, WILEY-VCH Verlag GmbH & Co. KGaA, 2013

[115] T. Kröner, Mass Transport and Kinetics in the Heterophasic Copolymerization of Propylene. Ph.D. Dissertation, Martin-Luther-Universität Halle-Wittenberg, Halle, Germany, 2014

[116] W. Kaminsky, Polyolefins: 50 years after Ziegler and Natta II, Advances in Polymer Science, Polyolefins by Metallocenes and Other Single-Site Catalysts, 2013, ISBN: 978-3-642-40804-5.

[117] A van der Wal, J.J Mulder, R.J Gaymans, Fracture of polypropylene: The effect of crystallinity, Polymer, 1998, Volume 39, Issue 22, 5477–5481

[119] A. v. Wal, J.J. Mulder, J. Oderkerk and R. J Gaymans, "Polypropylene-Rubber Blends: 1. The Effect of the Matrix Properties on the Impact Behaviour", Polymer,1998, 36 ,6781

[120] J. Crank, The Mathematics of Diffusion, ed. By J. Crank, G.S. Park, Academic, New York, 1968, 1-39

[121] C. Pellecchia, D. Pappalardo, G. Gruter, J. Macromolecules 1999, 32, 4491

[122] D.E. Thompson, K.B. McAuley, P.J. McLellan, Macromol React Eng 2007, 1, 264

[123] R. Spitz, V. Monteil* J Polym Sci Part A: Polym Chem 2010, 48, 2631.

[124] S. A. Shin, L. C. Simon, J. B. P. Soares, G. Scholz, T. F. McKenna Macromolecular Reaction Engineering, 2009, Volume 3, Issue 9

[125] S. Weiß, K-E. Militzer, K Gramlich, Thermische Verfahrenstechnik, Deutscher Verlag für Grundstoffindustrie, Leipzig, 1993

[126] R. Young, P. Lovell, Introduction to Polymers, Third Edition, CRC Press, 2011

[127] Y.V. Kissin, R. Ohnishi, T. Konakazawa, Propylene Polymerization with Titanium-Based Ziegler-Natta Catalysts: Effects of Temperature and Modifiers on Molecular Weight, Molecular Weight Distribution and Stereo-specificity, Macromolecular Chemistry and Physics, 2004, 205(3), 284-301

[128] J.A. Ewen, M.J. Elder, Eur. Pat. Appl. 426638, 1991.

[129] J. T. M. Pater, P. Roos, G. Weickert, , K. R. Westerterp, F. Shimitzu, G. Ko. Integral aspects of gas phase olefin polymerization: Kinetics, absorption and fluidization. In: K.-H. Reichert, H.-U. Moritz (Eds.), Sixth international workshop on polymer reaction engineering, Dechema Monograph, Vol. 134, 1998, 103–114.

[130] M. Kakugo, H. Sadatoshi, J. Sakai, M. Yokoyama. Growth of polypropylene particles in heterogeneous Ziegler–Natta polymerization. Macromolecules, 1989, 22, 3172–3177.

[131] M. A. Ferrero, M. G. Chiovetta. Catalyst fragmentation during propylene polymerization: Part IV. Comparison between gas phase and bulk polymerization processes. Polymer Engineering Science, 1991, 31(12), 904–911.

Curriculum Vitae

Personal data

Name: Miguel Angel Plata Acevedo

Date and place of birth: 18. March 1985 in Bogota (Colombia)

Citizenship: German

Contact: Phillipsring 29

55252 Mainz-Kastel; Germany

phone: +49-176-20278232

email: miguel.plata@chemie.uni-halle.de

Education

07/2013 – Martin Luther University Halle-Wittenberg
08/2017

Ph.D.-student in Polymer Reaction Engineering group of Prof. Dr.-Ing. M. Bartke

Project funded by Dutch Polymer Institute DPI #785.

HIPSTER: High Impact Polypropylene – Structure Evolution and impact on Reaction.

10/2008 - Friedrich Alexander University
01/2011

Department for Particle Technology by Prof. Dr.-Ing W. Peukert and Dr. rer. nat Schmidt.

Dipl.-Ing. degree in chemical and biological Engineering.

Diploma thesis: Production of polymeric micro particles by wet grinding in a stirred media mill and emulsion polymerization.

Professional experience

01/2018 – Dow silicones Deutschland GmbH
now

Senior Research Specialist

Process and Engineering R&D

07/2011 - Arkema GmbH
06/2013

Halogen Free research and development engineer.

List of publications:

- M. Plata, J. Schmidt, S. Tröger, W. Peukert Production of polymer particles below 5µm by wet grinding. Powder Technology (Volume 228, September 2012, Pages 84–90. Institute of Particle Technology, University of Erlangen-Nuremberg.
- A. J. Cancelas, M. A. Plata, M. A. Bashir, V. Monteil, T. F. L. McKenna. Solubility and Diffusivity of Propylene, Ethylene, and Propylene–Ethylene Mixtures in Polypropylene. Accepted by Macromolecular chemistry and physic (Volume 219, Issue 8, April 2018)
- M. Plata, M. Bartke. High impact Polypropylene: Morphology generation during Matrix-Stage and effects on the copolymerization. (In preparation).

Erklärung

Hiermit erkläre ich an Eides statte, dass ich meine Dissertation selbständig und ohne fremde Hilfe verfasst habe. Ich habe keine anderen als die von mir angegebenen Quellen und Hilfsmittel benutzt und habe die den benutzten Werken wörtlich oder inhaltlich entnommenen Stellen als solche kenntlich gemacht.

Des Weiteren erkläre ich, dass ich erstmals eine Dissertation einreiche und diese noch bei keiner anderen Institution eingereicht habe. Ich bin nicht vorbestraft und es gibt keine laufenden Ermittlungsverfahren gegen meine Person.

_____   _____
        Halle, den   Miguel Plata